# UCC28782 High-Density Active-Clamp Flyback Controller with EMI Dithering, X-Cap Discharge, and Bias Power Management

1 Features

- Active clamp recovers leakage inductance energy
- Adaptive control for fast zero voltage switching (ZVS) tracking and dead time optimization
- Integrated switching bias regulator supports USB Type-C™ PD wide output voltage range with one auxiliary winding
- EMI frequency dithering without trade-offs on transient response or audible noise
- Dynamic bias power management for digital isolator and GaN driver
- Programmable Adaptive Burst Mode (ABM) with internal compensation
- Active X-capacitor (X-cap) discharge
- Over-temperature, over-voltage, output short-circuit, over-current, over-power, and pin-fault protections
- Auto-recovery and group-latch fault options with fast latch-reset capability
- 4x4-mm 24-pin QFN package
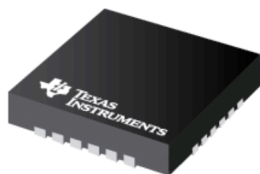
2 Applications

- High-density Type-C™ PD adapters for laptop, tablet, TV, set-top box, and printer
- USB power delivery and fast phone chargers
- AC-to-DC or DC-to-DC auxiliary power supply
- Audio soundbars and smart speakers
- Battery chargers for power tools and E-bikes
- USB wall outlets
- LED lighting

3 Description

The UCC28782 is a high-density active-clamp flyback (ACF) controller for USB Type C™ PD applications and allows for efficiencies over 93% by recovering the leakage inductance energy and adaptive ZVS tracking over the full load range.

With a maximum frequency of 1.5 MHz the magnetics can be minimized. Frequency dithering helps to improve EMI margin. The UCC28782 also integrates dynamic bias power management to optimize the gate drive for Si or GaN MOSFETs.

Adaptive Burst Mode (ABM) combined with Low Power Mode (LPM) and Standby Power mode (SBP) work together to increase light-load efficiency while reducing ripple and audible noise.

The UCC28782 also integrates an X-Cap discharge function to discharge the residual input voltage when power is removed.

The UCC28782 has multiple protection modes and options for retry or latch-off responses depending on the application needs. See Device Comparison Table.

Device Information[(1)]

PART NUMBER	PACKAGE	BODY SIZE
UCC28782	WQFN-24	4.0 mm × 4.0 mm

(1) For all available packages, see the orderable addendum at the end of the data sheet.
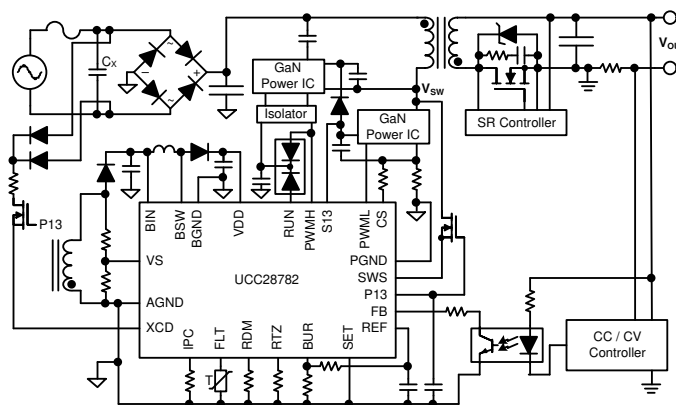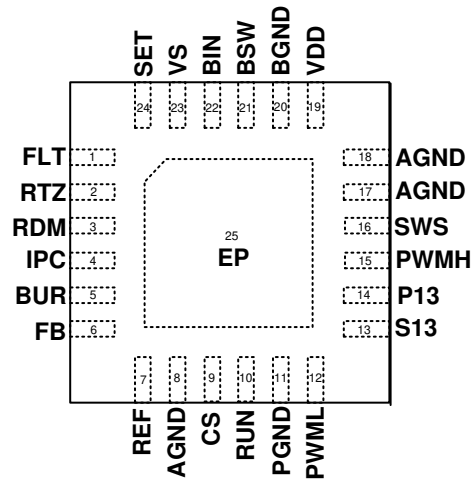

Simplified Typical Schematic

6 Pin Configuration and Functions

UCC28782A
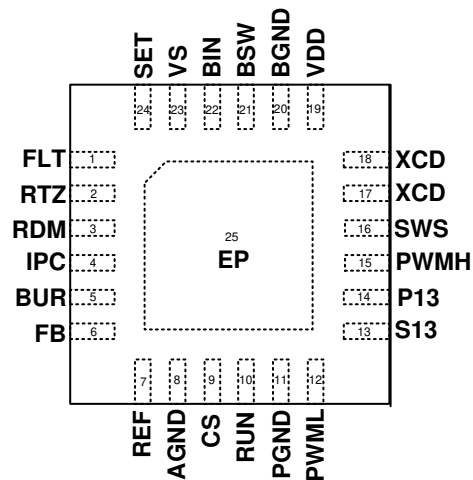

UCC28782AD, UCC28782BDL, UCC28782CD

Figure 6-1. RTW Package 24-Pin WQFN Top View

Pin Functions

PIN		TYPE[1]	DESCRIPTION
NAME	NUMBER		
FLT	1	I	The controller enters into the fault state if the FLT-pin voltage is pulled above 4.5 V or below 0.5 V. A 50-µA current source interfaces directly with an external NTC (negative temperature coefficient) thermistor to AGND pin for remote temperature sensing. The current source is active during the run state and inactive during the wait state. A 50-µs fault delay allows a filter capacitor to be placed on the FLT pin without false triggering the 0.5-V OTP fault when the controller enters into a run state from a wait state. Alternatively, a high-resistance voltage divider can be used to sense the bulk input capacitor voltage for line-OVP detection, and a 750-µs fault delay helps to prevent false triggering the 4.5-V input line-OVP from a short-duration bulk capacitor voltage overshoot during line surge and ESD strike events. When FLT-pin voltage is used for line-OVP detection, the external OTP can be implemented on CS pin.
RTZ	2	I	A resistor between this pin and AGND pin programs an adaptive delay for transition to zero voltage from the turn-off edge of the high-side clamp switch to the turn-on edge of the low-side switch. The parasitic capacitance between this pin and AGND needs to be minimized to avoid its effect on the dead-time calculation.
RDM	3	I	A resistor between this pin and AGND pin programs a synthesized demagnetization time used to control the on-time of the high-side switch to achieve zero voltage switching on the low-side switch. The controller applies a voltage on this pin that varies with the output voltage derived from the VS pin signal. The parasitic capacitance between this pin and AGND needs to be minimized to reduce its influence on the internal PWMH on-time calculation.
IPC	4	I	This pin is an intelligent power control (IPC) pin to optimize the converter efficiency. A 50-µA current source directly interfaces with a resistor (R_{IPC}) to AGND pin to program an increase in the peak current level at very light load; the burst frequency can be further reduced, helping to achieve low standby power and tiny-load power. If the IPC pin is connected to AGND without R_{IPC}, the peak current level in very light load is set to a minimum level for the output ripple or audible noise sensitive designs. R_{IPC} can also be connected between this pin and the CS pin or IPC pin can be directly connected to CS pin, so the 50-µA IPC current can create an output voltage dependent offset voltage on the CS pin for reducing output ripple in adaptive burst mode and improving light-load efficiency at lower output voltage level of a wide output voltage range design. IPC pin can be used to disable the PFC controller at all load condition of 5 V and 9 V outputs through a control switch to further improve the light load efficiency of higher power adapters.
BUR	5	I	This pin is used to program the burst threshold of the converter at light load. A resistor divider between REF pin and AGND pin is used to set a voltage at this pin to determine the peak current level when the converter enters adaptive burst mode (ABM). In addition, the Thevenin resistance on BUR pin (equivalent resistance of the divider resistors in parallel) is used to set an offset voltage for smooth mode transition. A 2.7-µA pull up current increases the peak current threshold when the converter enters low power mode (LPM) from ABM. A 5-µA pull down current reduces the peak current threshold when the converter enters into heavy load mode (adaptive amplitude modulation, AAM) from ABM.
FB	6	I	The feedback current signal to close the converter regulation loop is coupled to this pin. This pin presents a 4.25-V output that is designed to have 0-µA to 75-µA current pulled out of the pin corresponding to the converter operating from full-power to zero-power conditions. A 220-pF filter capacitor between FB pin and REF pin is recommended to desensitize the feedback signal from noise interference.
REF	7	O	The pin is a 5-V reference output that requires a 0.22-µF ceramic bypass capacitor to the AGND pin. This reference is used to power internal circuits and can supply a limited external load current. Pulling this pin low shuts down PWM action and initiates a VDD restart.
AGND	8	G	Analog ground and the ground return of PWMH and RUN drivers. Return all analog control signals to this ground.
CS	9	I	This is the current-sense input pin. This pin couples to the current-sense resistor through a line-compensation resistor to control the peak primary current in each switching cycle. An internal current source on this pin, proportional to the converter's input voltage, creates an offset voltage across the line-compensation resistor to balance the OPP level across line. The CS pin can also provide an alternative OTP function, when the FLT pin is being used for the line input-OVP. A small-signal diode in series with an NTC resistor is connected between PWMH pin and CS pin to form the OTP detection. When PWMH is high, the NTC resistor and the line-compensation resistor become a resistor divider from 5 V and creates a temperature dependent voltage on CS pin. When CS pin voltage is higher than 1.2 V in PWMH on state for 2 consecutive cycles, the OTP fault on CS pin is triggered.

PIN		TYPE[1]	DESCRIPTION
NAME	NUMBER		
RUN	10	O	This output pin is high when the controller is in a run state. This output is low during start-up, wait, and fault states. A 2.2-µs timer delays the initiation of PWML switching after this pin has gone high and S13-pin voltage is above the 10-V power good threshold. The pull up driving capability of both RUN and PWMH pins allows bias power management of a digital isolator and GaN power IC through a common-cathode small-signal diode, so the power consumption can be reduced in wait state.
PGND	11	G	Low-side ground return of the PWML driver. The internal level shifter allows the common return impedance to be eliminated, and improving higher frequency operation. For a GaN-based gate-injection transistor (GIT), this pin can be directly connected to the separate source pin of a GIT GaN device, which enhances the turn-off speed and decouples the additional voltage spike on the current-sense resistor and layout parasitic inductance of the gate driving loop. For a silicon (Si) power FET, this pin can be connected to the source for a smaller gate driving loop. For a GaN power IC with a logic PWM input, this pin can be referred to AGND.
PWML	12	O	Low-side switch gate driver output. The high-current capability (-0.5A/+1.9A) of PWML enables driving of a silicon power MOSFET with higher capacitive loading, a GIT GaN with continuous on-state current, or a GaN power IC with logic input. The maximum voltage level of PWML is clamped to the P13 pin voltage.
S13	13	O	S13 is coupled to P13 through an internal 2.8-Ω switch controlled by the RUN pin. When RUN is high, the S13 decoupling capacitor is charged up to 13 V by an internal soft-start current limiter. The S13 pin voltage needs to increase above 10 V to initiate PWML switching. When RUN is low, S13 is discharged by the S13 pin loading, such as GaN power IC. The power-on delay of the GaN power IC on S13 must be less than 2 µs to be responsive to PWML. A 22-nF ceramic capacitor between S13 and the driver ground is recommended. S13 can also perform power management on the PFC controller at the same time through a diode, such that PFC can be disabled at deep light load condition.
P13	14	O	P13 is a regulated 13-V output voltage derived from V_{VDD}. During V_{VDD} startup, P13 pin is connected to the VDD pin internally, so the external high-voltage depletion MOSFET, such as BSS126, can provide the controlled startup current to charge the VDD capacitor. After the initial startup, P13 recovers back to 13-V regulation. A 1-µF ceramic bypass capacitor is required from P13 to AGND. A 20-V Zener between this pin and AGND is recommended to protect this pin from overstress, when the connection between this pin and the BSS126 gate is fail-open or line surge energy is coupled to this pin.
PWMH	15	O	PWM output signal used to control the gate of the high-side clamp switch through an external high-voltage gate driver. The driving capability is designed to bias an external level-shifting isolator through a small-signal diode or can also transmit the signal to high-side driving circuitry through a pulse transformer. The maximum voltage level of PWMH is clamped to 5-V REF level.
SWS	16	I	This sensing input is used to monitor the switch-node voltage as it nears zero volts in normal operation for ZVS auto-tuning. The source of a high-voltage depletion-mode MOSFET, such as BSS126, is coupled to this pin through a current-limiting resistor, so only the useful switching characteristic below 15 V is monitored. During start-up, this pin is connected to the VDD pin internally to allow BSS126 to provide start-up current. The external current-limit resistor and a small bidirectional TVS across BSS126 gate and source should be added to protect the gate-to-source voltage from potential abnormal voltage stress. The resistor should be higher than 500 Ω. The clamping voltage of TVS should be less than BSS126 voltage rating but greater than 15 V. Moreover, the resistor and a 22-pF ceramic capacitor between the SWS pin and the bulk input capacitor ground form a small sensing delay to help the internal detection circuit to identify the ZVS characteristic correctly.

Product Folder Links: *UCC28782*

PIN		TYPE[1]	DESCRIPTION
NAME	**NUMBER**		
XCD	17, 18	I	X-cap discharge input pins with 2-mA maximum discharge current capability. The 6.5-V line zero-crossing (LZC) threshold on XCD pins is used to detect AC-line presence. When LZC is missing over an 84-ms timeout period, the discharge current is enabled for a maximum period of 300 ms followed by a 700-ms no current blanking time. For the latched-off fault protections, when AC-line recovers and LZC is detected again, the controller can reset the latch fault state almost immediately and will attempt to restart without waiting to fully discharge the bulk input capacitor. For the auto-recovery fault protections, if the controller is in 1.5-s auto-recovery fault state, LZC can reset the timer and speed up the restart attempt. The two redundant XCD pins help to provide the X-cap discharge function even when one pin is in fail-open condition. To form the discharge path, an anode of two high-voltage diode rectifiers is connected to each X-cap terminal, the two diode cathodes are connected together to a 26-kΩ high-voltage current-limiting resistance, and the drain-to-source connection of a high-voltage depletion MOSFET couples the resistance to the XCD pins. Two series 13-kΩ SMD resistors in 1206 size can be used as the current limiting device, and share the potential transient voltage from the AC-line. A 600-V rated MOSFET such as BSS126 is needed as the high voltage blocking device. The MOSFET gate is connected to the P13 pin, so the XCD pins can obtain enough signal headroom for LZC detection. If the X-cap discharge function is not needed, XCD pins must be connected to AGND pin to disable the function, and the diode-resistor-MOSFET path must be removed. Different from UCC28782AD, UCC28782BDL, and UCC28782CD, the same pin locations on UCC28782A are defined as two additional AGND pins, keeping the XCD-pin function disabled.
VDD	19	P	Controller bias power input. VDD pin is also the integrated boost converter output pin. A hold-up capacitor to BGND pin is required. For fixed-output applications where the boost converter is optional, VDD pin can directly connect to the rectified primary-side auxiliary winding voltage, so the boost-converter components can be eliminated. For wide-output design with the boost converter, a ceramic capacitor with 10-µF or 15-µF capacitance is recommended, and the minimum voltage rating is 25 V.
BGND	20	G	Boost converter return pin connected to the source terminal of the internal 30-V boost switch. The separate ground return simplifies PCB layout design to minimize the high di/dt switching loop along with the boost diode and VDD capacitor, so the noise-coupling effect to other sensitive nodes can be mitigated.
BSW	21	I	Boost converter switch node, connected to the drain terminal of internal 30-V boost switch. For wide output voltage applications, the boost inductor and boost diode anode are connected to this pin. For a fixed output voltage design, BIN and BSW pins should be connected to BGND pin, so the boost-converter control is disabled in order to lower the controller run current. A 22-µH inductor with higher than 0.4-A saturation current capability and less than 1 Ω resistance is recommended for boost inductor selection. If the maximum VDD-pin voltage is less than 30V, a 30-V rated Schottky diode not smaller than SOD-323 package is recommended as boost diode, so the BSW voltage stress from the diode reverse recovery effect can be avoided when the converter operates in short-duration CCM.
BIN	22	I	Boost converter input pin. For a wide output voltage application, when the boost converter is needed to improve the converter efficiency, BIN is connected to the rectified auxiliary-winding voltage. A 33-µF energy storage capacitor in parallel with a 10-µF ceramic capacitor is recommended. The 33-µF capacitor should be placed close to the auxiliary rectification diode and the auxiliary-winding ground terminal to minimize the rectification switching loop. The 10-µF cap can be placed close to the boost inductor and BGND pin to minimize the boost input switching loop. Together with a Schottky-type auxiliary diode in a SOD-123 package, less than 0.1-Ω winding resistance on the auxiliary winding is required to ensure the boost converter receives sufficient transformer energy under a very low output voltage condition, especially for the 3.3-V to 21-V output range. A small unidirectional 24-V TVS between BIN and AGND can protect the pin from exceeding its 30-V rating, when potential abnormal voltage stress occurs. If the boost converter is not needed, BIN and BSW should be connected to BGND pin.
VS	23	I	This voltage-sensing input pin is coupled to an auxiliary winding of the converter's transformer via a resistor divider. The pin and the associated external resistors are used to monitor the output and input voltages and switching edges of the converter at different moments within each switching cycle. The parasitic capacitance between this pin and AGND needs to be minimized to avoid the impact on the output voltage sensing and the dead-time calculation.
SET	24	I	This pin is used to configure the controller to be optimized for gallium nitride (GaN) power FETs or silicon (Si) power FETs on the primary side. Depending on the setting, it will optimize parameters of the ZVS control loop, dead-time adjustment, and protection features. When pulled high to REF pin, it is optimized for Si FETs. When pulled low to AGND, it is optimized for GaN FETs.
EP	25	G	The thermal pad must be connected to AGND.

(1)   I = Input, O = Output, P = Power, G = Ground

Product Folder Links: *UCC28782*

Table of Contents

4 Revision History

NOTE: Page numbers for previous revisions may differ from page numbers in the current version.

Changes from Revision C (August 2020) to Revision D (May 2021) **Page**

Changes from Revision B (June 2020) to Revision C (August 2020) **Page**

Changes from Revision A (May 2020) to Revision B (June 2020) **Page**

5 Device Comparison Table

ORDERABLE PART NUMBER	EMI Dither	X-CAPACITOR DISCHARGE	FAULT RESPONSE
UCC28782A	Disabled	No	All are auto-recovery (retry)
UCC28782AD	Enabled	Yes	All are auto-recovery (retry)
UCC28782BDL	Enabled	Yes	OVP, OPP, OCP, SCP, and OTP-on-FLT-pin are latch-off faults
UCC28782CD	Enabled	Yes	OVP and OTP-on-FLT-pin are latch-off faults

7 Specifications

7.1 Absolute Maximum Ratings

over operating free-air temperature range (unless otherwise noted) [1]

		MIN	MAX	UNIT
Input Voltage	VDD		38	V
	SWS	−6	38	
	SWS (transient, negative pulse width of 20 ns max., duty cycle ≤ 1%)	−10	38	
	VDD-SWS	−20	38	
	CS	−0.3	3.6	
	VS	−0.75	7	
	VS (transient, 100 ns max.)	−1	7	
	PGND	−1	4	
	PGND (transient, 25 ns max.)		5	
	RTZ, BUR, SET, RDM, IPC, FLT, FB	−0.3	7	
	XCD, BIN, BSW	−0.3	30	
	BSW (transient, 150 ns max.)	−1	30	
Output Voltage	REF, PWMH, RUN	−0.3	7	V
	P13, S13, PWML	−0.3	20	
Source Current	REF, P13, RTZ, RDM, IPC		Self–limiting	mA
	S13 (average)		15	
	VS		2	
	VS (transient, 100 ns max.)		2.5	
	FB		1	
	RUN (continuous)		5	
	PWML (continuous)		50	
	PWMH (continuous)		10	
	CS (transient, 30 ns max.)		1	
Sink Current	RUN (continuous)		8	mA
	PWML (continuous)		50	
	PWMH (continuous)		10	
	SWS, BSW		Self–limiting	
	XCD		25	
	FLT		0.3	
	BIN		1	
Operating junction temperature	T_J	−40	125	°C
Storage temperature	T_{stg}	−65	150	°C

(1) Stresses beyond those listed under *Absolute Maximum Rating* may cause permanent damage to the device. These are stress ratings only, which do not imply functional operation of the device at these or any other conditions beyond those indicated under *Recommended Operating Condition*. Exposure to absolute-maximum-rated conditions for extended periods may affect device reliability.

7.2 ESD Ratings

			VALUE	UNIT
$V_{(ESD)}$	Electrostatic discharge	Human body model (HBM), per ANSI/ESDA/ JEDEC JS-001, all pins[1]	±2000	V
		Charged device model (CDM), per JEDEC specification JESD22-C101, all pins[2]	±500	

(1)   JEDEC document JEP155 states that 500-V HBM allows safe manufacturing with a standard ESD control process.
(2)   JEDEC document JEP157 states that 250-V CDM allows safe manufacturing with a standard ESD control process.

7.3 Recommended Operating Conditions

over operating free-air temperature range (unless otherwise noted)

		MIN	NOM	MAX	UNIT
V_{VDD}	Bias supply operating voltage	14		34	V
C_{VDD}	VDD capacitor	10			µF
C_{P13}	P13 bypass capacitor	1			µF
C_{REF}	REF bypass capacitor	0.22			µF
T_J	Operating junction temperature	−40		125	°C

7.4 Thermal Information

	THERMAL METRIC[1]	DEVICE	UNIT
		RTW + Pad (WQFN)	
		24 PINS	
$R_{\theta JA}$	Junction-to-ambient thermal resistance	43.1	°C/W
$R_{\theta JC(top)}$	Junction-to-case (top) thermal resistance	31.6	°C/W
$R_{\theta JB}$	Junction-to-board thermal resistance	20.3	°C/W
Ψ_{JT}	Junction-to-top characterization parameter	0.5	°C/W
Ψ_{JB}	Junction-to-board characterization parameter	20.3	°C/W
$R_{\theta JC(bot)}$	Junction-to-case (bottom) thermal resistance	5.7	°C/W

(1)   For more information about traditional and new thermal metrics, see the Semiconductor and IC Package Thermal Metrics application report.

7.5 Electrical Characteristics

Unless otherwise stated: V_{VDD} = 20 V, V_{BIN} = 20 V, R_{RDM} = 115 kΩ, R_{RTZ} = 140 kΩ, V_{BUR} = 1.2 V, V_{SET} = 0 V, R_{NTC} = 50 kΩ, V_{VS} = 4 V, V_{SWS} = 0 V, I_{FB} = 0 µA, C_{PWML} = 0 pF, C_{PWMH} = 0 pF, C_{REF} = 0.22 µF, C_{P13} = 1 µF, and -40°C < T_J = T_A < 125°C

PARAMETER		TEST CONDITIONS	MIN	TYP	MAX	UNIT
VDD INPUT						
$I_{RUN(STOP)}$	Supply current, run state	No switching	0.88	2.2	2.66	mA
$I_{RUN(SW)}$	Supply current, run state	Switching, I_{VSL} = 0 µA	2.66	3	3.55	mA
I_{WAIT}	Supply current, wait state	I_{FB} = -85 µA, V_{BIN} = V_{BSW} = V_{VDD} = 20 V, sum of I_{BIN}, I_{BSW}, and I_{VDD}	452	580	695	µA
		I_{FB} = -85 µA, BIN and BSW pins to AGND, I_{VDD} only	465	540	658	µA
I_{START}	Supply current, start state	V_{VDD} = $V_{VDD(ON)}$ - 100 mV, V_{VS} = 0 V	150	235	301	µA
I_{FAULT}	Supply current, fault state	fault state		500	630	µA
$I_{VDD(LIMIT)}$	VDD startup current limit during startup	V_{VDD} increasing, V_{SWS} - V_{VDD} = 1 V, V_{VDD} = 16.5 V	1.2	2	2.53	mA
$V_{VDD(ON)}$	VDD turnon threshold	V_{VDD} increasing	16.31	17	17.91	V
$V_{VDD(OFF)}$	VDD turnoff threshold	V_{VDD} decreasing	9.94	10.6	11.17	V

Product Folder Links: UCC28782

Unless otherwise stated: V_{VDD} = 20 V, V_{BIN} = 20 V, R_{RDM} = 115 kΩ, R_{RTZ} = 140 kΩ, V_{BUR} = 1.2 V, V_{SET} = 0 V, R_{NTC} = 50 kΩ, V_{VS} = 4 V, V_{SWS} = 0 V, I_{FB} = 0 µA, C_{PWML} = 0 pF, C_{PWMH} = 0 pF, C_{REF} = 0.22 µF, C_{P13} = 1 µF, and -40ºC < T_J = T_A < 125ºC

PARAMETER		TEST CONDITIONS	MIN	TYP	MAX	UNIT
$V_{VDD(PCT)}$	Offset to power cycle for long output voltage overshoot	Offset above $V_{VDD(OFF)}$, I_{FB} = -85 µA	1.54	2.2	2.98	V
$V_{VDD(RST)}$	Logic reset threshold for latched fault	Voltage that VDD must cross H-L to reset a latched-off fault condition	3.3	4.3	4.61	V
$V_{VDD(BOOST)}$	VDD regulation level in boost mode	I_{VDD} = 0 mA to 30 mA, V_{BIN} = 9 V	17.6	18.5	19.4	V
BIN INPUT						
$V_{BIN(ON)}$	UVLO on voltage of V_{BIN} in boost mode	V_{BIN} increasing	2.03	2.2	2.42	V
$V_{BIN(OFF)}$	UVLO hysteresis below $V_{BIN(ON)}$ in boost mode	V_{BIN} decreasing	1.13	1.23	1.33	V
$V_{BIN(EN)}$	Highest V_{BIN} to enable boost mode	V_{BIN} decreasing	14.44	14.9	15.47	V
$V_{BIN(DIS)}$	Hysteresis above $V_{BIN(EN)}$ to disable boost mode	V_{BIN} increasing	0.12	0.16	0.18	V
BSW INPUT						
R_{BSW}	$R_{DS(on)}$ of internal boost switch		0.94	1.4	2.28	Ω
$I_{BSW(MAX)}$	Peak current threshold in CPC control		0.27	0.335	0.38	A
t_{BLEB}	Leading edge blanking time in boost mode		129	190	247	ns
f_{BSW}	Maximum switching frequency in CPC control, for UCC28782A only	V_{BIN} = 9 V	389	420	467	kHz
f_{BSW}	Maximum switching frequency in CPC control, for UCC28782AD, UCC28782BDL, and UCC28782CD only	V_{BIN} = 9 V	389	420	499	kHz
$t_{BOFF(MIN)}$	Minimum off time in COT control	I_{FB} = -85 µA	198	255	353	ns
		I_{BSW} = 500 mA	2.9	4.35	5.9	µs
P13 OUTPUT						
V_{P13}	P13 voltage level including load regulation	0 mA to 60 mA out of P13, run state, V_{VDD} = 20 V	12.0	12.8	13.6	V
$I_{P13(START)}$	Max sink current of P13 pin during startup	V_{P13} = 14 V	1.53	2.2	3.04	mA
$I_{P13(MAX)}$	Current sourcing limit of P13 pin	P13 shorted to AGND, V_{VDD} = 20 V	103.3	133	154.5	mA
$VR13_{(LINE)}$	Line regulation of V_{P13}	V_{VDD} = 15 V to 35 V	-6	2	8.7	mV
$V_{P13(OV)}$	Over voltage fault threshold above V_{P13}		1.35	2	2.54	V
R_{P13}	Dropout resistance of P13 regulator switch between VDD and P13 pins	(V_{VDD} - V_{P13}) / 30 mA, V_{VDD} = 11 V, 30 mA out of P13	8.5	13	22.7	Ω
S13 OUTPUT						
R_{S13}	$R_{DS(on)}$ of internal disconnect switch between P13 and S13 pins	(V_{P13} - V_{S13}) / 30 mA, V_{VDD} = 11 V, 30 mA out of S13	2.1	2.8	3.82	Ω
V_{S13_OK}	S13_OK threshold to enable switching	V_{RUN} = 5 V	9.63	10.2	10.7	V
$I_{S13(MAX)}$	Current sourcing limit of S13 pin	S13 shorted to AGND, V_{VDD} = 20 V	260.7	350	452.5	mA
REF OUTPUT						
V_{REF}	REF voltage level	I_{REF} = 0 A	4.9	5	5.13	V
$I_{REF(MAX)}$	Current sourcing limit of REF pin	REF shorted to AGND, V_{VDD} = 20 V	14.3	17	20.3	mA
$VR5_{(LINE)}$	Line regulation of V_{REF}	V_{VDD} = 12 V to 35 V	-7	-3	1	mV
$VR5_{(LOAD)}$	Load regulation of V_{REF}	0 mA to 1 mA out of REF, change in V_{REF}	-16	0.1	25	mV
VS INPUT						
V_{VSNC}	Negative clamp level	I_{VSL} = -1.25 mA, voltage below ground	221	287	344	mV
V_{ZCD}	Zero-crossing detection (ZCD) level	V_{VS} decreasing	12.4	35	67.2	mV
I_{VSB}	Input bias current	V_{VS} = 4 V	-0.23	0	0.31	µA
$V_{VS(SM1)}$	VS threshold voltage in SM1 startup mode		242.4	282	318.3	mV

Product Folder Links: *UCC28782*

Unless otherwise stated: V_{VDD} = 20 V, V_{BIN} = 20 V, R_{RDM} = 115 kΩ, R_{RTZ} = 140 kΩ, V_{BUR} = 1.2 V, V_{SET} = 0 V, R_{NTC} = 50 kΩ, V_{VS} = 4 V, V_{SWS} = 0 V, I_{FB} = 0 µA, C_{PWML} = 0 pF, C_{PWMH} = 0 pF, C_{REF} = 0.22 µF, C_{P13} = 1 µF, and -40ºC < T_J = T_A < 125ºC

PARAMETER		TEST CONDITIONS	MIN	TYP	MAX	UNIT
$V_{VS(SM2)}$	VS threshold voltage in SM2 startup mode		458.3	500	543	mV
$V_{VSLV(UP)}$	VS upper threshold out of low output voltage mode (LV mode)	V_{VS} increasing	2.41	2.49	2.6	V
$V_{VSLV(LR)}$	VS lower threshold into low output voltage mode (LV mode)	V_{VS} decreasing	2.3	2.39	2.49	V
t_{ZC}	Zero-crossing timeout delay		1.95	2.3	2.73	µs
$t_{D(ZCD)}$	Propagation delay from ZCD high to PWML 10 % high	V_{VS} step from 4 V to -0.1 V	23	50	81	ns
CS INPUT						
$V_{CST(MAX)}$	Peak-power threshold on CS pin out of LV mode	I_{VSL} = 0 µA, V_{VS} ≥ $V_{VSLV(UP)}$	767.4	801	836.4	mV
		I_{VSL} = -333 µA, V_{VS} ≥ $V_{VSLV(UP)}$	650	727	788.7	mV
		I_{VSL} = -666 µA, V_{VS} ≥ $V_{VSLV(UP)}$	570	600	651.8	mV
		I_{VSL} = -1.25 mA, V_{VS} ≥ $V_{VSLV(UP)}$	537.2	570	612	mV
$V_{CST(MAX)\_LV}$	Peak-power threshold on CS pin in LV mode	I_{VSL} = 0 mA, V_{VS} ≤ $V_{VSLV(LR)}$	593.7	628	663.9	mV
		I_{VSL} = -666 µA, V_{VS} ≤ $V_{VSLV(LR)}$	546	570	609.5	mV
		I_{VSL} = -1.25 mA, V_{VS} ≤ $V_{VSLV(LR)}$	511.2	540	584.7	mV
$V_{CST(MIN)}$	Minimum CS threshold voltage	V_{CS} increasing, I_{FB} = -85 µA	120.7	153	200.1	mV
K_{LC}	Line-compensation current ratio	I_{VSL} = -1.25 mA, I_{VSL} / current out of CS pin	21.6	25	29	A/A
$V_{CST(EMI)}$ [1]	EMI dithering magnitude on CS pin out of LV mode	$(V_{BUR}$ / $K_{BUR-CST})$ < V_{CST} < $V_{CST(MAX)}$, I_{VSL} < -646 µA, V_{VS} ≥ $V_{VSLV(UP)}$	78.4	96	113.6	mV
$V_{CST(EMI)\_LV}$ [1]	EMI dithering magnitude on CS pin in LV mode	$(V_{BUR}$ / $K_{BUR-CST})$ < V_{CST} < $V_{CST(MAX)}$, I_{VSL} < -646 µA, V_{VS} ≤ $V_{VSLV(LR)}$	29.3	36	42.7	mV
$V_{CST(SM1)}$	CS threshold voltage in SM1 startup mode	V_{VS} < $V_{VS(SM1)}$	177.5	200	222.9	mV
$V_{CST(SM2)}$	CS threshold voltage in SM2 startup mode	V_{VS} < $V_{VS(SM2)}$	470.4	500	531.4	mV
t_{CSLEB}	Leading-edge-blanking time	V_{SET} = 5 V, V_{CS} = 1 V	171.2	190	216.1	ns
		V_{SET} = 0 V, V_{CS} = 1 V	94.4	108	125	ns
$t_{D(CS)}$	Propagation delay of CS comparator high to PWML 90 % low	V_{CS} step from 0 V to 1 V	10	26	34.8	ns
f_{DITHER} [1]	EMI dithering frequency on CS pin	$(V_{BUR}$ / $K_{BUR-CST})$ < V_{CST} < $V_{CST(OPP)}$, I_{VSL} < -646 µA	20	23	27	kHz
BUR INPUT and Low-power MODE						
$K_{BUR-CST}$	Ratio of V_{BUR} to V_{CST}	V_{BUR} between 0.7 V and 2.4 V	3.82	3.98	4.09	V/V
$I_{BUR(LPM)}$	Bias source current of V_{BUR} offset in LPM		2.09	2.65	3.16	µA
$I_{BUR(AAM)}$	Bias sink current of V_{BUR} offset in AAM	V_{CST} > V_{BUR} / $K_{BUR-CST}$	3.76	4.85	5.81	µA
$f_{BUR(UP1)}$	First upper threshold of burst frequency in ABM		30.7	34.4	38.5	kHz
$f_{BUR(UP2)}$	Second upper threshold of burst frequency in ABM	V_{VS} = 2.2 V	41.8	51.2	58.9	kHz
$f_{BUR(LR)}$	Lower threshold of burst frequency in ABM		21.3	24.5	28.1	kHz
f_{LPM}	Burst frequency in low-power mode		23.3	25	26.9	kHz
IPC INPUT and SBP2 MODE						
$V_{CST\_IPC(UP)}$	Highest programmable V_{CST} range of SBP2 by IPC pin	V_{IPC} = 5 V	373.8	405	438.5	mV
K_{IPC}	Ratio of the programmable IPC voltage to V_{CST}	V_{IPC} between 1.8 V and 3.8 V	59.3	64	68.4	mV/V
$V_{CST\_IPC(LR)}$	Lowest programmable V_{CST} range of SBP2 by IPC pin	V_{IPC} = 1 V	247.5	273	307.7	mV

Product Folder Links: *UCC28782*

Unless otherwise stated: V_{VDD} = 20 V, V_{BIN} = 20 V, R_{RDM} = 115 kΩ, R_{RTZ} = 140 kΩ, V_{BUR} = 1.2 V, V_{SET} = 0 V, R_{NTC} = 50 kΩ, V_{VS} = 4 V, V_{SWS} = 0 V, I_{FB} = 0 µA, C_{PWML} = 0 pF, C_{PWMH} = 0 pF, C_{REF} = 0.22 µF, C_{P13} = 1 µF, and -40ºC < T_J = T_A < 125ºC

PARAMETER		TEST CONDITIONS	MIN	TYP	MAX	UNIT
$V_{CST\_IPC(MIN)}$	Minimum V_{CST} of SBP2 by grounding IPC pin	V_{IPC} = 0 V	128.1	154	191.5	mV
$I_{IPC(SBP2)}$	Bias source current of V_{IPC} offset in SBP2	I_{FB} = -85 µA	40.7	49	55.7	µA
$f_{SBP2(UP)}$	Upper threshold of burst frequency in SBP2		6	8.5	13.4	kHz
$f_{SBP2(LR)}$	Lower threshold of burst frequency in SBP2	V_{IPC} = 2 V	1	1.7	2	kHz
RUN						
V_{RUNH}	RUN pin high-level	I_{RUN} = -0.2 mA	4.6	4.78	5	V
V_{RUNL}	RUN pin low-level, for UCC28782A only	I_{RUN} = 1 mA	0.23	0.25	0.3	V
V_{RUNL}	RUN pin low-level, for UCC28782AD, UCC28782BDL, and UCC28782CD only	I_{RUN} = 1 mA	0.1	0.25	0.3	V
$I_{SRC(RUN)}$	RUN peak source current	V_{RUN} = 2.3 V	33	44	52	mA
		V_{RUN} = 3 V	14	20	25	mA
$t_{R(RUN)}$	Turn-on rise time of RUN, from 0 V to 2.5 V	C_{RUN} = 22 nF, V_{RUN} from 0 V to 2.5 V	0.4	0.79	1	µs
$t_{F(RUN)}$	Turn-off fall time of RUN, 90 % to 10 %	C_{RUN} = 10 pF		20	32	ns
PWML						
V_{PWMLH}	PWML pin high-level	I_{PWML} = -1 mA	12.1	12.85	13.6	V
V_{PWMLL}	PWML pin low-level	I_{PWML} = 1 mA		0.002	0.1	V
$I_{SRC(PWML)}$ [1]	PWML peak source current	V_{PWML} = 0 V	0.25	0.5	0.8	A
$I_{SNK(PWML)}$ [1]	PWML peak sink current	V_{PWML} = 13 V	1.2	1.9	2.8	A
$R_{SRC(PWML)}$	PWML pull-up resistance	I_{PWML} = -20 mA	3.1	4.3	6.1	Ω
$R_{SNK(PWML)}$	PWML pull-down resistance	I_{PWML} = 20 mA	0.5	1.1	1.9	Ω
$t_{R(PWML)}$	Turn-on rise time of PWML, 10 % to 90 %	C_{PWML} = 1.5 nF		30	53	ns
$t_{F(PWML)}$	Turn-off fall time of PWML, 90 % to 10 %	C_{PWML} = 1.5 nF		9	20	ns
$t_{D(RUN-PWML)}$	Delay from RUN high to PWML high	V_{S13} > 11 V	1.92	4.7	7.43	µs
$t_{ON(MIN)}$	Minimum on-time of PWML in LPM, for UCC28782A only	V_{SET} = 5 V, I_{FB} = -85 µA, V_{CS} = 1 V	68	105	172.5	ns
$t_{ON(MIN)}$	Minimum on-time of PWML in LPM, for UCC28782AD, UCC28782BDL, and UCC28782CD only	V_{SET} = 5 V, I_{FB} = -85 µA, V_{CS} = 1 V	68	105	175	ns
PWMH						
V_{PWMHH}	PWMH pin high-level	I_{PWMH} = -1 mA	4.39	4.66	4.83	V
V_{PWMHL}	PWMH pin low-level, for UCC28782A only	I_{PWMH} = 1 mA	0.19	0.198	0.21	V
V_{PWMHL}	PWMH pin low-level, for UCC28782AD, UCC28782BDL, and UCC28782CD only	I_{PWMH} = 1 mA	0.1	0.198	0.21	V
$I_{SRC(PWMH)}$	PWMH peak source current	V_{PWMH} = 2.5 V	16.5	21	26.2	mA
		V_{PWMH} = 3.5 V	3.8	6	7.6	mA
$t_{R(PWMH)}$	Turn-on rise time of PWMH, 10 % to 90 %, for UCC28782A only	C_{PWMH} = 10 pF		8	20	ns
$t_{R(PWMH)}$	Turn-on rise time of PWMH, 10 % to 90 %, for UCC28782AD, UCC28782BDL, and UCC28782CD only	C_{PWMH} = 10 pF		8	24	ns
$t_{F(PWMH)}$	Turn-off fall time of PWMH, 90 % to 10 %	C_{PWMH} = 10 pF		22	29	ns
$t_{D(VS-PWMH)}$	Dead time between VS high and PWMH 10 % high		10	18	28	ns
PROTECTION						
V_{OVP}	Over-voltage threshold	V_{VS} increasing	4.4	4.55	4.67	V
V_{OCP}	Over-current threshold	V_{CS} increasing	1.14	1.22	1.27	V

Product Folder Links: *UCC28782*

Unless otherwise stated: V_{VDD} = 20 V, V_{BIN} = 20 V, R_{RDM} = 115 kΩ, R_{RTZ} = 140 kΩ, V_{BUR} = 1.2 V, V_{SET} = 0 V, R_{NTC} = 50 kΩ, V_{VS} = 4 V, V_{SWS} = 0 V, I_{FB} = 0 µA, C_{PWML} = 0 pF, C_{PWMH} = 0 pF, C_{REF} = 0.22 µF, C_{P13} = 1 µF, and -40ºC < T_J = T_A < 125ºC

PARAMETER		TEST CONDITIONS	MIN	TYP	MAX	UNIT
$K_{OPP-PPL}$	Ratio of over-power threshold to peak-power threshold	$V_{CST(OPP)}$ / $V_{CST(MAX)}$, and $V_{CST(OPP)\_LV}$ / $V_{CST(MAX)\_LV}$	0.72	0.75	0.78	V/V
$I_{VSL(RUN)}$	VS line-sense run current	Current out of VS pin increasing	313	365	408.6	µA
$I_{VSL(STOP)}$	VS line-sense stop current	Current out of VS pin decreasing	255	305	336.4	µA
K_{VSL}	VS line sense ratio	$I_{VSL(STOP)}$ / $I_{VSL(RUN)}$	0.72	0.836	0.9	A/A
$R_{RDM(TH)}$	R_{RDM} threshold for CS pin fault		35	55	70	kΩ
$T_{J(STOP)}$	Thermal-shutdown temperature	Internal junction temperature	125	162		°C
V_{BOVPTH}	Shut-down voltage of V_{VDD} for boost output OVP		21.5	25	28.2	V
V_{BOVPR}	Recovery voltage of V_{VDD} for boost output OVP		16.8	20	23.3	V
t_{OPP}	OPP fault timer, for UCC28782A only	I_{FB} = 0 A	133.3	164	201.1	ms
t_{OPP}	OPP fault timer, for UCC28782AD, UCC28782BDL, and UCC28782CD only	I_{FB} = 0 A	130	164	201.1	ms
t_{BO}	Brown-out detection delay time	I_{VSL} < $I_{VSL(STOP)}$	28.8	55	85.2	ms
t_{CSF1}	Maximum PWML on-time for detecting CS pin fault	V_{SET} = 5 V	1.6	2.05	2.5	µs
t_{CSF0}	Maximum PWML on-time for detecting CS pin fault	R_{RDM} < $R_{RDM(TH)}$ for V_{SET} = 0 V	0.85	1.05	1.27	µs
t_{FDR}	Fault reset delay timer, for UCC28782A only	OCP, OPP, OVP, SCP or CS pin fault	1.2	1.5	2.22	s
t_{FDR}	Fault reset delay timer, for UCC28782AD, UCC28782BDL, and UCC28782CD only	OCP, OPP, OVP, SCP or CS pin fault	1.2	1.5	2.25	s
FLT INPUT						
V_{NTCTH}	NTC shut-down voltage	FLT voltage decreasing	0.47	0.5	0.52	V
R_{NTCTH}	NTC shut-down resistance	R_{NTC} decreasing	8.9	9.91	11.18	kΩ
R_{NTCR}	NTC recovery resistance	R_{NTC} increasing	21.2	23	26.4	kΩ
I_{FLT}	Input bias current for V_{FLT} at V_{IOVPTH}	V_{FLT} = 4.5 V	-0.1	0	0.1	µA
V_{IOVPTH}	Shut-down voltage of input OVP	FLT voltage increasing	4.3	4.5	4.67	V
V_{IOVPR}	Hysteresis of input OVP	FLT voltage increasing	57.7	74	87	mV
$t_{FLT(NTC)}$	Delay time of NTC fault		14	50	100	µs
$t_{FLT(IOVP)}$	Delay time of input OVP fault		555	750	917	µs
V_{FLTZ}	Clamp voltage of FLT pin	I_{FLT} = 150 µA	5.08	5.5	5.61	V
RTZ INPUT						
K_{TZ}	t_Z compensation ratio	Ratio of t_Z at I_{VSL} = -200 µA to t_Z at I_{VSL} = -733 µA	1.27	1.41	1.54	s/s
$t_{Z(MAX)}$	Maximum programmable dead time from PWMH low to PWML high	R_{RTZ} = 280 kΩ, I_{VSL} = -1 mA, V_{SET} = 5 V	397.8	478	592.8	ns
$t_{Z(MIN)}$	Minimum programmable dead time from PWMH low to PWML high	R_{RTZ} = 78.4 kΩ, I_{VSL} = -1 mA, V_{SET} = 0 V	56.1	70	89.1	ns
t_Z	Dead time from PWMH low to PWML high	I_{VSL} = -200 µA	152.2	175	212.7	ns
		I_{VSL} = -450 µA	129.2	150	190	ns
		I_{VSL} = -733 µA	109.7	125	147.2	ns
SWS INPUT						
$V_{TH(SWS)}$	SWS zero voltage threshold	V_{SET} = 5 V	8.1	8.5	9.1	V
		V_{SET} = 0 V	3.7	4.04	4.4	V
$t_{D(SWS-PWML)}$	Time between SWS low to PWML 10 % high	V_{SWS} step from 5 V to 0 V	11.4	17	24.8	ns
FB INPUT						

Product Folder Links: *UCC28782*

Unless otherwise stated: V_{VDD} = 20 V, V_{BIN} = 20 V, R_{RDM} = 115 kΩ, R_{RTZ} = 140 kΩ, V_{BUR} = 1.2 V, V_{SET} = 0 V, R_{NTC} = 50 kΩ, V_{VS} = 4 V, V_{SWS} = 0 V, I_{FB} = 0 μA, C_{PWML} = 0 pF, C_{PWMH} = 0 pF, C_{REF} = 0.22 μF, C_{P13} = 1 μF, and -40°C < T_J = T_A < 125°C

PARAMETER		TEST CONDITIONS	MIN	TYP	MAX	UNIT
$I_{FB(SBP)}$	Maximum control FB current	I_{FB} increasing	64.2	75	87.1	μA
$V_{FB(REG)}$	Regulated FB voltage level		4.02	4.25	4.53	V
R_{FBI}	FB input resistance		7.5	8.3	9.6	kΩ
dI_{COMP}/dt[(1)]	Slope of internal ramp compensation current		0.192	0.214	0.236	A/s
I_{COMP}	Magnitude of internal ramp compensation current		4	6.75	8	μA
RDM INPUT						
$t_{DM(MAX)}$	Maximum PWMH width with maximum tuning, for UCC28782A only	V_{SWS} = 12 V	6.32	6.95	7.53	μs
$t_{DM(MAX)}$	Maximum PWMH width with maximum tuning, for UCC28782AD, UCC28782BDL, and UCC28782CD only	V_{SWS} = 12 V	6.0	6.95	7.53	μs
$t_{DM(MIN)}$	Minimum PWMH width with minimum tuning, for UCC28782A only	V_{SWS} = 0 V	3.11	3.43	3.77	μs
$t_{DM(MIN)}$	Minimum PWMH width with minimum tuning, for UCC28782AD, UCC28782BDL, and UCC28782CD only	V_{SWS} = 0 V	3.0	3.43	3.77	μs
XCD INPUT (for UCC28782AD, UCC28782BDL, and UCC28782CD only)						
$V_{XCD(LR)}$	XCD lower zero-crossing threshold		5.9	6.62	7.2	V
$V_{XCD(UP)}$	XCD upper zero-crossing threshold		6.8	7.5	7.9	V
$I_{XCD(0)}$	Leakage current in XCD wait state	V_{XCD} = 15 V		0.3	1.7	μA
$I_{XCD(1)}$	First-step XCD sense current	V_{XCD} = 15 V	0.32	0.4	0.46	mA
$I_{XCD(2)}$	Second-step XCD sense current	V_{XCD} = 15 V	0.61	0.775	0.91	mA
$I_{XCD(3)}$	Third-step XCD sense current	V_{XCD} = 15 V	0.73	1.15	1.6	mA
$I_{XCD(4)}$	Fourth-step XCD sense current	V_{XCD} = 15 V	1.2	1.53	1.81	mA
$I_{XCD(MAX)}$	Maximum XCD discharge current	V_{XCD} = 15 V	1.65	2	2.5	mA
$V_{XCD(OVP)}$	Clamping voltage for XCD OVP	I_{XCD} = 20 mA	23	26	30	V
$t_{XCD(STEP)}$	Dwell time for each XCD sense step, for UCC28782A only		10	12	14	ms
$t_{XCD(STEP)}$	Dwell time for each XCD sense step, for UCC28782AD, UCC28782BDL, and UCC28782CD only		9	12	14	ms
$t_{XCD(MAX)}$	Maximum XCD discharge time		230.4	300	373.3	ms
$t_{XCD(WAIT)}$	XCD wait time			700	1071	ms

(1)   Ensured by design, not tested in production

7.6 Typical Characteristics

V_{VDD} = 20V, R_{RDM} = 115 kΩ, R_{RTZ} = 140 kΩ, V_{SET} = 0 V, and T_J = T_A = 25 °C (unless otherwise noted)
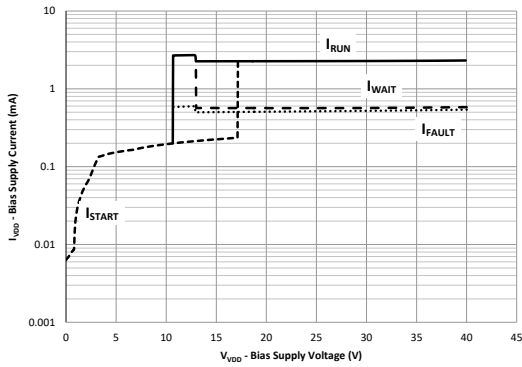
Figure 7-1. VDD Bias-Supply Current vs. VDD Bias-Supply Voltage
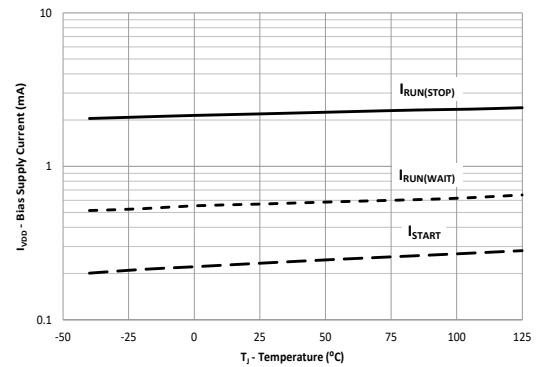

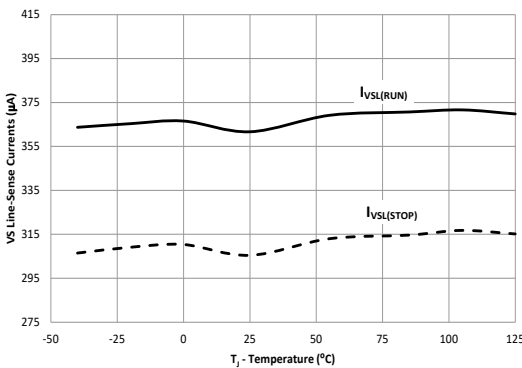Figure 7-2. VDD Bias-Supply Current vs. Temperature

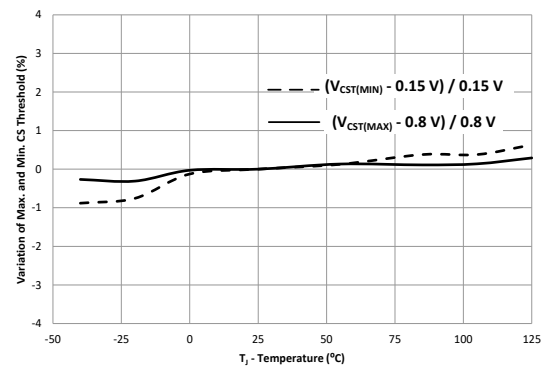Figure 7-3. VS Line-Sense Currents vs. Temperature

Figure 7-4. Percentage Variation of Maximum and Minimum CS Thresholds vs. Temperature
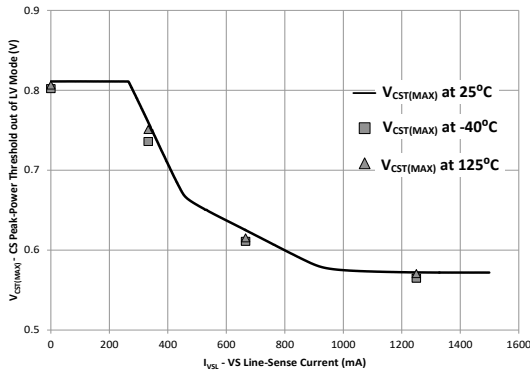

Figure 7-5. CS Peak-Power Threshold for V_{VS} > $V_{VSLV(UP)}$ vs. VS Line-Sense Currents
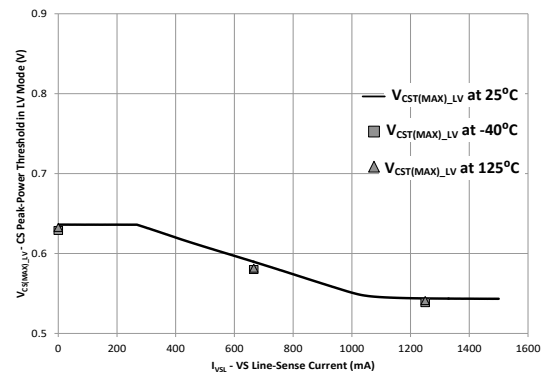

Figure 7-6. CS Peak-Power Threshold for V_{VS} < $V_{VSLV(LR)}$ vs. VS Line-Sense Currents
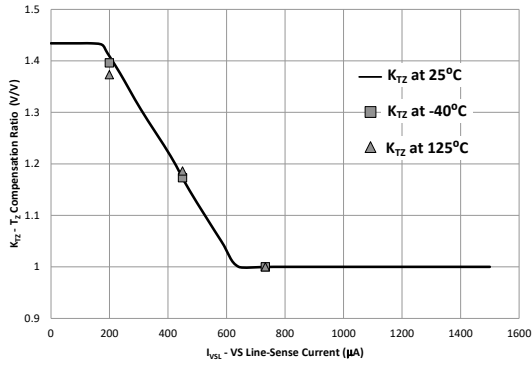
Product Folder Links: *UCC28782*

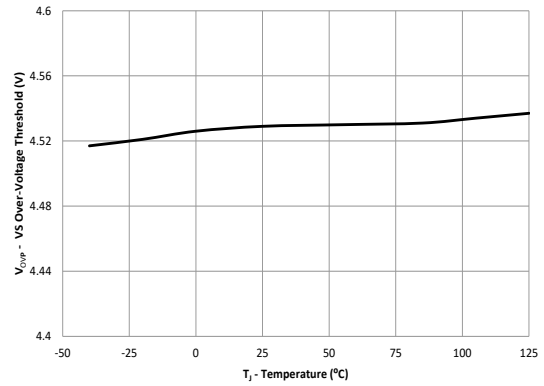Figure 7-7. t_Z Compensation Ratio (K_TZ) vs. VS Line-Sense Currents

Figure 7-8. VS Over-Voltage Threshold vs. Temperature

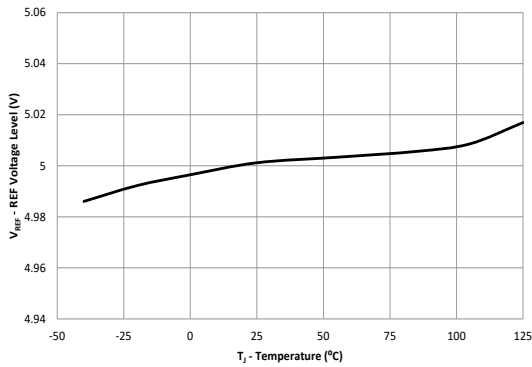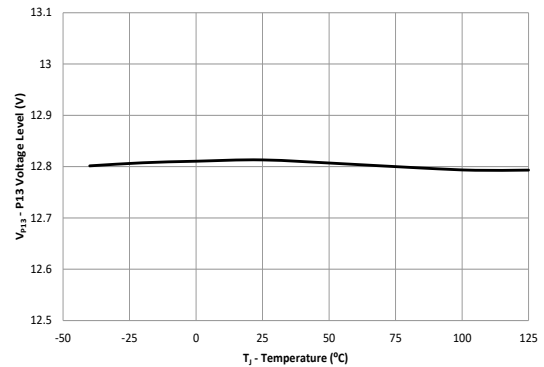Figure 7-9. REF Voltage vs. Temperature

Figure 7-10. P13 Voltage vs. Temperature
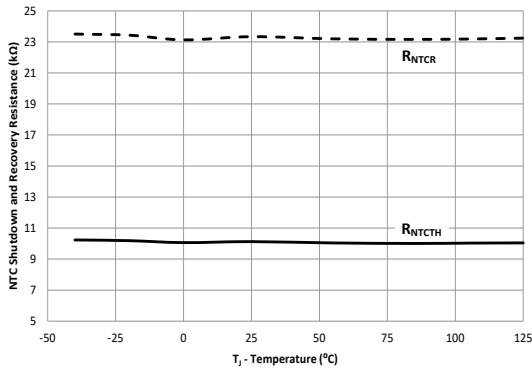
Figure 7-11. FLT OTP Thresholds vs. Junction Temperature

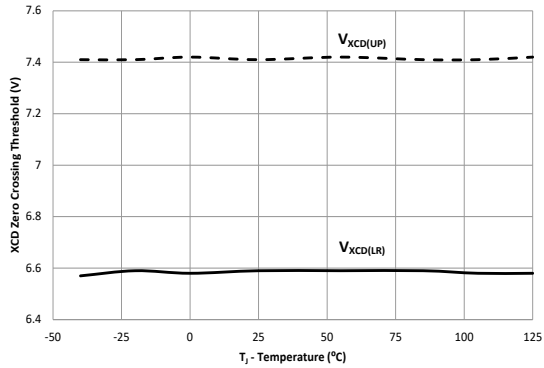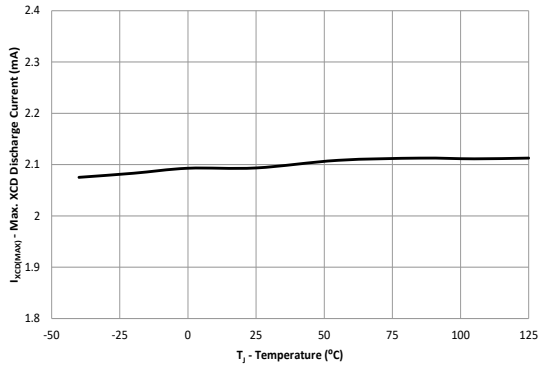Figure 7-12. XCD Thresholds vs. Junction Temperature

Product Folder Links: *UCC28782*

Figure 7-13. Max. XCD Discharge Current vs. Junction Temperature
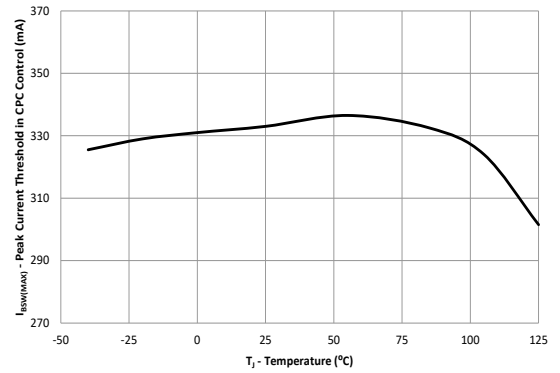
Figure 7-14. BSW Peak Current Thresholds vs. Junction Temperature

Product Folder Links: *UCC28782*

8 Detailed Description

8.1 Overview

The UCC28782 is a transition-mode (TM) active-clamp flyback (ACF) controller equipped with advanced control schemes to enable significant size reduction of passive components for higher power density and higher average efficiency. Its control law is optimized for Silicon (Si) and Gallium Nitride (GaN) power FETs in a half-bridge configuration and is capable of driving high-frequency AC/DC converters up to 1.5 MHz.

The zero-voltage switching (ZVS) control of the UCC28782 is capable of auto-tuning the on-time of a high-side clamp switch (Q_H) by using a unique lossless ZVS sensing network connected between the switch-node voltage (V_{SW}) and the SWS pin. The ACF controller is designed to adaptively achieve targeted full-ZVS or partial-ZVS conditions for the low-side main switch (Q_L) with minimum circulating energy over wide operating conditions. Auto-tuning eliminates the risk of losing ZVS due to component tolerance, temperature, and input/output voltage variations, since the Q_H on-time is corrected cycle-by-cycle.

Dead-times between PWML (controls Q_L) and PWMH (controls Q_H) are optimally adjusted to help minimize the circulating energy required for ZVS. Therefore, the overall system efficiency can be significantly improved and more consistent efficiency can be obtained in mass production of the soft-switching topology. The programming features of the RTZ, RDM, BUR, IPC, and SET pins provide rich flexibility to optimize the power stage efficiency across a range of output power and operating frequency levels.

The UCC28782 uses five different operating modes in steady state to maximize efficiency over wide load and line ranges. Adaptive amplitude modulation (AAM) adjusts the peak primary current at higher load levels. Adaptive burst mode (ABM) modulates the pulse count of each burst packet in the medium load range. Low power mode (LPM) reduces the peak primary current of each two-pulse burst packet in the light load range. Two stand-by power modes (SBP1 and SBP2) minimize the power loss during very light load and no load conditions. During the system transient events such as the output load step down and output voltage ramp down, V_{VDD} may be reduced close to the 10.5-V UVLO-off threshold, so the survival mode is triggered to maintain V_{VDD} above 13 V and to reduce the size of the hold-up VDD capacitor.

The frequency-dither function is active in AAM to help reduce conducted-EMI noise and allow EMI filter size reduction. The 23-kHz dithering pattern and magnitude are designed to avoid audible noise, minimize efficiency influence, and desensitize the effect of the output voltage feedback loop response effect on the EMI attenuation. The two-level dither magnitude is adjusted automatically based on the output voltage level, so dither-induced output ripple is reduced at lower output voltages to meet more stringent ripple requirements. The dither function at low line can be programmed into disable mode based on the brown-in voltage setting, so the option provides design flexibility to balance the worst-case low-line efficiency and EMI. The dither fading feature smoothly disables the dither signal when the output load is close to the transition point between AAM and ABM. The 23-kHz dither frequency is high enough to allow a higher control-loop bandwidth for improved load transient response without distorting the dither signal and impairing EMI.

The unique burst mode control in ABM, LPM, and two SBP modes maximizes the light-load efficiency of the ACF power stage while avoiding the concerns of conventional burst operation - such as high output ripple and audible noise. The internal ramp compensation can stabilize the burst control loop without an additional compensation network. The burst control provides an enable signal through the RUN pin to dynamically manage the static current of the half-bridge driver and also adaptively disables the drive signal of Q_H. The internal drivers of RUN and PWMH can supply and disconnect the 5-V bias voltage to a digital isolator or a level-shifter through a small-signal diode. The disconnect switch inside the S13 pin can directly control the 13-V bias voltage to a low-side GaN driver. These power management functions with RUN, PWMH, and S13 pins can be used to minimize the quiescent power consumed by those devices during burst off time, further improving the converter's light-load efficiency and reducing its stand-by power.

The S13 and IPC pins of the UCC28782 can be adapted to manage an upstream PFC stage to maximize the light-load efficiency of higher power USB-PD adapters. The S13 pin can supply a 13-V bias voltage to the PFC controller whenever the ACF controller is in the run state. The pin disconnects the bias voltage during the wait states of the burst mode operation. When the burst frequency is reduced in very light load conditions, the bias voltage will decay below UVLO and shut down PFC controller, so the power loss from PFC can be eliminated. When ACF operates at 5-V and 9-V output levels, the IPC pin can control the gate of an external small signal

MOSFET to pull down on the COMP pin of the PFC controller. When the power factor requirement is not needed for the low-power output rails of USB-PD adapters, disabling the PFC converter and controller improves the average efficiency and standby power significantly.

The PWML output is a strong driver for a Si power MOSFET with high capacitive loading, a GaN-based gate injection transistor (GIT) with continuous on-state current, or a GaN power IC with logic input. The maximum voltage level of PWML is clamped at 13 V to balance the conduction loss reduction and gate charge loss of Si MOSFET. A dedicated driver ground return pin (PGND) minimizes the parasitic impedance and noise coupling of the PWML gate-drive loop to achieve faster switching speed and reduced turn-off loss of Q_L. The short 15-ns propagation delay and narrow 110-ns minimum on-time enable more accurate ZVS control and higher switching frequency operation.

Controller bias power over a wide output voltage range is simplified with the integrated boost regulator of the UCC28782 using a single auxiliary winding on the primary side. The boost conversion mode provides an 18.5-V regulation level for the VDD pin from the rectified auxiliary-winding voltage at the BIN pin. Compared to the commonly-used high-voltage linear regulator plus multiple auxiliary windings, the boost-regulator power consumption, component footprint, and thermal stress can be greatly reduced for a higher power-density design. The boost switch, regulator control loop, and cycle-by-cycle robust protections are fully integrated. The boost switch node pin (BSW) and the dedicated regulator ground return pin (BGND) interface with a small external boost inductor, a boost schottky diode, and filter capacitors needed to form a tight switching loop.

During initial power up or VDD restart, the regulator is disabled and ACF stops switching, so UCC28782 starts up the VDD supply voltage with an external high-voltage depletion-mode MOSFET between the ACF switch node and the SWS pin. Fast startup is achieved with low stand-by power overhead, compared with using the conventional high-voltage startup resistance to VDD. Moreover, the P13 pin biases the gate of the depletion-mode FET to also allow this MOSFET to be used in lossless ZVS-sensing. This arrangement avoids additional sensing devices.

The enhanced switching control of UCC28782 mitigates excessive drain-to-source voltage stress on a synchronous rectifier (SR) caused by over-charged clamping capacitor voltage or temporary continuous conduction mode (CCM), so the power loss of an SR snubber can be reduced for higher efficiency. During output voltage ramp-down and LPM-to-ABM transition events, a unique PWMH on-time control extends the Q_H on-time momentarily. This control helps to avoid the case of Q_H being turned off during an instant where a large voltage-balancing negative current is flowing through Q_H to equalize an over-charged clamp capacitor voltage closer to the reflected output voltage. Additional PWML timing controls can avoid premature Q_L turn-on before the magnetizing current reaches to zero through an improved zero-crossing detection (ZCD) scheme of the VS pin.

The UCC28782 also integrates more robust protection features tailored to maximize the system reliability and safety. These features include active X-capacitor discharge, internal soft start, brown in/out, output over-voltage (OVP), input line over-voltage (IOVP), output over-power (OPP), system over-temperature (OTP), switch over-current (OCP), output short-circuit protection (SCP), and pin faults. The controller provides both auto-recovery and latch-off response options for OVP, OPP, OTP, OCP, and SCP faults.

The X-capacitor discharge function can actively discharge the residual voltage on X2 safety capacitors to a safe level after AC-line voltage removal is detected through the XCD pins of UCC28782 and its external sensing circuit. If the AC-line voltage recovers within 2 seconds after the line removal, the controller will reset the fault state immediately and will attempt to restart without waiting to fully discharge the bulk input capacitor or VDD capacitor. Grounding the two XCD pins disables this function and eliminates the sensing circuit. Unlike other conventional flyback controllers, UCC28782 provides the design flexibility of using the X-capacitor discharge function based on application power level as it is decoupled from VDD startup and brown-in/out detection functions. Since those two functions are implemented on the SWS and VS pins, respectively, UCC28782 maintains the two functions even when the XCD-related components are fully removed.

8.2 Functional Block Diagram

Copyright © 2019, Texas Instruments Incorporated

Product Folder Links: *UCC28782*
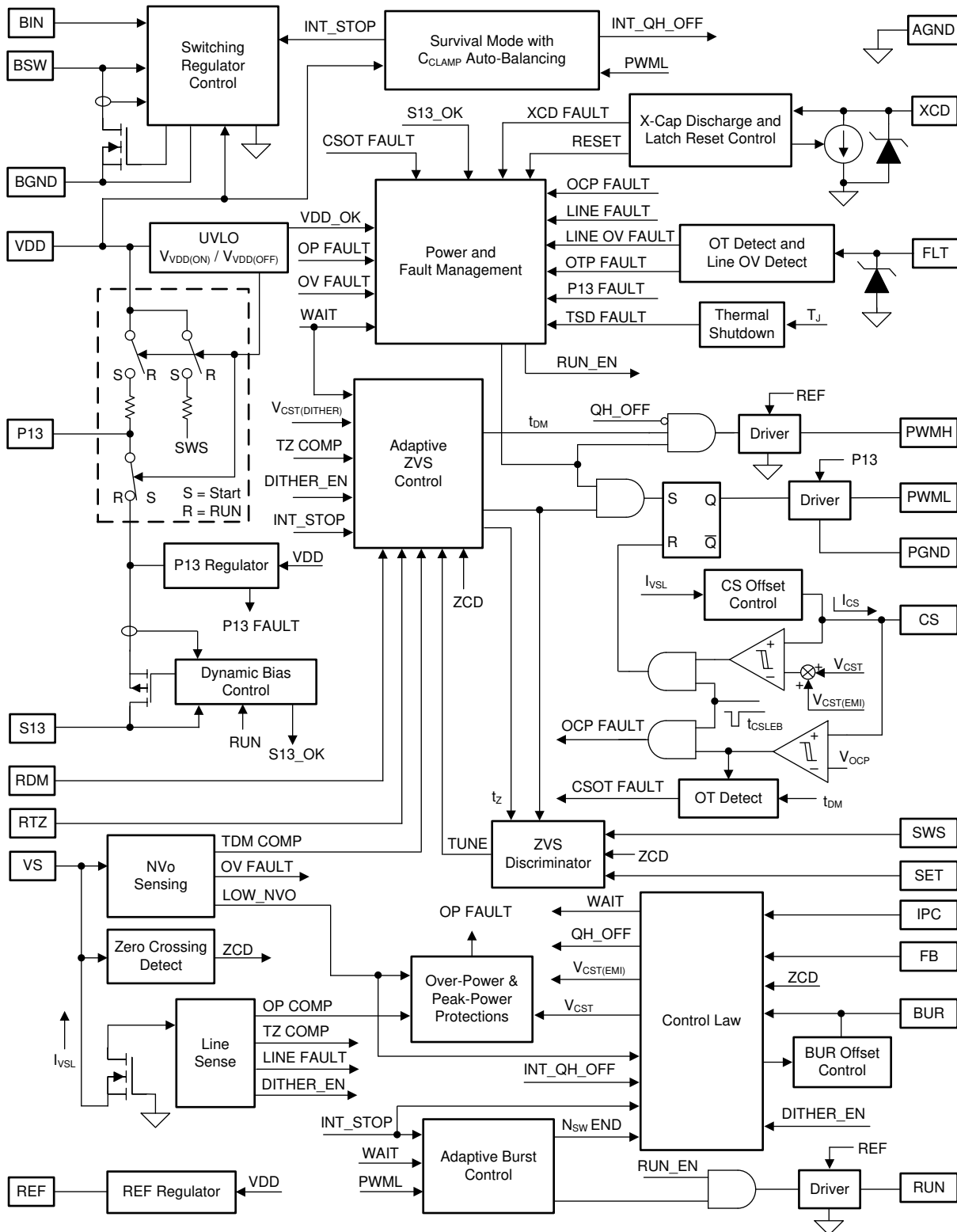
8.3 Detailed Pin Description

8.3.1 BUR Pin (Programmable Burst Mode)

The voltage at the BUR pin (V_{BUR}) sets a target peak current-sense threshold at the CS pin ($V_{CST(BUR)}$) which programs the onset of adaptive burst mode (ABM). V_{BUR} also determines the clamped peak current level of switching cycles in each burst packet. When V_{BUR} is set higher, ABM will start at heavier output load conditions with higher peak primary current, so the benefit is higher light-load efficiency but the side effect is larger burst-mode output voltage ripple. Therefore, 50% to 60% of output load at high line is the recommended highest load condition to enter ABM ($I_{O(BUR)}$) for both Si and GaN-based ACF designs.

The relationship between V_{BUR} and $V_{CST(BUR)}$ is a constant gain of $K_{BUR-CST}$, so targeting $V_{CST(BUR)}$ just requires properly selecting the resistor divider on the BUR pin formed by R_{BUR1} and R_{BUR2}. V_{BUR} should be set between 0.7 V and 2.4 V, which constitute internal limits. If V_{BUR} is less than 0.7 V, $V_{CST(BUR)}$ holds at 0.7 V / $K_{BUR-CST}$. If V_{BUR} is higher than 2.4 V, $V_{CST(BUR)}$ holds at 2.4 V / $K_{BUR-CST}$. Targeting an excessively low or high percentage of load for entering ABM will engage one of these internal limits.

$$R_{BUR2} = \frac{R_{BUR1}K_{BUR-CST}V_{CST(BUR)}}{V_{REF} - K_{BUR-CST}V_{CST(BUR)}} = \frac{4 \times R_{BUR1}V_{CST(BUR)}}{5V - 4 \times V_{CST(BUR)}}$$

(1)

In order to enhance the mode transition between ABM and LPM, a programmable offset voltage ($\Delta V_{BUR(LPM)}$) is generated on top of the V_{BUR} setting in ABM through an internal 2.7-µA current source ($I_{BUR(LPM)}$), as shown in Figure 8-1. In ABM, V_{BUR} is set through the resistor voltage divider to fulfill the target average efficiency. On transition from ABM to LPM, $I_{BUR(LPM)}$ is enabled in LPM and flows out of the BUR pin, so $\Delta V_{BUR(LPM)}$ can be programmed based on the Thevenin resistance on the BUR pin, which can be expressed as

$$\Delta V_{BUR(LPM)} = I_{BUR(LPM)}(R_{BUR1}//R_{BUR2})$$

(2)
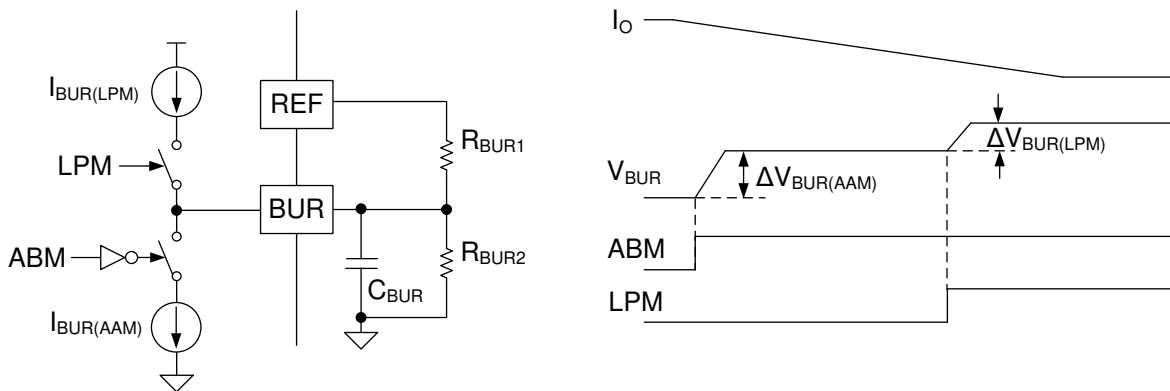
Copyright © 2019, Texas Instruments Incorporated

Figure 8-1. Hysteresis Voltage Generation on BUR Pin

When V_{BUR} steps higher on transition into LPM, the initial peak magnetizing current in LPM is increased with larger energy per switching cycle in each burst packet. This increases the output voltage which forces higher feedback current to restore regulation. Higher feedback current causes UCC28782 to stay in LPM, forming a hysteresis effect. If $\Delta V_{BUR(LPM)}$ is designed too small, it is possible that mode toggling between LPM and ABM can occur resulting in audible noise. For that situation, $\Delta V_{BUR(LPM)}$ greater than 100 mV is recommended.

To minimize the effects of external noise coupling on V_{BUR}, a filter capacitor on the BUR pin (C_{BUR}) may be needed. C_{BUR} needs to be properly designed to minimize the delay in generating ΔV_{BUR} during mode transitions. It is recommended that C_{BUR} should be sized small enough to ensure $\Delta V_{BUR(LPM)}$ settles within 40 µs, corresponding to the burst frequency of 25 kHz in LPM (f_{LPM}). Based on three RC time constants,

representing 95% of a settled steady-state value from a step response, the design guide for C_{BUR} is expressed as

$$C_{BUR} \leq 40\mu s \times \frac{R_{BUR1} + R_{BUR2}}{3R_{BUR1}R_{BUR2}}$$

(3)

In order to enhance the mode transition between ABM and AAM, a programmable offset voltage ($\Delta V_{BUR(AAM)}$) is generated to lower the V_{BUR} with an internal 5-µA pull-down current ($I_{BUR(AAM)}$), as shown in Figure 8-1. After transition from ABM to AAM, $I_{BUR(AAM)}$ is enabled in AAM and flows into the BUR pin, so $\Delta V_{BUR(AAM)}$ is also programmed based on the Thevenin resistance on the BUR pin, which can be expressed as

$$\Delta V_{BUR(AAM)} = I_{BUR(AAM)}(R_{BUR1}//R_{BUR2})$$

(4)

When V_{BUR} reduces after transition to AAM, the initial peak magnetizing current in AAM is reduced with less energy per switching cycle, which forces UCC28782 to stay in AAM. If $\Delta V_{BUR(AAM)}$ is too small, it is possible that either mode toggling between ABM and AAM or low-frequency ABM burst packets less than 20 kHz can occur and result in audible noise concern. For that situation, $\Delta V_{BUR(AAM)}$ greater than 150 mV is recommended. In some power stage designs, LPM in hard switching condition may cover a wider output load current range, so the light-load efficiency in LPM may be lower than ABM with ZVS condition. Besides, the ABM-to-AAM mode transition may be affected potentially when the load current condition of LPM-to-ABM transition is too close to the load current condition of ABM-AAM transition.

In order to narrow down the output load current range in LPM, lower $V_{BUR(ABM)}$, smaller $\Delta V_{BUR(LPM)}$, larger R_{OPP}, and smaller C_{CS} help to reduce the peak magnetizing current in LPM. If the LPM energy needs to be further reduced but V_{BUR} in AAM is limited by the 0.7-V minimum programmable level, the optional application circuit in Figure 8-2 can be considered. When the output load current is reduced, duty cycle of each burst packet becomes smaller, so as the duty cycle of RUN-pin voltage. C_{BUR} is discharged by the RUN driver through the small-signal diode (D_{BUR}) and the current limit resistor (R_{RUN}). Proper selection of R_{RUN} value can further reduce $V_{BUR(ABM)}$ when the load current is reduced close to the transition point from ABM to LPM. One example BUR-pin setting is R_{BUR1} = 182 kΩ, R_{BUR2} = 37.4 kΩ, C_{BUR} = 330 pF, and R_{RUN} = 20 kΩ.
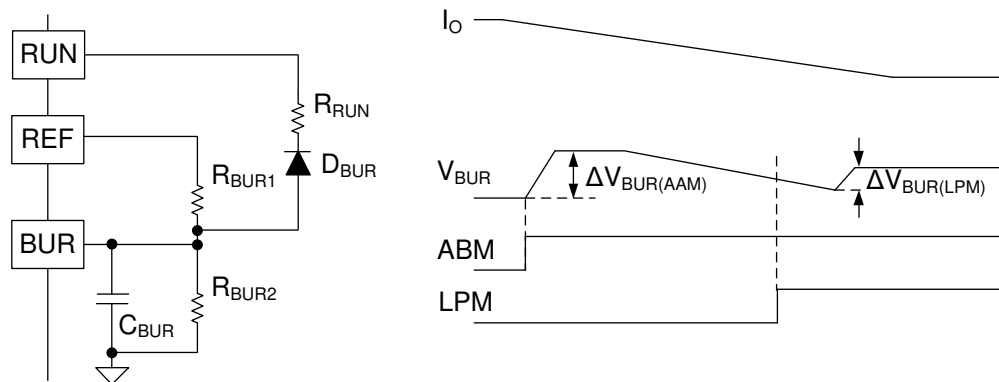

Figure 8-2. Optional Application Circuit to Reduce V_{BUR} in LPM

8.3.2 FB Pin (Feedback Pin)

The FB pin usually connects to the collector of an optocoupler output transistor through an external current-limiting resistor (R_{FB}). A maximum of 20 kΩ for R_{FB} is recommended. The feedback network of UCC28782 is shown in Figure 8-3. A high-quality ceramic by-pass capacitor between FB pin and REF pin (C_{FB}) is required for decoupling I_{FB} from switching noise interference. A minimum of 220 pF is recommended for C_{FB} . An internal 8-kΩ resistor (R_{FBI}) at the FB pin in conjunction with the external C_{FB} forms an effective low-pass filter. Section 9 provides a detailed design guide on the secondary-side compensation network of V_O feedback loop, to improve the load transient response and also limit the I_{FB} ripple of ABM mode within the recommended range.
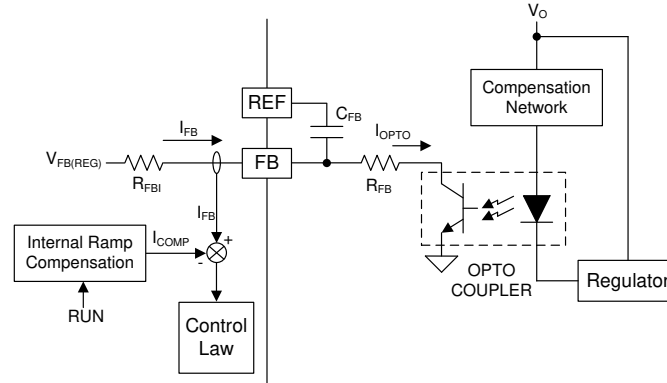
Copyright © 2019, Texas Instruments Incorporated

Figure 8-3. External Feedback Network Connected to the FB Pin

Depending on the operating mode, the controller interprets the current flowing out of the FB pin (I_{FB}) to regulate the output voltage. For AAM and LPM modes based on peak current control, I_{FB} is converted into an internal peak current-sense threshold (V_{CST}) to modulate the amplitude of the current-sense signal on the CS pin. For example, when the output voltage (V_O) is lower than the regulation level set by the shunt regulator, the absolute current level of I_{FB} reduces, causing a higher V_{CST} to increase more power to the output load. In ABM, the burst control loop takes over the V_O regulation, where V_{CST} is clamped to $V_{CST(BUR)}$ and the ripple component of I_{FB} participates in the modulation of the burst off time.

Figure 8-4 illustrates the operating principle of the ABM. A burst of switching pulses raises the output voltage V_O which increases I_{FB}. At the end of the burst, the load current discharges the output capacitor, which decreases V_O and I_{FB}. UCC28782 injects a noise-free internal ramp compensation current (I_{COMP}) superimposed on I_{FB} in order to stabilize the ABM operation. When the RUN pin is high, I_{COMP} is reset to 0 µA. When the RUN pin goes low, I_{COMP} is gradually increased to 6 µA with a positive slope of 0.214 A/s. The summation of I_{FB} and I_{COMP} is compared with $I_{TH(FB)}$ to trigger the next burst event. The magnitude and sharp slope of I_{COMP} help to push switching ripple and high-frequency noise component of I_{OPTO} away from $I_{TH(FB)}$.
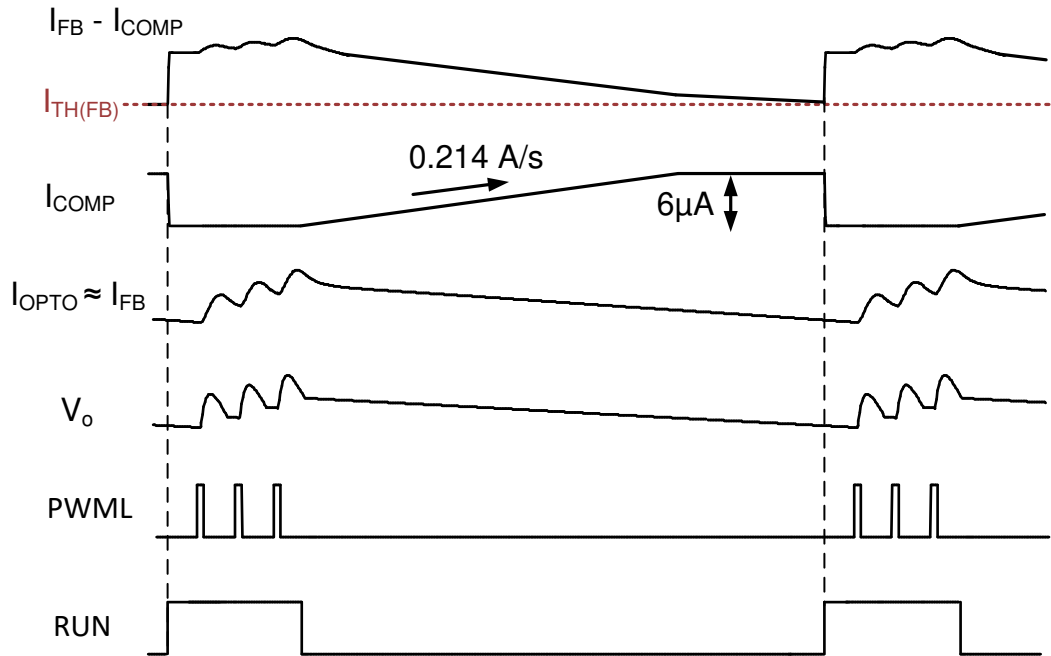
Copyright © 2019, Texas Instruments Incorporated

Figure 8-4. Concept of Burst Control with an Internal Ramp Compensation

8.3.3 REF Pin (Internal 5-V Bias)

The output of the internal 5-V regulator of the controller is connected to the REF pin. REF provides bias current to most of the functional blocks in the UCC28782. It requires a high-quality ceramic by-pass capacitor (C_{REF}) to AGND to decouple switching noise and to reduce the voltage transients as the controller transitions from wait state to run state. The minimum C_{REF} value is 0.22 µF, and a high quality dielectric material should be used, such as a X7R.

The output short-circuit current ($I_{S(REF)}$) of the REF regulator is self-limited to approximately 17 mA. 5-V bias is only available after the under-voltage lock-out (UVLO) circuit enables the operation of UCC28782 after V_{VDD} reaches $V_{VDD(ON)}$. This pin can be used to perform an external shutdown function. A small-signal switch can be used to pull this pin voltage below the power-good threshold of 4.5V, so the controller will stop switching, force a VDD restart cycle, and turn off the REF current.

8.3.4 VDD Pin (Device Bias Supply)

The VDD pin is the primary bias for the internal 5-V REF regulator, internal 13-V P13 regulator, other internal references, and the undervoltage lock-out (UVLO) circuit. As shown in Figure 8-5, the UVLO circuit connected to the VDD pin controls the internal power-path switches among VDD, P13, and SWS pins, in order to allow an external depletion-mode MOSFET (Q_S) to be able to perform both V_{VDD} startup and switch-node voltage (V_{SW}) sensing for ZVS control after startup. During startup, SWS and P13 pins are connected to VDD pin allowing Q_S to charge the VDD capacitor (C_{VDD}) from the V_{SW}. After VDD startup completes, the ZVS discriminator block and switching logic are enabled. Then, the transformer starts delivering energy to the output capacitor (C_O) every switching cycle, so both output voltage (V_O) and auxiliary winding voltage (V_{AUX}) increase. As V_{AUX} is high enough, the auxiliary winding will take over to power V_{VDD}. The UVLO circuit provides a turn-on threshold of $V_{VDD(ON)}$ at 17 V and turn-off threshold of $V_{VDD(OFF)}$ at 10.6 V. For fixed output voltage ACF converter designs, the wide V_{VDD} range can accommodate lower values of VDD capacitor (C_{VDD}) and support shorter power-on delays. For ACF designs requiring wide output voltage range, the integrated switching regulator converts the rectified V_{AUX} to an 18.5-V regulation level of V_{VDD}. Compared with the conventional bias approach with a high-voltage linear regulator and multiple auxiliary windings, the footprint and conversion efficiency of the integrated switching regulator are improved greatly. For a wide-output design using the bias regulator, a 10 to 15-µF ceramic VDD capacitor is recommended to hold up V_{VDD} during soft start and to provide decoupling for the regulator switching loop. Section 8.4.10 of this datasheet describes the details on the startup sequencing with the switching regulator.

For a fixed output voltage design, both the BIN and BSW pins should be shorted to BGND, and the rectified V_{AUX} is directly connected to the VDD pin. As V_{VDD} reaches $V_{VDD(ON)}$, the SWS pin is disconnected from the VDD pin by the internal power path switch, so the C_{VDD} size has to be sufficient to hold V_{VDD} higher than $V_{VDD(OFF)}$ until the positive auxiliary winding voltage is high enough to take over bias power delivery during V_O soft start. Therefore, the calculation of minimum capacitance ($C_{VDD(MIN)}$) needs to consider the discharging effect from the sink current of the UCC28782 during switching in its run state ($I_{RUN(SW)}$), the average operating current of driver (I_{DR}), and the average gate charge current of half-bridge FETs (I_{Qg}) throughout the longest time of V_O soft start ($t_{SS(MAX)}$).

$$C_{VDD(MIN)} = \frac{(I_{RUN(SW)} + I_{DR} + I_{Qg})t_{SS(MAX)}}{V_{VDD(ON)} - V_{VDD(OFF)}}$$

(5)

$t_{SS(MAX)}$ estimation should consider the averaged soft-start current ($I_{SEC(SS)}$) on the secondary side of ACF, the constant-current output load ($I_{O(SS)}$) (if any), maximum output capacitance ($C_{O(MAX)}$), and a 0.7-ms time-out potentially being triggered in the startup sequence. 1 ms is applied in the equation to be the worst-case condition of the 0.7-ms timer.

$$t_{SS(MAX)} = \frac{C_{O(MAX)}V_O}{I_{SEC(SS)} - I_{O(SS)}} + 1ms$$

(6)

During V_O soft start, V_{CST} reaches the maximum current threshold on the CS pin ($V_{CST(MAX)}$) , so $I_{SEC(SS)}$ at the minimum voltage of the input bulk capacitor ($V_{BULK(MIN)}$) can be approximated as:

$$I_{SEC(SS)} = \frac{N_{PS}V_{CST(MAX)}}{2R_{CS}} \frac{V_{BULK(MIN)}}{V_{BULK(MIN)} + N_{PS}(V_O + V_F)}$$

(7)

where R_{CS} is the current sense resistor, N_{PS} is primary-to-secondary turns ratio, and V_F is the forward voltage drop of the secondary rectifier.

8.3.5 P13 and SWS Pins

The P13 pin provides a regulated voltage to the gate of the depletion-mode MOSFET (Q_S), enabling Q_S to serve both V_{VDD} start-up and loss-less ZVS-sensing from the high-voltage switch node (V_{SW}) through the SWS pin. During V_{VDD} start-up, the UVLO circuit controls two power-path switches connecting SWS and P13 pins to VDD pin with two internal current-limit resistors (R_{DDS} and R_{DDH}), as shown in Figure 8-5. In this configuration, Q_S behaves as a current source to charge the VDD capacitor (C_{VDD}). R_{DDS} is set at 5 kΩ when $V_{VDD} < 1.8$ V to limit the maximum fault current under a VDD short-to-GND condition. R_{DDS} is reduced to 500 Ω when $V_{VDD} >$ 1.8 V to allow V_{VDD} to charge faster. The maximum charge current (I_{SWS}) is affected by R_{DDS}, the external series resistance (R_{SWS}) from SWS pin to Q_S, and the threshold voltage of Q_S ($V_{TH(Qs)}$). I_{SWS} can be calculated as

$$I_{SWS} = \frac{V_{TH(Qs)}}{R_{DDS} + R_{SWS}}$$

(8)
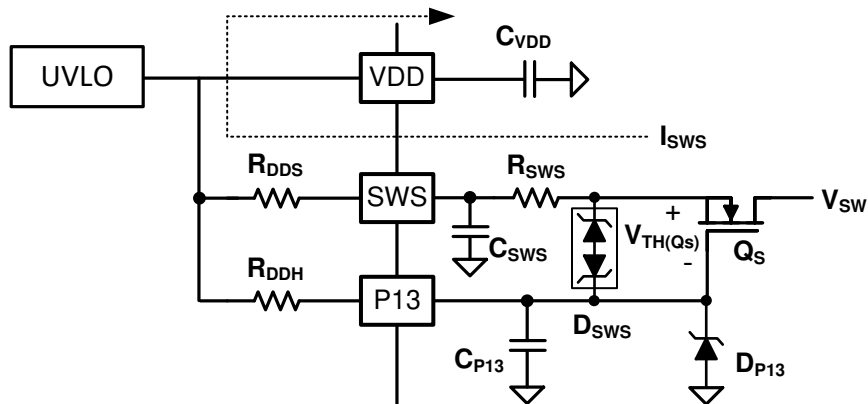
Copyright © 2019, Texas Instruments Incorporated

Figure 8-5. Operation of the VDD Startup Circuit

After V_{VDD} reaches $V_{VDD(ON)}$, the two power-path switches open the connections between SWS, P13, and VDD pins. At this point, a third power-path switch connects an internal 13-V regulator to the P13 pin for configuring Q_S to perform loss-less ZVS sensing. Since Q_S gate is fixed at 13 V, when the drain pin voltage of Q_S becomes higher than the sum of Q_S threshold voltage ($V_{TH(Qs)}$) and the 13-V gate voltage, Q_S turns off and the source pin voltage of Q_S can no longer follow the drain pin voltage change. This gate control method makes Q_S act as a high-voltage blocking device with the drain pin connected to V_{SW}. When the controller is switching, whenever V_{SW} is lower than 13 V, Q_S turns on and forces the source pin voltage to follow V_{SW}, becoming a replica of the V_{SW} waveform at the lower voltage level, as illustrated in Figure 8-6.

The limited window for monitoring the V_{SW} waveform is sufficient for ZVS control of the UCC28782, since the ZVS tuning threshold ($V_{TH(SWS)}$) is set at 8.5 V for $V_{SET} = 5$ V and set at 4 V for $V_{SET} = 0$ V. The 8.5-V threshold is the auto-tuning target of the internal adaptive ZVS control loop for realizing a partial-ZVS condition on an ACF using Si primary switches. On the other hand, performing full ZVS operation is more suitable for an ACF with GaN primary switches. Using a 4-V threshold helps to compensate for sensing delay between V_{SW} and the SWS pin.

Product Folder Links: *UCC28782*

The internal 13-V regulator requires a high-quality ceramic by-pass capacitor (C_{P13}) between the P13 pin and AGND pin for noise filtering and providing compensation to the P13 regulator. The minimum C_{P13} value is 1 μF and an X7R-type dielectric capacitor with 25-V rating or better is recommended. The controller enters a fault state if the P13 pin is open or shorted to AGND during V_{VDD} start-up, or if V_{P13} overshoot is higher than $V_{P13(OV)}$ of 15 V in run state. The output short-circuit current of P13 regulator ($I_{P13(MAX)}$) is self-limited to approximately 130 mA.

During AAM and ABM if the negative magnetizing current is large enough, a low-side GaN device may operate in the reverse conduction condition before it turns on each switching cycle, so V_{SW} may be around -5 V for a brief inteval and it appears on the SWS pin. The SWS-pin design of UCC28782 can sustain -6 V (continuous) and -10 V (transient) stress to enhance the robust operation of the GaN ACF power stage.

During this interval, Q_S is in the on-state and its body diode may conduct for a short time when the voltage drop across the on-state resistance of Q_S is high enough. The external R_{SWS} can limit the forward current flowing through the Q_S body diode, so the reverse recovery charge of the body diode can be significantly reduced. Too high of R_{SWS} value weakens the start-up charge current of C_{VDD} and results in a longer start-up time. R_{SWS} should be slightly higher than 500 Ω. A small back-to-back TVS across BSS126 gate-to-source should be added to protect the gate-to-source voltage from potential abnormal voltage stress. The TVS clamping voltage should be less than the BSS126 gate-to-source voltage rating but should not conduct below 15 V.

R_{SWS} and a ceramic capacitor (C_{SWS}) between the SWS pin and the bulk input capacitor ground form a small sensing delay to help the internal detection circuit to identify the ZVS characteristic correctly. The delay is to ensure that the ZCD detection on the VS pin happens earlier than the ZVS detection on the SWS pin, such that the ZVS control can auto-tune the PWMH on-time in the proper direction. The minimum value of C_{SWS} is 22 pF.
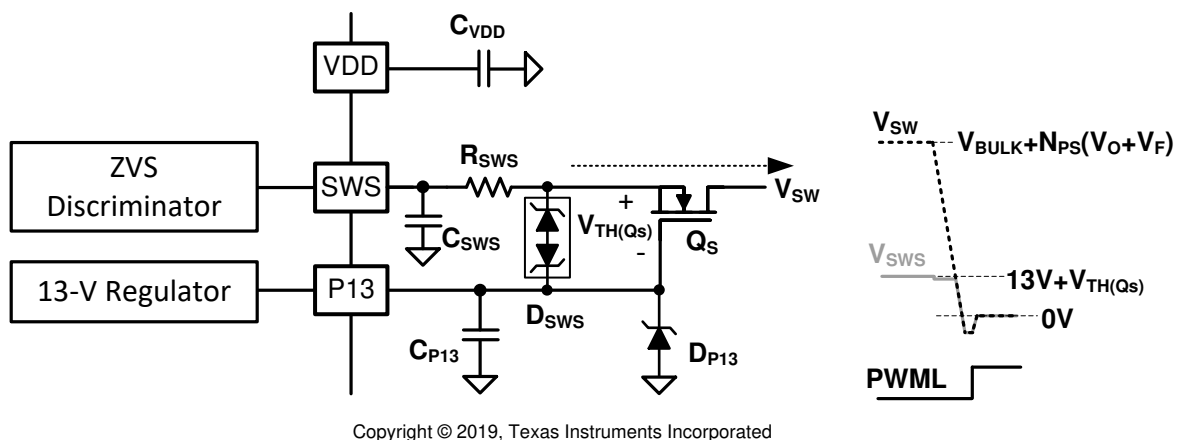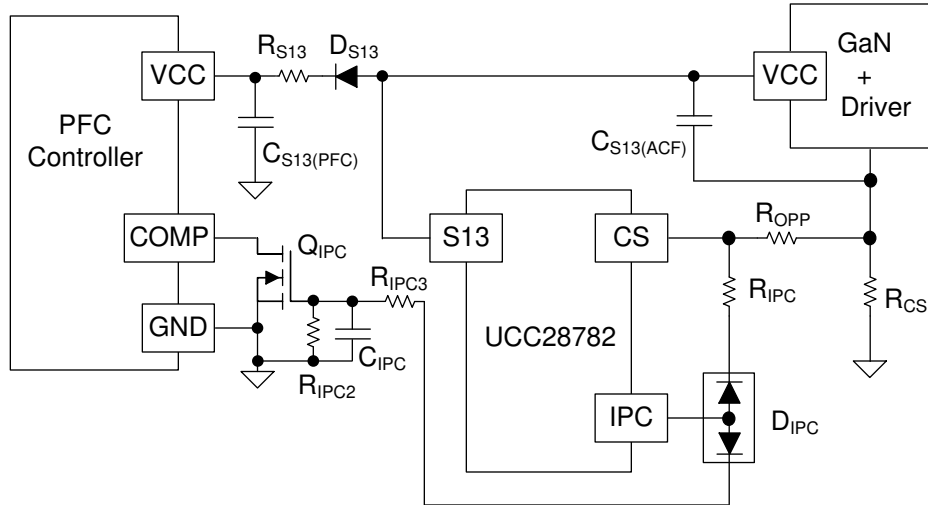

Copyright © 2019, Texas Instruments Incorporated

Figure 8-6. ZVS Sensing by Reusing the VDD Startup Circuit

8.3.6 S13 Pin

As shown in Figure 8-7, the S13 pin (switched 13-V rail) is used to perform bias-power management for a low-side GaN power IC of ACF, along with an example application where it also powers a PFC controller. This configuration enables to minimize the power-loss contribution to so-called "tiny-load" input power and stand-by power. One example of tiny-load input power requirement is that the input power must be less than 0.5 W with an output load of 0.25 W at 20 V.

S13 is sourced by P13 through an internal 2.8-Ω switch controlled by the RUN pin. Figure 8-8 illustrates the power-up sequence of the S13 pin. When RUN is high, the S13 decoupling capacitor is charged up to 13 V and the charge current is controlled by an internal soft-start current limiter. The S13-pin voltage must increase above the 10-V power-good threshold ($V_{S13(OK)}$) in order to initiate PWML switching of each burst cycle. When RUN is low, V_{S13} is discharged by the loading on S13. The power-on delay of the GaN power IC on the S13 pin must be less than 2 μs to be responsive to PWML. If not, the VDD or P13 pin may be a more suitable bias supply for devices with long power-on delay, but the wait-state power consumption will be compromised. A 22-nF ceramic capacitor as $C_{S13(ACF)}$ is recommended. If the S13 pin is not used, it can be connected to the P13 pin in order to eliminate the delay effect on PWML switching in every low-frequency burst cycle.

Copyright © 2019, Texas Instruments Incorporated

Figure 8-7. Power Management Function for the ACF GaN Power IC and PFC Controller
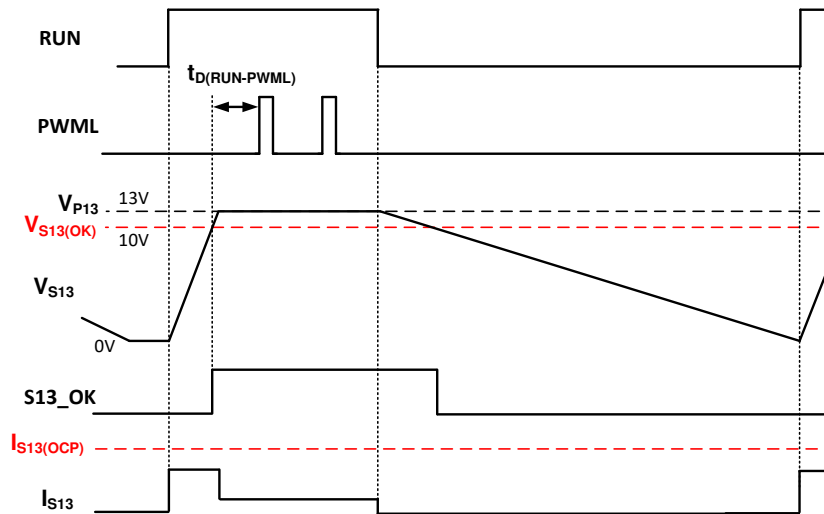
Copyright © 2019, Texas Instruments Incorporated

Figure 8-8. Power-up Sequence of the S13 Pin

When the S13 pin supplies both an ACF GaN power IC and a PFC controller at the same time, a low-voltage rectifier diode (D_{S13}) between the S13 pin and the PFC controller bias VCC pin is needed, so the local decoupling capacitor for each powered device can be separated. The decoupling capacitor of the PFC controller ($C_{S13(PFC)}$) is usually larger than the one for a GaN power IC, such that the bias voltage of the GaN power IC will discharge more quickly without affecting the PFC bias voltage and PFC output voltage regulation. If the S13 pin supplies a PFC controller only, the rectifier diode is not needed.

During start-up before VDD reaches the $V_{VDD(ON)}$ threshold, the S13 switch stays off, so the S13-pin loading will not consume any of the charging current of VDD capacitor flowing from SWS pin to VDD pin, thereby enabling a fast start-up sequence. Under this condition, the PFC controller will be off resulting in a lower PFC bus voltage below 400 V. For USB-PD adapter applications, the output voltage start-up condition is 5V/0A before the PD power path switch between ACF output and USB-C port is applied. Hence, there is no need for the PFC bus voltage to be immediately regulated to 400 V before ACF starts switching. Even for non USB-PD applications, the integrated bias regulator of UCC28782 is able to perform 18.5-V VDD regulation when the output voltage is at a very low level, so the S13 function still allows the PFC bus voltage to build up at the beginning of output voltage start-up.

8.3.7 IPC Pin (Intelligent Power Control Pin)

Under certain conditions, the IPC pin provides a 50-µA current from an internal source ($I_{IPC(SBP2)}$) which is controlled by logic as shown in Figure 8-9. The voltage on the VS pin is sampled during the demagnetization time to obtain an indication of the reflected output voltage (NVO). When the VS-pin voltage is lower than the 2.4-V lower LV mode threshold ($V_{VSLV(LR)}$), the LOW_NVO logic signal is pulled high, and the current source is enabled during the run state of all normal control modes (SBP1, SBP2, LPM, ABM, and AAM).

When the sampled VS-pin voltage is higher than the 2.5-V upper LV mode threshold ($V_{VSLV(UP)}$), the LOW_NVO logic signal becomes low. In the LOW_NVO = 0 V case, the 50-µA current source is enabled in the run state of SBP2 mode only.

To minimize stand-by power, the 50-µA source is always disabled during the wait state of any control mode. Additionally, if V_{VDD} falls lower than the 13-V survival-mode threshold, the INT_STOP logic signal is pulled high and the current source is disabled during survival mode operation, irrespective of the V_{VS} level.
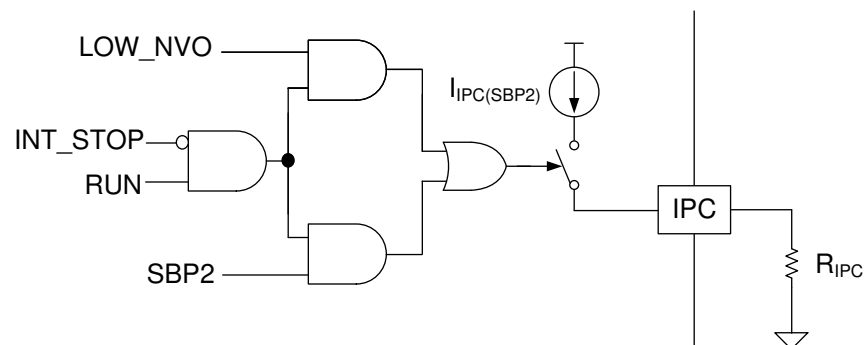
Copyright © 2019, Texas Instruments Incorporated

**Figure 8-9. Control Circuit Diagram to the IPC-Pin Current Source**

The multi-function IPC pin can be programmed to obtain one or more of the following benefits:

1. Reduction of input power for special light-load and stand-by conditions.
2. Improvement of light-load efficiency at lower output voltages, such as 5 V and 9 V.
3. Reduction of burst-mode output ripple at lower output voltages.
4. Reduction of the over-power limit at lower output voltages.
5. Power management of a PFC controller, together with the S13 pin.

To implement the 1st benefit, a resistor R_{IPC} is connected from IPC pin to AGND pin. The 50-µA current source establishes a voltage (V_{IPC}) across R_{IPC} to program an increase in the CS-pin peak primary current threshold at very light loads. The transfer function between V_{IPC} and the CS threshold (V_{CST_IPC}) in SBP2 mode is illustrated in Figure 8-10.

Proper sizing of R_{IPC} to AGND can further reduce the burst frequency in SBP2 for so-called "tiny-load" power and for stand-by power. An example of a tiny-load input power specification is that the input power must be less than 0.5 W when the output power is 0.25 W at the 20-V output. An example of a stand-by power specification is that the input power must be less than 75 mW at no load at the 5-V output.

When V_{IPC} is less than 0.9 V (or IPC is shorted to AGND), V_{CST_IPC} threshold stays at the minimum level of 0.15 V. When V_{IPC} is set between 0.9 V and 1.8V, V_{CST_IPC} is clamped at 0.27 V. For V_{IPC} between 1.8 V and 3.8 V, there is a linear programmable V_{CST_IPC} range between 0.27 V and 0.4 V. When V_{IPC} is greater than 3.8 V, V_{CST_IPC} remains clamped to 0.4 V. Be aware that high settings of V_{CST_IPC} may, in some cases, introduce higher output ripple in deep light-load condition or provoke audible noise.
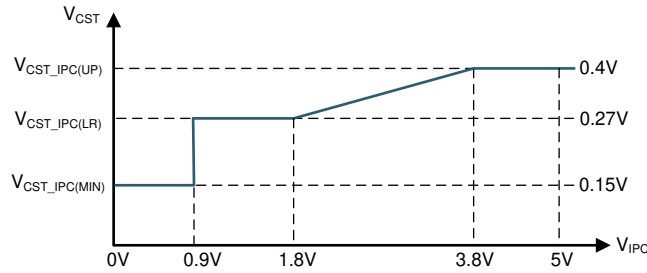
Copyright © 2019, Texas Instruments Incorporated

Figure 8-10. IPC Transfer Function to Program the SBP2 Peak Current Threshold

Since the enable status of the IPC current source contains the very useful output voltage information from the LOW_NVO logic state, the IPC pin can be used to further optimize power stage performance over a wide output voltage range. To gain the 2nd, 3rd, and 4th benefits of the IPC function, R_{IPC} should be connected between the IPC pin and the CS pin, so that the current source can create additional CS-pin offset voltage on R_{OPP} when V_{VS} < 2.4 V. With higher CS offset, the operating range of the V_{CST} signal will be higher than the actual power stage peak current. This forces the controller to operate in AAM mode for a wider actual output load range, and forces the burst-mode threshold down to a lower power level.

For 100-W USB-PD adapters as example, the 20-V output is designed to deliver 100 W full power, but the 5-V output requires only 15 W full power. When the 20-V output enters ABM below 50 W, the majority of the 5-V output load range may operate in burst mode. Figure 8-11 compares the control law difference between the two IPC-pin connections.

When R_{IPC} is connected to AGND, the peak magnetizing current ($i_{M(+)}$) correlated with the $V_{CST(BUR)}$ setting of the higher power 20-V output is too high for the lower-power 5-V output. With higher energy per cycle at the 5-V output, the AAM mode must transition into ABM mode at a heavier load condition, and the hard switching operating modes such as LPM will cover a wider output load range. Therefore, the 5-V average efficiency is impaired by the hard switching operation, and the output ripple is compromised by the burst mode setting.

When the R_{IPC} is connected to CS, however, the output voltage feedback loop increases the V_{CST} level to overcome the CS offset voltage in AAM, such that the AAM-ABM transition point can be pushed to a lighter output load. Since the output load range covered by the soft switching operating modes (AAM and ABM) is extended with this IPC configuration, the average efficiency at the low-power voltage levels can be improved. Moreover, since the peak current becomes lower in burst mode, the output ripple magnitude is reduced as well.

Figure 8-11 points out the side effect of the IPC-to-CS connection if the R_{IPC} setting is the same. Since 50 µA is enabled in the run state of SBP2, the lower peak magnetizing current of the IPC-to-CS connection makes the SBP2 burst frequency higher and results in weakening the stand-by power improvement. Therefore, a higher R_{IPC} is needed to increase V_{CST_IPC} to compensate the peak current change.

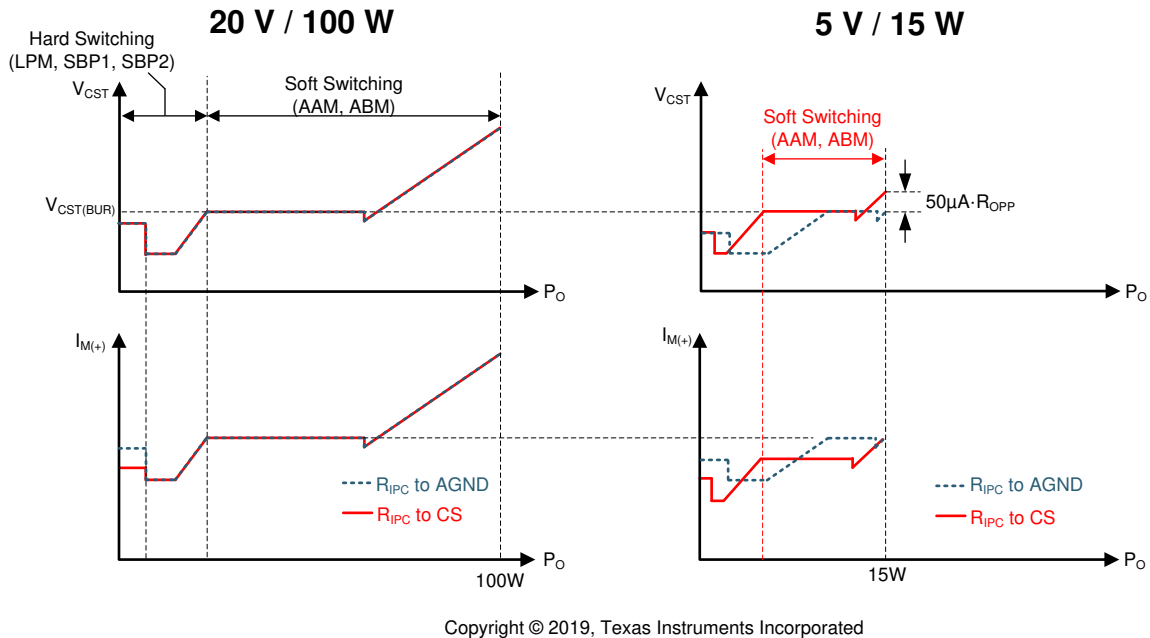Copyright © 2019, Texas Instruments Incorporated

Figure 8-11. Effect of the CS-pin Offset Voltage from the IPC Pin

For the 5th benefit, the IPC pin can also be used to disable a PFC controller (if used) at all load conditions for 5-V and 9-V outputs to further improve the light-load efficiency of higher power adapters. As shown in Figure 8-7, the diode D_{IPC} in series with R_{IPC} is placed between IPC and CS pins, and V_{IPC} established at IPC is used to drive a small-signal switch Q_{IPC} to disable the PFC controller such as UCC28056.

When V_{IPC} is higher than its threshold voltage, Q_{IPC} can pull low the COMP pin voltage of a PFC controller, so its switching is disabled. As a consequence, PFC output voltage drops from the typical 400-V regulation level to the peak value of the AC line. This lowers the ACF bulk voltage, which reduces the ZVS energy, which increases ACF power stage efficiency for low voltage outputs. Furthermore, the power loss of the PFC power stage is out of the efficiency equation. One design example for those components are $C_{S13(ACF)}$ = 22 nF, $C_{S13(PFC)}$ = 0.22 µF, C_{IPC} = 10 nF, R_{IPC} = 69.8 kΩ, R_{IPC2} = 10 MΩ, and R_{IPC3} = 20 kΩ. Choose Q_{IPC} with threshold voltage less than 1.5 V to ensure that V_{IPC} is sufficient to achieve low Rds(on) even at very low burst frequencies.

8.3.8 RUN Pin (Driver and Bias Source for Isolator)

The RUN pin is a logic-level output signal which enables PWM switching when active high. When RUN is low, all PWML and PWMH switching is disabled and the controller enters a low-current wait state. (The boost regulator, however, operates independently of the RUN signal.)

In addition to enabling switching, RUN is capable of sourcing considerable current to bias an external gate driver and perform a power management function to a high-side digital isolator. It generates a 5-V logic output when the driver should be active, and pulls down to less than 0.5 V when the driver should be disabled. During the off-time of any burst mode, the RUN pin serves as a power-management function to dynamically reduce the static bias current of the isolator/ driver, so light-load efficiency can be further improved and stand-by power can be minimized.

As RUN goes high, while its voltage is less than 3 V, a 44-mA peak pull-up current is supplied from the internal P13 regulator. With this current, the RUN driver can quickly charge the primary-side decoupling capacitor of a digital isolator above its UVLO(ON) threshold. A Schottky diode can block discharge of this capacitor when RUN goes low. When the RUN voltage goes above 3 V, P13 stops providing current and the pull-up is supplied from the REF regulator, so the peak driving capability will be limited in order to avoid triggering the over-current protection of the REF regulator. When RUN is low for a long burst off-time, the decoupling capacitor of the digital isolator will be gradually discharged below its UVLO(OFF) threshold, so the isolator power loss can be minimized.

There are three delays between RUN going high to the first PWML pulse going high in each burst packet. The first delay is a fixed 2.2-μs delay time, intended to provide an appropriate "wake-up" time for UCC28782 and the gate driver to transition from a wait state to a run state. The second delay is gated by the 10-V power-good threshold of the S13 pin. PWML will not go high until S13 voltage exceeds 10 V. The third delay is another 2.2-μs timeout, t_{ZC} in the electrical table, intended to turn on the low-side switch of the first switching cycle per burst packet around the valley point of DCM ringing by waiting for the zero-crossing detection (ZCD) on the auxiliary winding voltage (V_{AUX}). If ZCD is detected (on the VS input) before the t_{ZC} timeout elapses, PWML is immediately driven. If no ZCD is detected, PWML is driven when t_{ZC} elapses. The first two delays can be concurrent; the third delay is sequential.

Therefore, the minimum total delay time is 2.2 μs typically if $V_{S13} > 10$ V and ZCD is detected immediately after the 2.2-μs wake-up time. If $V_{S13} < 10$ V, the total delay time with tolerance over temperature is listed as $t_{D(RUN-PWML)}$ in the electrical table.
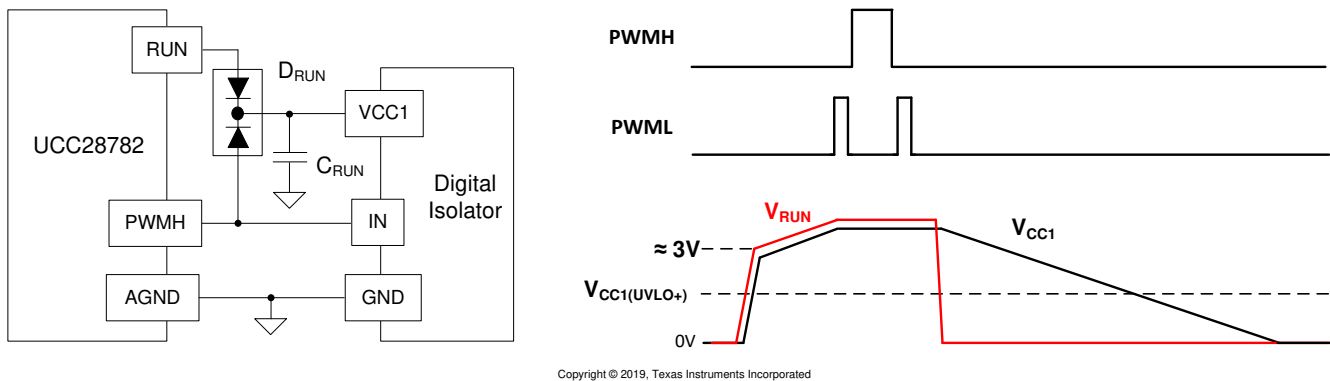

Copyright © 2019, Texas Instruments Incorporated

Figure 8-12. Power Management Function for the Digital Isolator

8.3.9 PWMH and AGND Pins

The PWMH pin controls the gate of the high-side clamp switch through an external high-voltage gate driver. The PWMH driver ground return is referenced to the AGND pin. The maximum voltage level of PWMH is clamped to 5-V REF level. As PWMH goes high, when its voltage is less than 3 V, a 21-mA peak pull-up current is supplied from the P13 regulator. When the PWMH voltage goes above 3 V, the pull-up is supplied from the REF regulator instead, so the peak driving capability will be limited less than 6 mA in order to avoid the high current loading from tripping the over current protection of the REF regulator.

As shown in Figure 8-12, since the RUN driver charges the decoupling capacitor of a digital isolator first through one small-signal diode at the beginning of every burst cycle, the sourcing current of PWMH is sufficient to send the control signal to the isolator and supply the continuous isolator operating current together with the RUN driver at the same time through another small-signal diode. The high peak driving capability of PWMH provides the flexibility of signal transmission through a digitally isolated gate-driver with opto-compatible input. If the PWMH pin is provided to a half-bridge GaN device with an internal high side driver, the PWMH driver is mainly treated as a logic signal output.

In any case, it is prudent to choose a high-side isolator or gate-driver with minimal power-up delay on both input and output sides to avoid missing several PWMH pulses to the high-side switch. Furthermore, signal transfer from input to output should be edge-triggered to avoid asynchronous high-side turn-on in the middle of a PWMH pulse, as may happen with level-triggered isolators. This can avoid high-side switch turn-off during significant current and its resultant voltage spike.

AGND pin is the ground return for all the analog control signals, RUN driver, and PWMH driver. It is required to implement a careful layout separation from other noisy ground return paths, such as PGND, BGND, and power stage ground. The thermal pad should be connected to the AGND pin directly and could be a Kelvin connection point to the related external components. For details of the grounding layout guideline and noise decoupling techniques, one can refer to the Section 9.1 of this datasheet.

8.3.10 PWML and PGND Pins

The PWML pin is the low-side switch gate-drive, for which ground return is referenced to the PGND pin. The strong driver with 0.5-A peak source and 1.9-A peak sink capability can control either a silicon power MOSFET with a higher gate-to-source capacitance, a cascode GaN, an E-mode gate-injection-transistor (GIT) GaN with continuous on-state current, or a GaN power IC with logic PWM input. The maximum voltage level of PWML is clamped to the P13 pin voltage. The 13-V clamped gate voltage provides an optimal gate-drive for low on-state resistance and lower gate-driving loss. An external gate resistor in parallel with a fast recovery diode can be used to further reduce the turn on speed without compromising the turn off switching loss. Slower turn on speed mitigates the voltage stress across the secondary-side rectifier when the high-side switch is disabled in deep light load condition, and reduces the switching-node dV/dt to a safe level for reducing stress on the high-voltage high side driver. A decoupling capacitor much larger than the PWML capacitive loading should be placed between P13 and PGND pins to decouple the gate drive loop to allow operation at higher switching frequency. The 15-ns propagation delay of the PWML driver enables a higher frequency operation and more consistent ZVS switching.

Figure 8-13 shows the example PWML driving network for a GIT GaN device and for a silicon MOSFET. The turn on speed is controlled by R_{G2}. The turn off speed can be maintained by the two fast recovery diodes, D_{G1} and D_{G2}. R_{G1} provides a continuous driving path to maintain the on state and low $R_{DS(on)}$ of a GIT GaN. C_G avoids the small R_{G2} from affecting the on state current. PGND can be directly connected to the separate source terminal of a GIT GaN to achieve a kelvin connection, so the driver loop parasitic inductance can be decoupled.
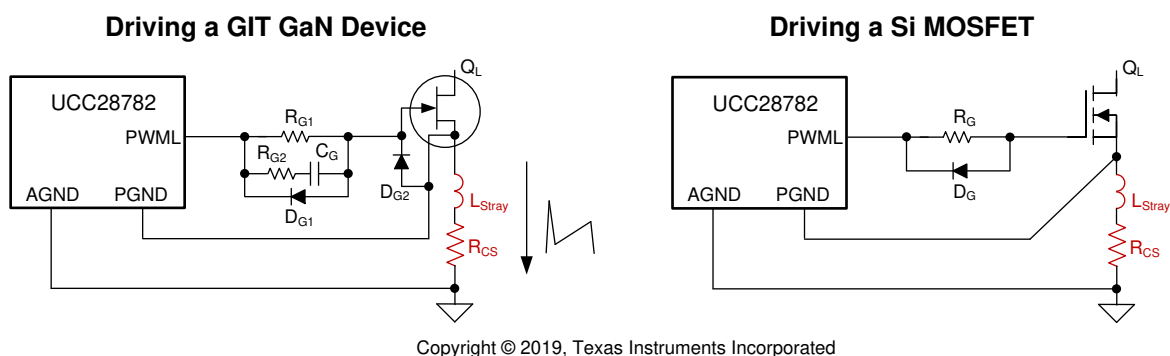
Driving a GIT GaN Device   **Driving a Si MOSFET**

Copyright © 2019, Texas Instruments Incorporated

Figure 8-13. The PWML Driver and the PGND Driver Ground Return

An internal low-voltage level shifter is included between PGND and the ground return pin for analog control signals (AGND), so PGND can be connected separately to the top of the current sense resistor (R_{CS}) to achieve a Kelvin connection. When hard switching condition occurs, the lumped parasitic capacitor on the switch node is discharged, so a positive voltage spike is created across R_{CS}. In soft switching condition, the negative magnetizing current flowing through R_{CS} can create a negative voltage spike on R_{CS}. The level shifter is designed to handle 5-V positive transient spike and -1-V negative stress between PGND pin and AGND pin.

8.3.11 SET Pin

Due to different capacitance non-linearity between Si and GaN power FETs as well as different propagation delays of their drivers, the SET pin is provided to program critical parameters of UCC28782 for the two different power stages. Firstly, this pin sets the zero voltage threshold ($V_{TH(SWS)}$) at the SWS input pin to be two different auto-tuning targets for ZVS control. When SET pin is tied to AGND, $V_{TH(SWS)}$ is set at its low level of 4 V for realizing full ZVS, which allows the low-side switch (Q_L) to be turned on when the switch-node voltage drops close to 0 V. When SET pin is tied to REF pin, $V_{TH(SWS)}$ is set at 8.5 V for implementing partial ZVS, which makes Q_L turn on at around 8.5 V. Secondly, the SET pin also selects the current sense leading edge blanking time (t_{CSLEB}) to accommodate different delays of the gate drivers; 110 ns for V_{SET} = 0 V and 190 ns for V_{SET} = 5 V. Thirdly, the minimum PWML on-time ($t_{ON(MIN)}$) in low-power mode and standby-power mode is 110 ns for V_{SET} = 0 V, and is 100 ns for V_{SET} = 5 V. Finally, the maximum PWML on-time to detect CS pin fault (t_{CSF}). t_{CSF} for V_{SET} = 5 V (t_{CSF1}) is set at 2 µs. t_{CSF} for V_{SET} = 0 V (t_{CSF0}) depends on R_{RDM}, which is configured to 1 µs under $R_{RDM} < R_{RDM(TH)}$ and to 2 µs under $R_{RDM} \geq R_{RDM(TH)}$.

8.3.12 RTZ Pin (Sets Delay for Transition Time to Zero)

The dead-time between PWMH falling edge and PWML rising edge (t_Z) serves as the wait time for V_{SW} transition from its high level down to the target ZVS point. Since the optimal t_Z varies with V_{BULK}, the internal dead-time optimizer automatically extends t_Z as V_{BULK} is less than the highest voltage of the input bulk capacitor ($V_{BULK(MAX)}$). The circulating energy for ZVS can be further reduced, obtaining higher efficiency at low line versus a fixed dead-time over a wide line voltage range. A resistor on the RTZ pin (R_{RTZ}) programs the minimum t_Z ($t_{Z(MIN)}$) at $V_{BULK(MAX)}$, which is the sum of the propagation delay of the high-side driver ($t_{D(DR)}$) and the minimum resonant transition time of V_{SW} falling edge ($t_{LC(MIN)}$).

$$R_{RTZ} = K_{RTZ} \times t_{Z(MIN)} = K_{RTZ} \times \left(t_{D(DR)} + t_{LC(MIN)} \right)$$

(9)

where K_{RTZ} is equal to 11.2×10^{11} (unit: F^{-1}) for $V_{SET} = 0$ V, and 5.6×10^{11} (unit: F^{-1}) for $V_{SET} = 5$ V.
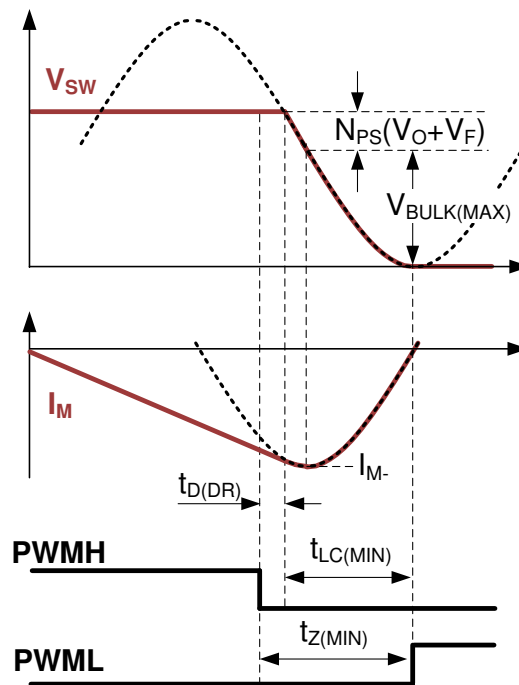

Figure 8-14. RTZ Setting for the Falling-edge Transition of V_{SW}

As illustrated in Figure 8-14, when PWMH turns off Q_H after $t_{D(DR)}$ delay, the negative magnetizing current (i_{M-}) becomes an initial condition of the resonant tank formed by magnetizing inductance (L_M) and the switch-node capacitance (C_{SW}). C_{SW} is the total capacitive loading on the switch-node, including all junction capacitance (C_{OSS}) of switching devices, stray capacitance of the boot-strap diode, intra-winding capacitance of the transformer, the snubber capacitor, and parasitic capacitance of the PCB traces between switch-node and ground. Unlike a conventional valley-switching flyback converter, the resonance of an active clamp flyback converter at high line does not begin at the peak of the sinusoidal trajectory. The transition time of V_{SW} takes less than half of the resonant period. The following $t_{LC(MIN)}$ expression quantifies the transition time for R_{RTZ} calculation, where an arccosine term represents the initial angle at the beginning of resonance. As an example, the value of π minus the arccosine term at $V_{BULK(MAX)}$ of 375 V, V_O of 20 V, and N_{PS} of 5 is around 0.585π, which is close to one quarter of the resonant period.

$$t_{LC(MIN)} = [\pi - \cos^{-1}(\frac{N_{PS}(V_O + V_F)}{V_{BULK(MAX)}})] \times \sqrt{L_M C_{SW}}$$

(10)

Product Folder Links: UCC28782

8.3.13 RDM Pin (Sets Synthesized Demagnetization Time for ZVS Tuning)

The R_{RDM} resistor provides the power stage information to the t_{DM} optimizer for auto-tuning the on-time of PWMH to achieve ZVS within a given t_Z discharge time. The following equation calculates the resistance, based on the knowledge of the primary magnetizing inductance (L_M), auxiliary-to-primary turns ratio (N_A/N_P), the values of the resistor divider (R_{VS1} and R_{VS2}) from the auxiliary winding to VS pin, and the current sense resistor (R_{CS}). Among those parameters, L_M contributes the most variation due to its typically wider tolerance. The optimizer is equipped with wide enough on-time tuning range of PWMH to cover tolerance errors. Therefore, just typical values are enough for the calculation.

$$R_{RDM} = \frac{N_A R_{VS2}}{N_P (R_{VS1} + R_{VS2})} \frac{K_{DM} L_M}{R_{CS}}$$

(11)

where K_{DM} is equal to 5.25×10^9 (unit: F^{-1}) for both V_{SET} = 5 V and 0 V.

8.3.14 BIN, BSW, and BGND Pins

A high-impedance resistor is integrated inside the BIN pin to sense the bias regulator input voltage and determine the regulator operating mode. A 30-V rated MOSFET (Q_{BSW}) with 1.4-Ω $R_{DS(on)}$ is integrated in the controller, whose drain is connected to the BSW pin and the source is to the BGND pin. When V_{BIN} is less than the 2.2-V UVLO(ON) threshold ($V_{BIN(ON)}$) and V_{VDD} is still higher than the 13-V survival mode threshold ($V_{VDD(PCT)}$ + $V_{VDD(OFF)}$), the regulator remains in the disabled condition. If the survival mode is triggered by V_{VDD} < 13 V, Q_{BSW} is forced to switch regardless of V_{BIN} < $V_{BIN(ON)}$ or not, and the regulator operates in continuous conduction mode (CCM) to charge C_{VDD} quickly. If V_{VDD} > 13 V, Q_{BSW} switching is enabled when V_{BIN} > $V_{BIN(ON)}$, and the regulator operates in transition mode or discontinuous conduction mode (DCM) to boost V_{VDD} to the 18.5-V regulation level ($V_{VDD(BOOST)}$). When the regulator starts switching, the 190-ns leading edge blanking time of Q_{BSW} is used to sample V_{BIN} for under-voltage. If V_{BIN} drops below the 1-V UVLO(OFF) threshold ($V_{BIN(ON)}$ - $V_{BIN(OFF)}$), the regulator switching will be terminated immediately.

When the ACF output voltage increases and V_{BIN} reaches to the 15-V boost disable threshold ($V_{BIN(EN)}$ + $V_{BIN(DIS)}$), so the regulator will stop switching and V_{VDD} is directly supplied from the rectified auxiliary winding voltage through the boost inductor and boost diode. When V_{BIN} drops below the 14.8-V boost enable threshold ($V_{BIN(EN)}$), the switching regulator will take over boosting of the VDD supply.

Two separate capacitors are recommended for the regulator input capacitor bank of the BIN pin. One is placed closer to the auxiliary winding and its rectification diode, so the switching loop of the primary auxiliary winding output can be minimized. A 33-μF chip ceramic capacitor is recommended for energy storage. The other capacitor is placed closer to the boost inductor, BSW, and BGND pins, so the regulator input switching loop can be reduced as well. A 10-μF chip ceramic capacitor is recommended for high-frequency decoupling. Ground return of the regulator output capacitor (C_{VDD}) should be connected back to the BGND pin as close as possible in order to minimize the regulator output switching loop area. Rather than with the BGND pin, the low-noise ground terminal of C_{VDD} should be used to connect the BGND net to the AGND pin with a low impedance copper trace or copper pour.

When the boost inductor current flowing through Q_{BSW} reaches to the 0.33-A peak current threshold, Q_{BSW} turns off in every boost switching cycle. A 30-V rated Schottky diode with higher than 0.4-A rated peak current capability is needed between the BSW and VDD pins in order to handle the 0.33-A switching current. The boost inductor between the BIN and BSW pins should support higher than 0.4-A saturation current capability. Higher current peaks may ring through the inductor whenever C_{BIN} is charged higher than C_{VDD}.

As the following equation shows, the inductance (L_B) is determined based on the largest total supply current to the loading on the VDD pin and the highest boost switching frequency selection (f_{BSW}), which is limited by maximum boost switching frequency ($f_{BSW(MAX)}$) of the control loop. The minimum inductance is 22 μH (±10%) regardless of calculation result. Magnetic shielding is recommended to help avoid inducing noise into nearby networks.

$$L_B = \frac{2(V_{VDD(REG)} - V_{BIN}) \cdot I_{VDD}}{i_{BSW(MAX)}{}^2 \cdot f_{BSW}}$$

(12)

The voltage drop on the DC winding resistance of the boost inductor (R_{LB}) and $R_{DS(ON)}$ of Q_{BSW} (R_{BSW}) reduces the actual voltage across the boost inductance from V_{BIN}. The boost inductor voltage needs to be high enough to build up the inductor current quickly. Therefore, it is recommended to choose the R_{LB} low enough to make the total resistive voltage drop at 0.33 A lower than the 1-V boost UVLO(OFF) threshold.

$$R_{LB} < \frac{V_{BIN(ON)} - V_{BIN(OFF)} - I_{BSW(MAX)}R_{BSW}}{I_{BSW(MAX)}}$$

(13)

When the ACF operates in the LPM, SBP1, and SBP2 modes, the high side switch is disabled, so the leakage inductance energy will charge the clamping capacitor and C_{BIN} in every ACF switching cycle. If the leakage inductance energy is big enough to build up V_{BIN} higher than 30 V under those operating modes, a unidirectional TVS between the BIN pin and AGND pin will be needed to protect the 30-V rated BIN and BSW pins. A high-voltage Schottky auxiliary winding rectifier diode maximizes the C_{BIN} voltage in the survival mode, so the regulator in CCM mode can transfer the stored C_{BIN} charge to C_{VDD}. The more survival mode energy is absorbed by the auxiliary power supply, the less residual energy is delivered to the output capacitor. This will ensure that the output voltage can stay within regulation range during survival mode under no-load condition.

8.3.15 XCD Pin

The XCD pin performs X-capacitor discharge and the fault-latch fast-reset functions in conjunction with the recommended external detection circuits, shown in Figure 8-15. The first application circuit allows to perform the two functions at the same time. The second application circuit achieves the fault-latch fast-reset only. **The two application circuits must be connected to the AC input but not the DC input, in order to avoid the thermal issue of those sensing components caused by enabling the discharge current repetitively.** If neither function is needed, directly shorting the two XCD pins to the AGND pin disables the XCD pin functions, so the controller wait-state current is further reduced. The external sensing circuit must be removed.
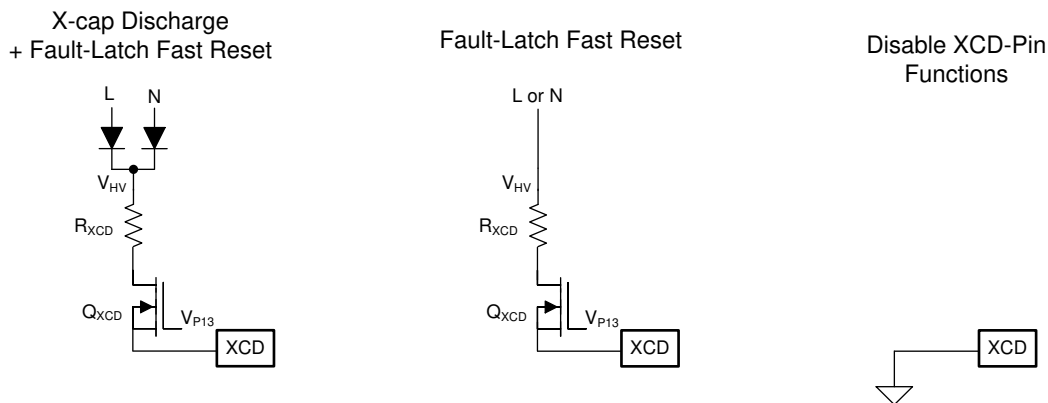
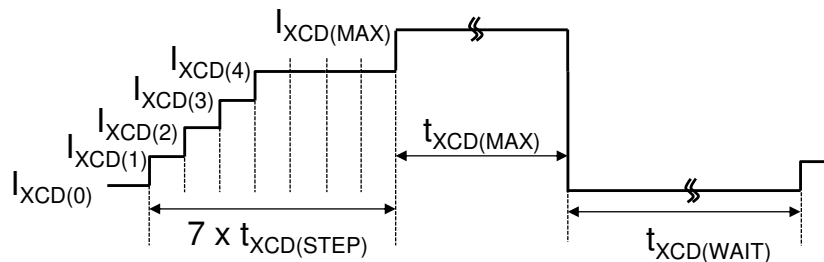Copyright © 2019, Texas Instruments Incorporated

Figure 8-15. XCD-pin Application Circuits

To form the discharge path in the first circuit, the anode nodes of two high-voltage diode rectifiers are connected to each X-cap terminal, the two diode cathodes are connected together to a 26-kΩ current limit resistance (R_{XCD}), and the drain-to-source of a high-voltage depletion MOSFET (Q_{XCD}) couples the resistance to XCD pins. Since R_{XCD} needs to sustain the high voltage drop from the XCD-pin current, two series 13-kΩ SMD resistors in 1206 size with 26-kΩ total resistance are required to meet the voltage de-rating. A 600-V rated MOSFET such as BSS126 is needed as the high voltage blocking device. The MOSFET gate is connected to the P13 pin, so

the highest voltage level of the XCD pins is limited to the sum of the P13-pin voltage and the threshold voltage of BSS126. The voltage level gives sufficient headroom over the 6.5-V line zero-crossing (LZC) threshold.

In case of single-fault event where one XCD pin is in fail-open condition, the redundant XCD pin helps to maintain the X-cap discharge function. In case of the single-fault event of BSS126 involving its drain-to-source in fail-short condition, an internal 26-V clamp helps to protect the XCD pin from exceeding its voltage rating. The current-limiting resistance (R_{XCD}) limits the fault current below the maximum clamping capability, however the value of R_{XCD} should avoid reducing the normal discharge current. A total resistance of 26 kΩ ±5% meets both criteria. The internal clamping function can also help to dissipate some of the line surge energy accumulated on the XCD pins in order to limit the pin voltage below its 30-V rating.

After the AC line is disconnected, X-capacitors in the EMI filters on the AC side of the diode-bridge rectifier must have means to discharge its residual voltage to a safe level within a certain time. Typically a high voltage discharge resistor bank is placed in parallel with the capacitor to form a discharge path. The value of the resistance is chosen to discharge the capacitance within the required time period. However, if the capacitance is large enough, the necessary lower value of discharge resistance will increase the standby power. UCC28782 provides an active X-capacitor discharge function with 2-mA maximum discharge current capability to reduce the standby power. The discharge current is activated only when the detection criteria for the AC-line removal condition is met. The 6.5-V line zero-crossing (LZC) threshold on XCD pins is used to detect AC-line presence. When LZC is missing over an 84-ms detection timeout period, the discharge current is enabled for a maximum period of 300 ms followed by a 700-ms blanking time with no current. To detect the zero crossing reliably, as well as to save power consumption, a stair-case test current shown in Figure 8-16 is generated within the 84-ms detection time. The worst-case discharge current and timing are designed to discharge the X-capacitor up to 1 μF.
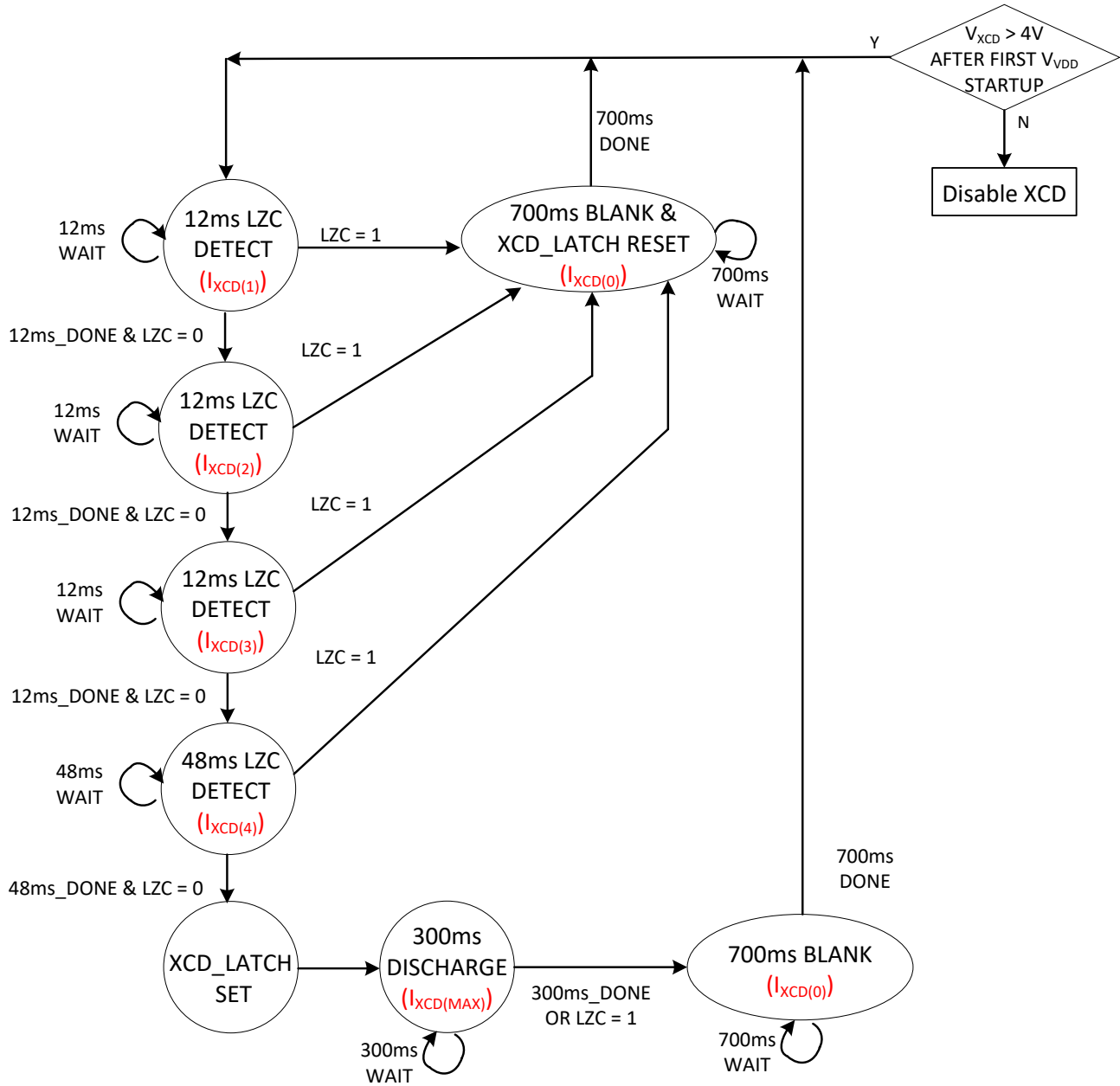

Copyright © 2019, Texas Instruments Incorporated

Figure 8-16. Step-current Profile into the XCD Pins for the X-cap Discharge Function

The four test current levels are designed to overcome the impact of leakage current from the bridge diode over a wide line range. Without enough test current level in a 12-ms period, the diode leakage current will prevent the XCD-pin voltage from reaching close to the 6.5-V LZC threshold. A higher AC line voltage or a higher diode junction temperature requires a higher test current due to the increased diode leakage current. When the AC line is connected, the four stair-case current levels and the 700-ms time out after the completion of LZC detection helps to minimize the average current sink from AC main and thereby the static power loss. For the first three current levels, every 12-ms time-out event commands the test current to increment. The last test current level has to be sustained for 48 ms without LZC, before triggering the 2-mA discharge mode. Whenever LZC is detected, any higher-level test-current steps are aborted and the 700-ms wait-state is initiated. Figure 8-17 shows the flow chart of X-capacitor discharge and the fault-latch reset sequence.

Note that the XCD-LATCH referenced in Figure 8-17 is not the same as the Fault-Latch. XCD-LATCH is a latch that is set when loss of AC line is confirmed. When set, this state allows the Fault-Latch to be reset and allows X-capacitor discharge to proceed.

Figure 8-17. The State Diagram of the XCD-pin Function

Whenever any system protection triggers the fault-latch, the converter switching is terminated and V_{VDD} restart cycle occurs between $V_{VDD(ON)}$ and $V_{VDD(OFF)}$. In this mode, the XCD pin function continues to operate, since the internal circuitry is separately biased from V_{VDD} instead of from V_{REF}. When the AC line is disconnected, the large bulk input capacitor of the ACF prevents V_{VDD} from decaying below the 4.3-V fault reset threshold quickly enough. If the AC line recovers too fast without the XCD pin detection, the controller will still stay in a latched condition and output voltage fails to retry. The two XCD-pin detection circuits can inform the controller the instant of AC line recovery based on the LZC detection concept, so the controller can directly reset the fault condition more quickly.

The second application circuit performs the fault-latch fast-reset without the need for the two high voltage diodes, so essential sensing components become fewer. In the first application circuit with both line and neutral connections, the frequency of the XCD-pin signal is twice the AC-line frequency, and the 12-ms timeout is long

enough for V_{XCD} to reach the LZC threshold when the test current becomes sufficient. On the other hand, since the current-limit resistor is connected directly to either line or neutral of the AC input in the second application circuit, only the line-frequency waveform on the XCD pins can trigger the LZC threshold. Because the 12-ms timeout is shorter than a 50-Hz or 60-Hz line cycle, the LZC detection time requires two 12-ms timeout periods to allow the latch reset function to be triggered correctly. Considering the average static current into the XCD pins and the circuit power loss, the second application circuit is lower than the first one. At a high-line condition, the second circuit only needs to use the second step current of 775 µA to detect LZC, while the first circuit may need to increase to the third or fourth step current in order to obtain a valid LZC detection.

Shorting the XCD pins to AGND disables both functions automatically. After V_{VDD} first reaches $V_{VDD(ON)}$, a 80-µA test current is sourced out of the XCD pin, in order to reliably identify the XCD-pin short with a low-impedance path to the AGND pin. If XCD is shorted to AGND, any path to L and N must be open to prevent R_{XCD} from overheating. When V_{XCD} is lower than 4 V before the RUN-pin first pulls high, the function is disabled and the internal circuit will stop sourcing current from V_{VDD}. Different from the first two application circuits, when a latch-off fault happens, the only way to reset the fault condition for this connection is to wait for V_{VDD} to drop below the 4.3-V logic reset threshold ($V_{VDD(RST)}$) first before the next V_{VDD} restart cycle occurs. With large bulk capacitance, V_{VDD} may cycle for several minutes before its energy is depleted low enough to drop to 4.3V. This connection may be more useful for the all auto-recovery fault setting, or for the latch-off fault setting with no stringent latch reset time limitation.

8.3.16 CS, VS, and FLT Pins

The CS pin is the current-sense input. The internal peak current control loop limits the highest magnetizing current, and Section 8.4.4 in this datasheet describes the peak current change in different operation modes. The VS pin is a multi-function sensing input, which detects the input voltage, the output voltage, and the zero-current-crossing (ZCD) through the auxiliary winding voltage, for optimizing ACF performance and providing critical protections. The FLT pin is a dual-purpose fault detection pin for the over-temperature protection or the input over-voltage protection. The system protection functions of the three pins are introduced in Section 8.4.14.

Product Folder Links: *UCC28782*

8.4 Device Functional Modes

8.4.1 Adaptive ZVS Control with Auto-Tuning

Figure 8-18 shows the simplified block diagram explaining the ZVS control of UCC28782. A high-voltage sensing network provides a replica of the switch node voltage waveform (V_{SW}) with a limited "visible" lower voltage range that the SWS pin can handle. The ZVS discriminator identifies the ZVS condition and determines the adjustment direction for the on-time of PWMH (t_{DM}) by detecting if V_{SW} reaches a predetermined ZVS threshold, $V_{TH(SWS)}$, within t_Z, where t_Z is the targeted zero voltage transition time of V_{SW} controlled by the PWMH-to-PWML dead-time optimizer.

In Figure 8-18, V_{SW} of the current switching cycle in the dashed line has not reached $V_{TH(SWS)}$ after t_Z expires. The ZVS discriminator sends a TUNE signal to increase t_{DM} for the next switching cycle in the solid line, such that the negative magnetizing current (I_{M-}) can be increased to bring V_{SW} down to a lower level in the same t_Z. After a few switching cycles, the t_{DM} optimizer settles and locks into ZVS operation of the low-side switch (Q_L). In steady-state, there is a fine adjustment on t_{DM}, which is the least significant bit (LSB) of the ZVS tuning loop. This small change of t_{DM} in each switching cycle is too small to significantly move the ZVS condition away from the desired operating point. Figure 8-19 demonstrates how fast the ZVS control can lock into ZVS operation. Before the ZVS loop is settled, UCC28782 starts in a valley-switching mode as t_{DM} is not long enough to create sufficient I_{M-}. Within 15 switching cycles, the ZVS tuning loop settles and begins toggling t_{DM} with an LSB.
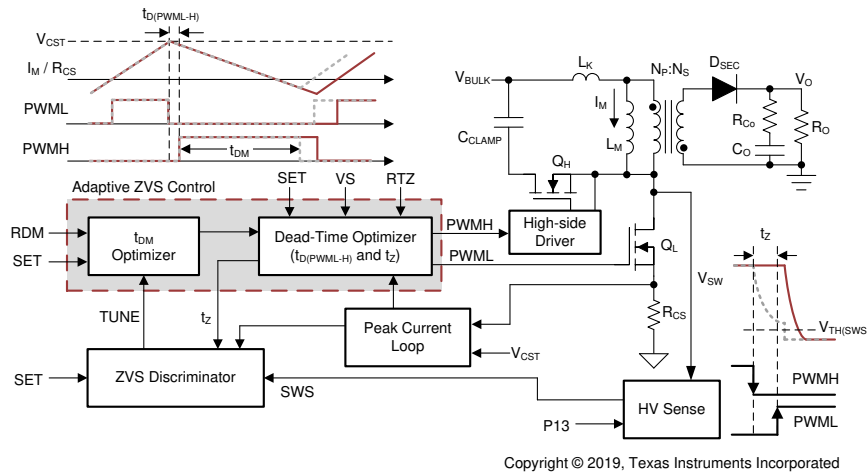

Copyright © 2019, Texas Instruments Incorporated

Figure 8-18. Block Diagram of Adaptive ZVS Control
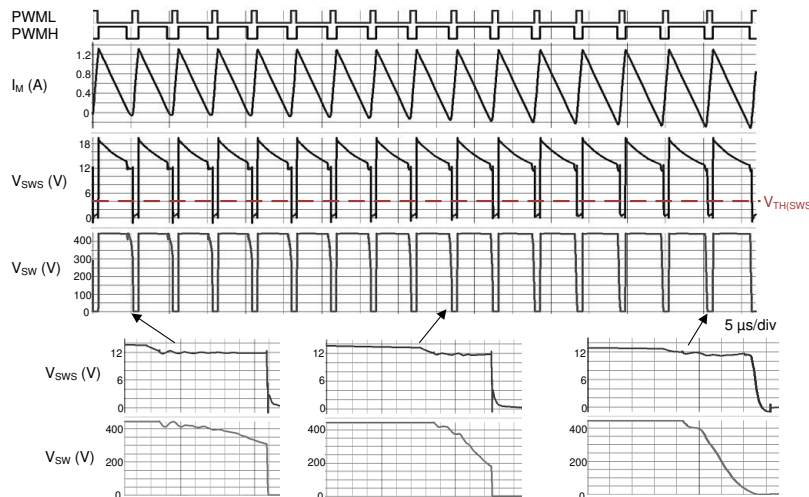
Figure 8-19. Auto-Tuning Process of Adaptive ZVS Control

Product Folder Links: *UCC28782*

8.4.2 Dead-Time Optimization

The dead-time optimizer in Figure 8-18 controls the two dead-times: the dead-time between PWMH falling edge and PWML rising edge (t_Z), as well as the dead-time between PWML falling edge and PWMH rising edge ($t_{D(PWML-H)}$).

Similar to UCC28780, the adaptive control law for t_Z of UCC28782 utilizes the line feed-forward signal to extend t_Z as V_{BULK} reduces, as shown in Figure 8-20. The VS pin senses V_{BULK} through the auxiliary winding voltage (V_{AUX}) when the low-side switch (Q_L) is on. The auxiliary winding creates a line-sensing current (I_{VSL}) out of the VS pin flowing through the upper resistor of the voltage divider on VS pin (R_{VS1}). Minimum t_Z ($t_{Z(MIN)}$) is set at $V_{BULK(MAX)}$ through the RTZ pin. When I_{VSL} is lower than 666 µA, t_Z linearly increases and the maximum t_Z extension is 140% of $t_{Z(MIN)}$.
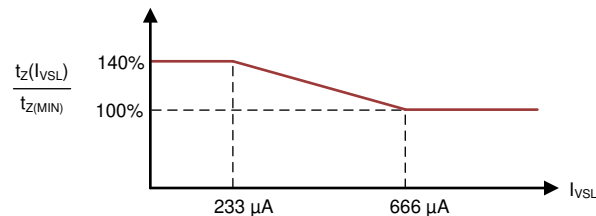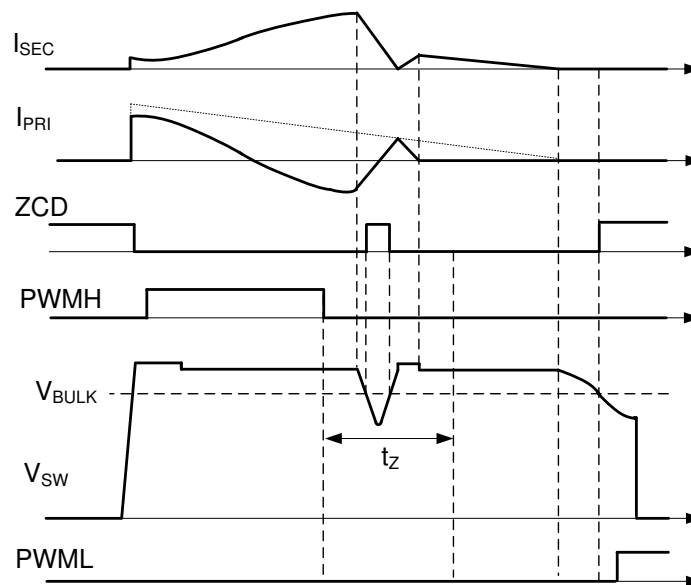

Figure 8-20. t_Z Control Optimized for Wide Input Voltage Range

Copyright © 2019, Texas Instruments Incorporated

Figure 8-21. The Enhanced t_Z Control for CCM Avoidance

The enhanced t_Z control of UCC28782 helps to avoid voltage stress on the secondary rectifier due to temporary continuous conduction mode (CCM) operation. If the high side switch turns off under a higher than normal negative resonant current instance, the switch node voltage (V_{SW}) and the auxiliary winding voltage (V_{AUX}) will drop very fast, because a higher di/dt current flows through the leakage inductance. At the same instant, if the magnetizing current has not decayed down to zero yet, the current will continue to flow in the secondary rectifier, so the switch node voltage will recover back to a high level again and results in a short-duration voltage dip behavior within the t_Z period. If a ACF controller turns on the low-side switch after t_Z expires but the magnetizing current is still positive, the limited turn off speed of the synchronous rectifier (SR) will result in a higher di/dt current as the low-side switch turns on, so a high voltage spike is generated on the SR drain-to-source voltage. Then, the FET voltage rating or the snubber design on the secondary side may need to be compromised, which are the typical concerns of flyback topology in CCM. Therefore, the VS pin of UCC28782 can detect this event and avoid low-side switch turn on after t_Z expires under this situation.

The concept is to detect the ZCD signal once again at the instant of t_Z expiration, such that the controller will not respond to the false ZCD signal after the high side switch turns off. When the duration of the voltage dip is shorter than t_Z setting, the ZCD signal will change back to its original low state at the t_Z expiration instance. When there is no valid switch node voltage transition detected from the ZCD signal at the instance, the controller will wait for another ZCD rising edge to trigger the low-side switch turn-on of the next cycle. Since the next ZCD signal could be a real indication of the magnetizing current reached to 0 A, the CCM turn-off event of secondary rectifier will not occur. Figure 8-21 illustrates the issue and the operation principle of the improved switching control in UCC28782.

The control law for $t_{D(PWML-H)}$ of UCC28782 is adaptive with the slope variation of the switching node voltage, regardless of the SET-pin voltage. One reason of applying the adaptive control is to generate a minimum dead time for reducing the body diode conduction time of the high-side Si switch or the reverse conduction time of the high-side GaN switch. Another reason is to avoid the risk of hard switching. Since the rising slope of the switch node voltage varies with different peak magnetizing currents as output load changes, using a fixed dead-time can potentially cause hard-switching on the high-side clamp switch (Q_H) if the dead-time is not long enough.
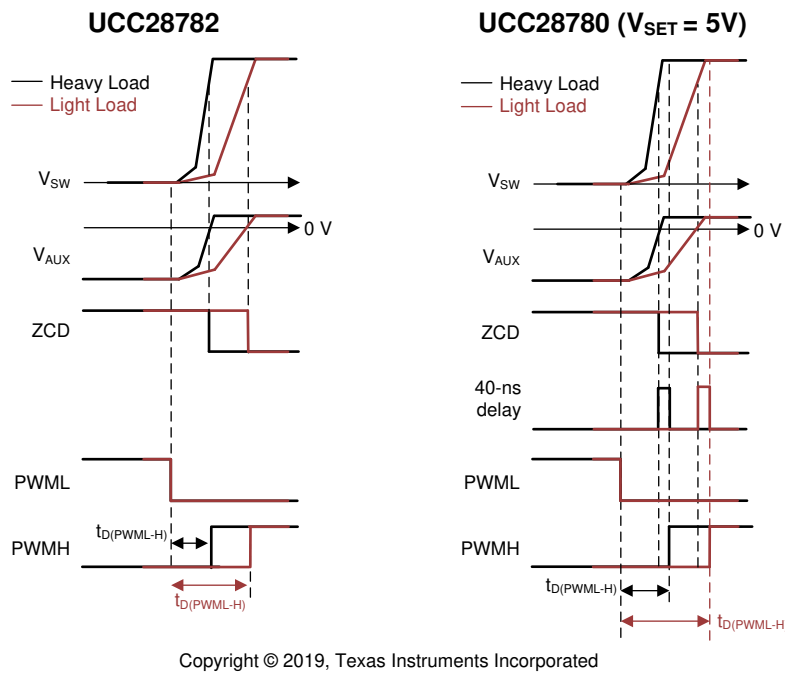

Figure 8-22. $t_{D(PWML-H)}$ Control Optimized for GaN and Si FETs

For the GaN ACF with UCC28780, a fixed 40-ns dead time from PWML falling edge to PWMH rising edge is applied for the SET pin connected to GND. For the Si ACF with UCC28780, the adaptive dead time adjustment based on the ZCD falling edge plus 40-ns delay is applied for the SET pin connected to the REF pin. The enhanced $t_{D(PWML-H)}$ control of UCC28782 helps to further reduce the body diode conduction time of the high side Si switch or the reverse conduction time of the high-side GaN switch without risk of hard switching on the high side switch. Moreover, the same dead time control is generalized for both SET-pin connections. After the ZCD falling edge is detected, the PWMH driver of UCC28782 will pull high immediately, and the extra 40-ns delay in UCC28780 is removed. For the GaN ACF with UCC28782, as long as the VS-pin delay from the parasitic capacitive loading is reduced by a proper layout arrangement, it is possible to shorten the reverse conduction time in heavy load, and also eliminate the concern of high-side hard switching in light load. For the Si ACF with UCC28782, the propagation delay of the high-side driver already provides enough margin for switch node voltage settled to a high level after ZCD falling edge is triggered, so there is no need to introduce an extra 40-ns delay like UCC28780.

8.4.3 EMI Dither and Dither Fading Function

The frequency dither function in AAM reduces the conducted EMI noise and results in EMI filter size reduction. Conventionally, the dither carrier frequency is in the range of hundreds of Hz. However, when the control loop bandwidth is pushed higher in order to improve the load transient response, the control loop will be able to correct the disturbance from the dither signal, and weakens the EMI frequency spreading effectiveness. Even though increasing the dither frequency to few kHz can reduce the influence of the control loop, the audible noise issue will occur. For UCC28782, since the ACF is able to run at a higher switching frequency in AAM, the dither frequency can be optimized at 23 kHz, so as to avoid audible noise and desensitize the loop response effect on the EMI attenuation.

UCC28782 enhances the response of the ZVS control loop, such that the ZVS performance can be maintained in most switching cycles even under a strong EMI dither condition. A triangular dither signal is superimposed on the feedback voltage signal V_{CST}, so it is challenging to calculate the proper PWMH on time cycle by cycle to keep similar negative magnetizing current for ZVS. The novel feed-forward control method is applied to allow the ZVS loop to correct the timing error much faster, so ZVS can be maintained and the efficiency will not suffer.

Conventionally, the dither magnitude is fixed across the whole output voltage range. Since the higher output voltage condition needs to deliver a higher output power, the EMI issue is typically more severe, so a stronger dither signal is needed for more conducted EMI reduction. In the lower output voltage condition, the output ripple specification is usually much tighter, so a strong dither signal may aggravate the output voltage ripple and create the design tradeoff. For UCC28782, the two-level dither magnitude is adjusted automatically based on the output voltage level, so the perturbed output ripple at the lower output voltage condition can be reduced to meet a more stringent ripple requirement, and the strong dither can still be applied to the higher output voltage condition for the better EMI performance. Specifically, when V_{VS} is lower than 2.4 V during the demagnetization time (the LOW_NVO logic signal is high), the peak-to-peak dither magnitude on CS pin is reduced to around 36 mV. When V_{VS} is higher than 2.5 V, the peak-to-peak dither magnitude on CS pin is increased to around 98 mV.

Since the low-line efficiency usually determines the power stage thermal limit, the efficiency will drop further when EMI dither is enabled. Since the bulk capacitor ripple voltage at low line is bigger than at high line and AAM mode forces variable frequency operation, the line frequency causes nature dither frequency anyway even without applying the internal EMI dither. Therefore, taking advantage of AAM mode, the dither function at low line can be disabled based on the brown-in voltage setting, so the option provides design flexibility to trade-off the worst-case low-line efficiency and EMI. Specifically, when i_{VSL} is higher than 646 µA, the EMI dither function is enabled. When i_{VSL} is lower than 580 µA, the EMI dither function is disabled. If the brown-in point is set at 75 Vac, this means that the EMI dither is disabled for 90 Vac and 115 Vac.

The dither fading feature allows the dither signal to be smoothly disabled, when the output load current is close to the transition point between AAM and ABM. As shown in Figure 8-23, $V_{CST(MAX)}$ and $V_{CST(BUR)}$ are used as the two voltage-clamping targets to the perturbed V_{CST} signal. When the V_{CST} reaches $V_{CST(MAX)}$, the top of the V_{CST} ripple content is clipped by the internal clamp circuit, so the influence of the EMI dither on the peak power capability can be eliminated. When the V_{CST} reaches $V_{CST(BUR)}$, the bottom of the V_{CST} ripple content is clipped by an another internal clamp circuit, so the influence of the EMI dither on the ABM waveform is removed.
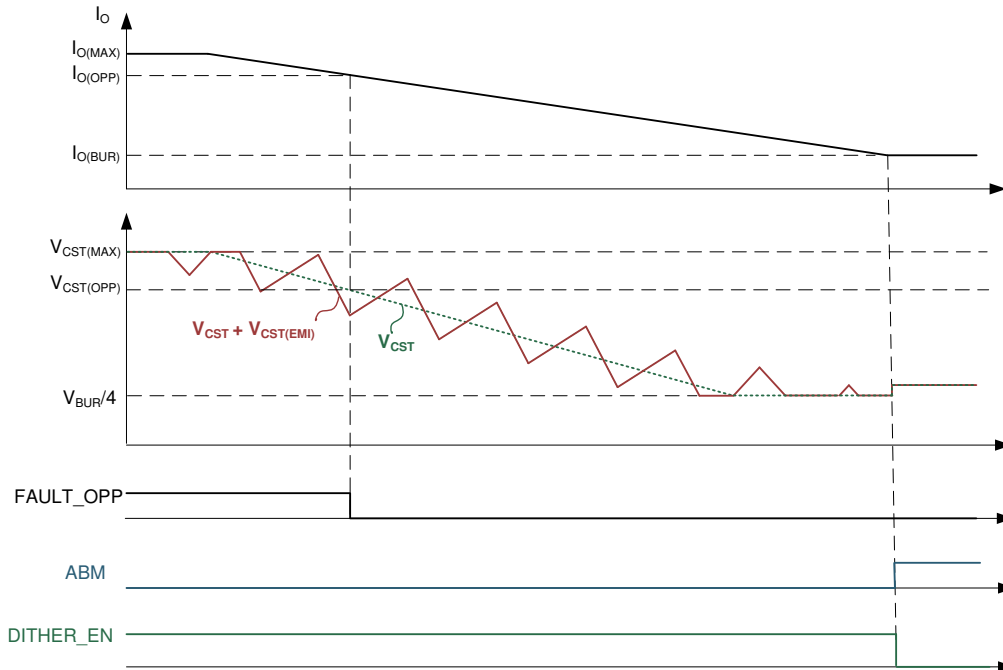
Copyright © 2019, Texas Instruments Incorporated

Figure 8-23. Dither Fading Feature in AAM

8.4.4 Control Law across Entire Load Range

UCC28782 contains six modes of operation summarized in Table 8-1. Starting from heavier load, the AAM mode forces PWML and PWMH into complementary switching with ZVS tuning enabled. ABM mode generates a group of PWML and PWMH pulses as a burst packet, and adjusts the burst off-time to regulate the output voltage. At the same time, the burst frequency variation is confined above 20kHz by adjusting the number of PWML and PWMH pulses per packet to mitigate audible noise and reduce burst output ripple. In LPM, SBP1, and SBP2 modes, PWMH and the ZVS tuning loop are disabled, so the converter operates in valley-switching. The survival mode is to maintain V_{VDD} higher than $V_{VDD(OFF)}$ in a long burst off time, and also performs the clamping capacitor balancing function to reduce the voltage stress of the secondary-side rectifier.

Table 8-1. Functional Modes

	MODE	OPERATION	PWMH	ZVS
AAM	Adaptive Amplitude Modulation	ACF operation with PWML and PWMH in complementary switching	Enabled	Yes
ABM	Adaptive Burst Mode	Variable $f_{BUR} > f_{BUR(LR)}$, ACF operation in complementary switching	Enabled	Yes
LPM	Low Power Mode	Fix $f_{BUR} \approx f_{LPM}$, valley-switching	Disabled	No
SBP1	First StandBy Power Mode	Variable f_{BUR} between $f_{SBP2(LR)}$ and $f_{SBP2(UP)}$, valley-switching	Disabled	No
SBP2	Second StandBy Power Mode	Variable $f_{BUR} < f_{SBP2(UP)}$ as $V_{BUR} < 0.9$ V; Variable $f_{BUR} < f_{SBP2(LR)}$ as $V_{BUR} > 0.9$ V; Both are in valley-switching	Disabled	No
INT_STOP	Survival Mode	When $V_{VDD} < V_{VDD(OFF)} + V_{VDD(PCT)}$, a series of PWML pulses followed by a long PWMH pulse is generated	Enabled in the last switching cycle of a survival-mode burst packet	No

Figure 8-24 and Figure 8-25 show the critical parameter changes among the five operating modes, where V_{CST} is the peak current threshold compared with the current-sense voltage from the CS pin, f_{SW} is the switching frequency of PWML, f_{BUR} is the burst frequency, and N_{SW} is the pulse number of PWML cycles per burst packet.

Figure 8-24 represents the control mode difference under the two VS-pin voltage ranges, when the IPC-pin voltage is less than 0.9 V or IPC is connected to AGND. Figure 8-25 illustrates the modified control mode, when the IPC-pin voltage setting is higher than 0.9 V. The following section explains the detailed operation of each mode. The VS-pin voltage and IPC-pin voltage effects will also be introduced in the following section.
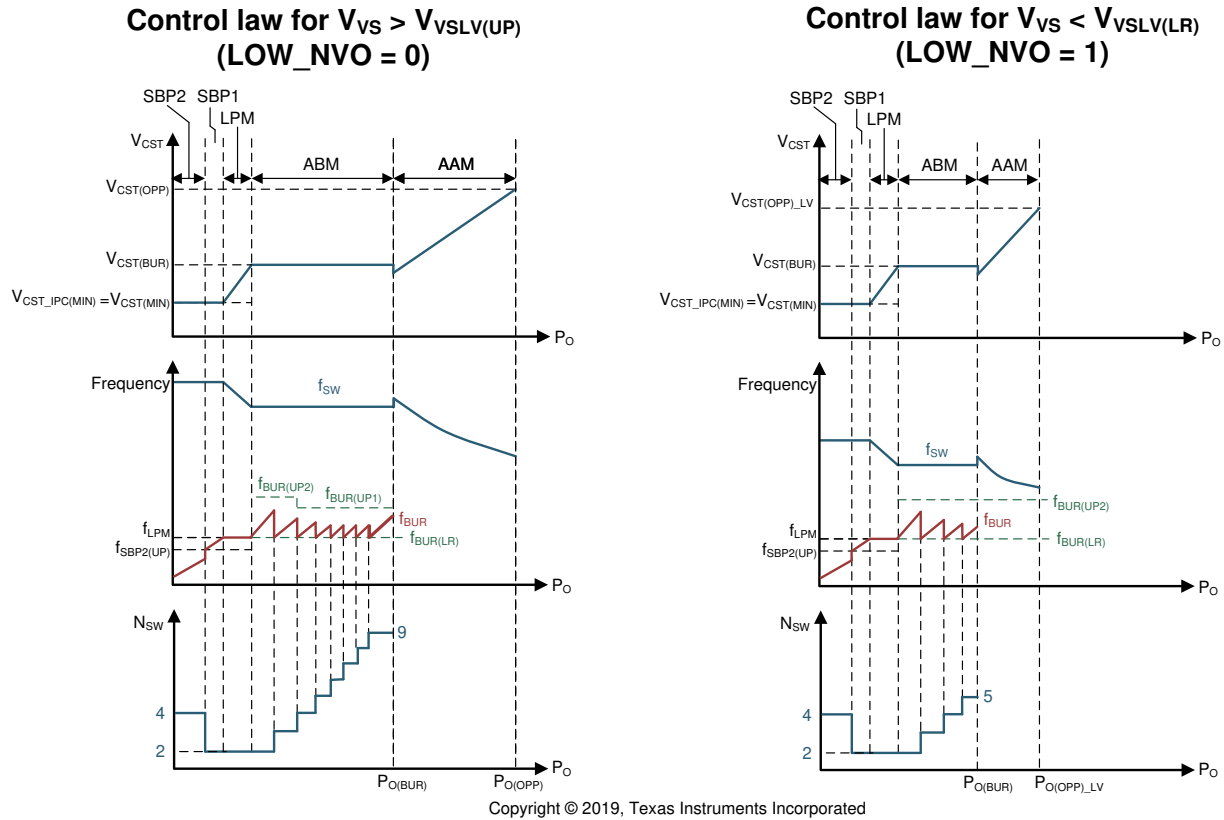

Copyright © 2019, Texas Instruments Incorporated

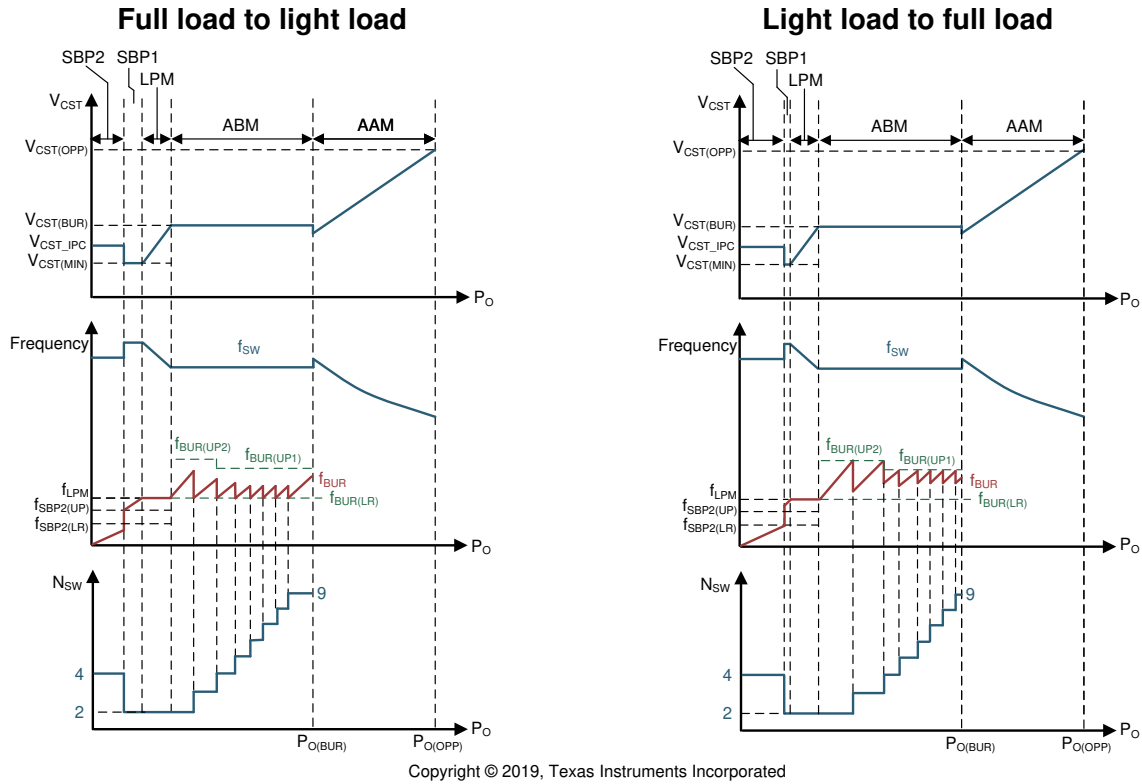**Figure 8-24. Control Law Over Entire Load Range Based on the V_{VS} Condition as V_{IPC} < 0.9 V**

Figure 8-25. Control Law Under Different Load Sweep Direction as $V_{IPC} > 0.9$ V and $V_{VS} > V_{VSLV(UP)}$

8.4.5 Adaptive Amplitude Modulation (AAM)

The switching pattern in AAM forces PWML and PWMH to alternate in a complementary fashion with dead-time in between, as shown in Figure 8-26. As the load current reduces, the negative magnetizing current (I_{M-}) stays the same, while the positive magnetizing current (I_{M+}) reduces by the internal peak current loop to regulate the output voltage. I_{M+} generates a current-feedback signal (V_{CS}) on the CS pin through a current-sense resistor (R_{CS}) in series with Q_L source and a peak current threshold (V_{CST}) in the current loop controls the peak current variation. Due to the nature of transition-mode (TM) operation, lowering the peak current with lighter load conditions results in higher switching frequency. When the load current increases to an over-power condition ($I_{O(OPP)}$) where V_{CST} correspondingly reaches an OPP threshold ($V_{CST(OPP)}$) of the peak current loop, the OPP fault response will be triggered after a 160-ms timeout. The RUN signal stays high in AAM, so the half-bridge driver remains active.
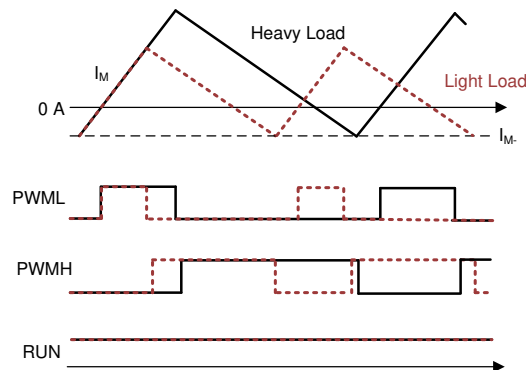

Figure 8-26. PWM Pattern in AAM

Product Folder Links: *UCC28782*

8.4.6 Adaptive Burst Mode (ABM)

As the load current reduces to $I_{O(BUR)}$ where V_{CS} reaches the $V_{CST(BUR)}$ threshold, the control mode transitions to ABM starts and V_{CS} is clamped. The peak magnetizing current and the switching frequency (f_{SW}) of each switching cycle are fixed for a given input voltage level. $V_{CST(BUR)}$ is programmed by the BUR pin voltage (V_{BUR}). The PWM pattern of ABM is shown in Figure 8-27. When RUN goes high, a delay time between RUN and PWML ($t_{D(RUN-PWML)}$) is given to allow both the gate driver and the UCC28782 time to wake up from a wait state to a run state. PWML is set as the first pulse to build up the bootstrap voltage of the high-side driver before PWMH starts switching. The first PWML pulse turns on Q_L close to a valley point of the DCM ringing on the switch-node voltage (V_{SW}) by sensing the condition of zero crossing detection (ZCD) on the auxiliary winding voltage (V_{AUX}). The following switching cycles operate in a ZVS condition, since PWMH is enabled. As the number of PWML pulses (N_{SW}) in the burst packet reaches its target value, the RUN pin pulls low after the ZCD of the last switching cycle is detected, and forces the half-bridge driver and UCC28782 into a wait state for the quiescent current reduction of both devices. In this mode, the minimum off-time of the RUN signal is 2.2 µs and the minimum on-time of PWML is limited to the leading-edge blanking time (t_{CSLEB}) of the peak current loop. However, more grouped pulses means more risk of higher output ripple and higher audible noise. The following equation estimates how burst frequency (f_{BUR}) varies with output load and other parameters.

$$f_{BUR} = \frac{I_O}{I_{O(BUR)}} \frac{f_{SW}}{N_{SW}}$$

(14)

As $I_O < I_{O(BUR)}$, f_{BUR} can become lower than the audible noise range if N_{SW} is fixed. In ABM, N_{SW} is modulated to ensure f_{BUR} stays above 20 kHz by monitoring f_{BUR} in each burst period. As I_O reduces, f_{BUR} becomes lower and reaches a predetermined low-level frequency threshold ($f_{BUR(LR)}$) of 25 kHz. The ABM loop commands N_{sw} of both PWML and PWMH to be reduced by one pulse to maintain f_{BUR} above $f_{BUR(LR)}$. At the same time, the burst frequency ripple on the output voltage reduces as N_{SW} drops with the load reduction. As I_O increases, f_{BUR} becomes higher and reaches a predetermined high-level frequency threshold ($f_{BUR(UP)}$). The ABM loop commands N_{SW} to be increased by one pulse to push f_{BUR} back below $f_{BUR(UP)}$.

The maximum N_{SW} and the $f_{BUR(UP)}$ thresholds are modified based on the output voltage condition, i.e., the positive VS-pin voltage level. When the V_{VS} sampled at the PWMH falling edge is less than the 2.4-V threshold ($V_{VSLV(LR)}$), the maximum N_{SW} is 5 pulses and the $f_{BUR(UP2)}$ is 50 kHz. When the sampled V_{VS} is higher than the 2.5-V threshold ($V_{VSLV(UP)}$), the maximum N_{SW} is 9 pulses, the $f_{BUR(UP2)}$ is 50 kHz for $N_{SW} \leq 3$, and the $f_{BUR(UP1)}$ is 34 kHz for $N_{SW} > 3$. The IPC-pin voltage does not affect the parameters in ABM mode.

This algorithm maximizes the number of pulses in each burst packet to improve light-load efficiency, while also limiting the burst output ripple and audible noise. As I_O is close to the boundary between AAM and ABM, the two burst packets with the maximum pulse count may start to bundle together. In order to mitigate the output ripple and audible noise concerns, when the bundled burst packet appears two times within eight sequential burst cycles, the 5-µA current sink into the BUR pin is enabled to reduce V_{BUR} . The less energy per cycle with a lower V_{BUR} will force the control loop to transition from ABM to AAM smoothly in order to allow the peak current increase to maintain the output voltage regulation.
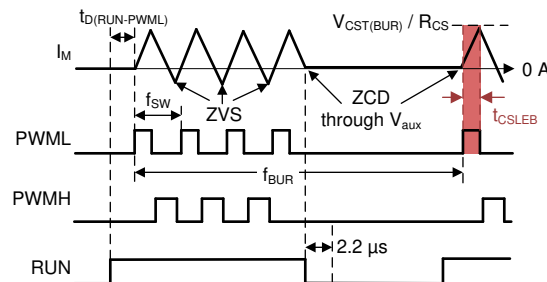

Figure 8-27. PWM Pattern in ABM

8.4.7 Low Power Mode (LPM)

As N_{SW} drops to two in ABM and the condition of f_{BUR} less than $f_{BUR(LR)}$ is qualified under two consecutive burst periods, UCC28782 enters into LPM mode and disables PWMH. The purpose of LPM is to provide a soft peak current transition between $V_{CST(BUR)}$ and $V_{CST(MIN)}$. LPM fixes N_{SW} at two and sets f_{BUR} equal to f_{LPM} of 25 kHz. In LPM mode, V_{CST} is controlled to regulate the output voltage. At the start of each burst packet, after RUN pulls high, $t_{D(RUN-PWML)}$ is used to wake up both the gate driver and UCC28782. With PWMH disabled, the two PWML pulses turn on Q_L close to valley-switching by sensing ZCD. When ZCD is detected again at the end of the second pulse, the RUN pin goes low and the UCC28782 enters its low-power wait state. For LPM mode with the SET pin connected to REF, the minimum on-time of PWML can be further reduced to $t_{ON(MIN)}$, to allow the peak magnetizing current to be reduced below the level limited by t_{CSLEB} of the peak current loop. In this condition, operation of the LPM control loop is changed from a current-mode control to a voltage-mode control, so the on-time adjustment of PWML is not limited to t_{CSLEB}. When the silicon ACF is used and the SET pin is connected to REF, the high capacitance region of the low-side switch will introduce a higher peak current overshoot than the GaN ACF. With this feature, before f_{BUR} starts to fall below f_{LPM} and enters the audible frequency range of SBP mode, the peak current is low enough to limit the magnitude of audible excitation. For the LPM mode with GaN ACF by connecting the SET pin to AGND, the minimum on-time of PWML will still be limited by t_{CSLEB}.
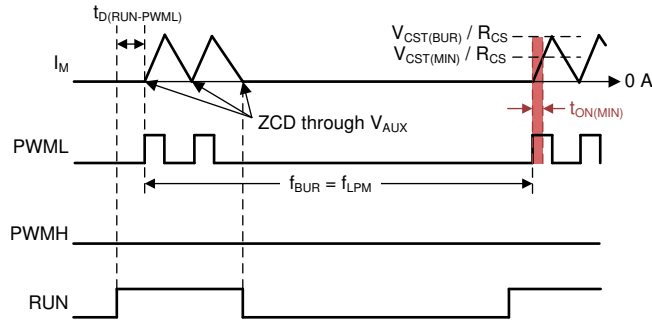

Figure 8-28. PWM Pattern in LPM

8.4.8 First Standby Power Mode (SBP1)

As V_{CST} drops to $V_{CST(MIN)}$, UCC28782 enters into SBP1 mode and PWMH continues to stay disabled. The purpose of SBP1 is to lower f_{BUR} in order to minimize power loss. SBP1 fixes N_{SW} at two and V_{CST} to $V_{CST(MIN)}$, while the burst off-time is adjusted to regulate the output voltage. As f_{BUR} is well below f_{LPM}, the switching-related loss can be minimized. In addition, lowering f_{BUR} forces both the gate driver and UCC28782 to remain in wait states longer to minimize the static power loss. The equivalent static current of the UCC28782 in SBP can be represented as

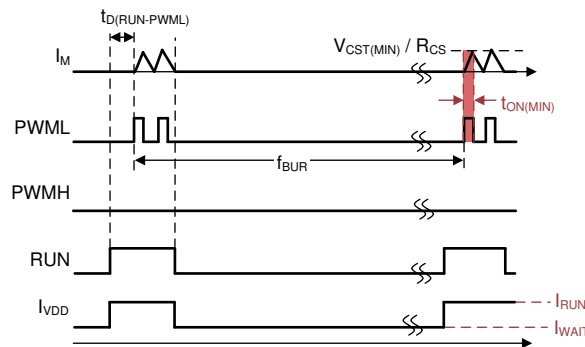$$I_{VDD(SBP)} = (I_{RUN} - I_{WAIT})(\frac{2}{f_{SW(SBP)}} + t_{D(RUN-PWML)})f_{BUR} + I_{WAIT}$$

(15)

Figure 8-29. PWM Pattern in SBP1

Product Folder Links: UCC28782

8.4.9 Second Standby Power Mode (SBP2)

When f_{BUR} is below the 8.5-kHz upper burst frequency threshold ($f_{SBP2(UP)}$), UCC28782 exits SBP1 mode and enters into SBP2 mode. Compared with the SBP1 mode, the pulse count is doubled and V_{CST} can be programmed by the IPC pin. The V_{CST} programmable range in SBP2 is between 0.27 V and 0.4 V. The purpose of SBP2 is to further lower f_{BUR} in order to minimize standby power.

The f_{BUR} condition to trigger the mode transition from SBP2 to SBP1 depends on the IPC pin voltage setting as well. If V_{IPC} is set lower than 0.9 V or the IPC pin is shorted to AGND, V_{CST} is equal to $V_{CST\_IPC(MIN)}$, and the mode transition occurs when f_{BUR} is increased above the same 8.5-kHz threshold. On the other hand, if V_{IPC} is set higher than 0.9 V, V_{CST} is higher than 0.27 V, and the mode transition occurs when f_{BUR} is increased above the 1.7-kHz lower burst frequency threshold ($f_{SBP2(LR)}$). The purpose of skipping the burst frequency range between 1.7 kHz and 8.5 kHz is to avoid the most sensitive audible frequency range to the human ear. The frequency skipping is only enabled, when the peak current is set higher by $V_{IPC} > 0.9$ V.
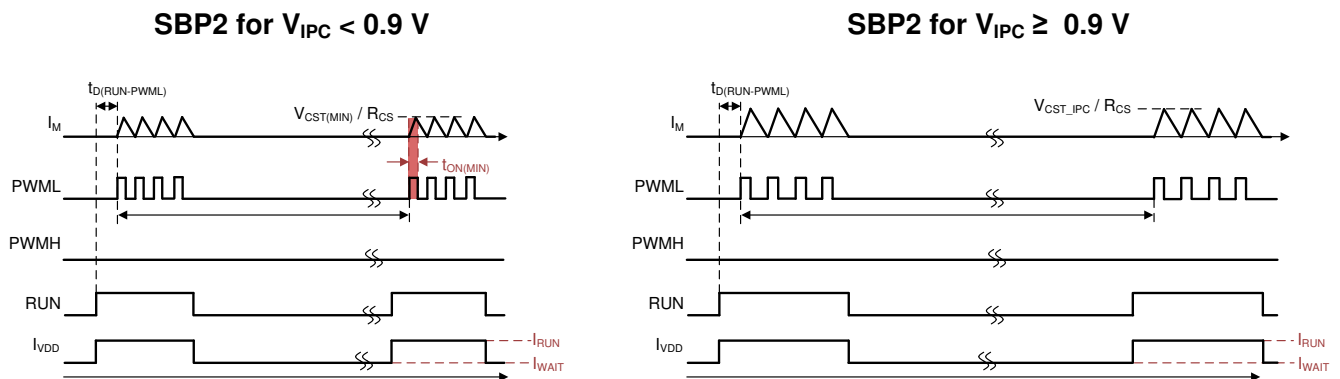
Copyright © 2019, Texas Instruments Incorporated

Figure 8-30. PWM Pattern in SBP2

8.4.10 Startup Sequence

Figure 8-31 shows the simplified block diagram related with the VDD startup function of UCC28782, and Figure 8-32 addresses the startup sequence. The detailed description on the startup waveforms is :

1. Time interval A: The UVLO circuit commands the two internal power-path switches (Q_{DDS} and Q_{DDP}) to close the connections between SWS, VDD, and P13 pins through two serial current-limiting resistors (R_{DDS} and R_{DDP}). The depletion-mode MOSFET (Q_S) starts sourcing charge current (I_{SWS}) safely from the high-voltage switch-node voltage (V_{SW}) to the VDD capacitor (C_{VDD}). Before V_{VDD} reaches 1.8 V, I_{SWS} is limited by the high-resistance R_{DDS} of 5 kΩ to prevent potential device damage if C_{VDD} or VDD pin is shorted to ground.
2. Time interval B: After V_{VDD} rises above 1.8 V, R_{DDS} is reduced to a smaller resistance of 0.5 kΩ. I_{SWS} is increased to charge C_{VDD} faster. The maximum charge current during VDD startup can be quantified by Equation 8.
3. Time interval C: As V_{VDD} reaches $V_{VDD(ON)}$ of 17 V, the ULVO circuit turns-off Q_{DDS} to disconnect the source pin of Q_S to C_{VDD}, and turns-off Q_{DDP} to break the gate-to-source connection of Q_S, so Q_S loses its current-charge capability. V_{VDD} then starts to drop, because the 5-V regulator on REF pin starts to charge up the reference capacitor (C_{REF}) to 5 V, for which the maximum charge current ($I_{SE(REF)}$) is self-limited at around 17 mA. After V_{REF} is settled, the UVLO circuit turns-on another power-path switch (Q_{P13}), so an internal 13-V regulator is connected to the P13 pin. The voltage on the P13 pin capacitor (C_{P13}) starts to be discharged by the regulator.
4. Time interval D: While discharging the recommended 1 μF on C_{P13} , the sink current of the 13-V regulator ($I_{P13(START)}$) is self-limited at around 2.2 mA, so it takes longer than 10 μs to settle to 13 V. If V_{P13} reaches 13 V in less than 10 μs, the P13 pin open fault is triggered to protect the device. Once V_{P13} has settled to 13 V without the fault event, RUN pin goes high and UCC28782 enters a run state with $I_{VDD} = I_{RUN}$.
5. Time interval E: There is a minimum 2.2-μs delay from RUN going high to PWML starting to switch in order to wake-up the gate driver and UCC28782. In this interval, the 2.8-Ω power path switch between the P13 pin

and the S13 pin is enabled, so the S13-pin decoupling capacitor (C_{S13}) is charged up and the charge current is supplied from C_{P13} and the P13 regulator. If 2.2-µs delay is timed out before V_{S13} reaches to the 10-V power good threshold (V_{S13_OK}), the PWML switching instance will be further delayed.

6. Time interval F: This is the soft-start region of peak magnetizing current. The first purpose is to limit the supply current if the output is short. The second purpose is to push the switching frequency higher than the audible frequency range during repetitive startup situations. At the beginning of V_O soft-start, the peak current is limited by two V_{CST} thresholds. The first V_{CST} startup threshold ($V_{CST(SM1)}$) is clamped at 0.2 V and the following second threshold ($V_{CST(SM2)}$) is 0.5 V. When $V_{CST} = V_{CST(SM1)}$, PWMH is disabled if the sampled VS pin voltage (V_{VS}) < 0.28 V, and the first five PWML pulses are forced to stay at this current level. After the sampled V_{VS} exceeds 0.28 V and the first five PWML pulses are generated, the peak current threshold changes from $V_{CST(SM1)}$ to $V_{CST(SM2)}$. In case of the inability to build up V_O with $V_{CST(SM1)}$ at the beginning of the V_O soft-start due to excessively large output capacitor and/or constant-current output load, there is an internal time-out of 0.7 ms to force V_{CST} to switch to $V_{CST(SM2)}$. At this moment, the BIN-pin capacitor voltage increases with V_O proportionally. If V_{BIN} is less than the 2.2-V UVLO threshold (VBIN(ON)), the bias switching regulator is disabled.

7. Time interval G: When V_{BIN} is higher than 2.2 V, the bias switching regulator enters into the boost switching mode, and starts to build up the V_{VDD} toward the 18.5-V regulation level.

8. Time interval H: When V_{VS} rises above 0.5 V, V_{CST} is allowed to reach $V_{CST(MAX)}$, so the ramp rate of V_O startup becomes faster. When PWML is in a high state, I_{VDD} can be larger than I_{RUN}, because the 5-V regulator provides the line-sensing current pulse (I_{VSL}) on the VS pin to sense V_{BULK} condition.

9. Time interval I: Higher V_{BIN} results in a lower switching frequency of the bias regulator, because more energy in the boost inductor (L_B) is transferred to C_{VDD} every switching cycle.

10. Time interval J: When V_{BIN} increases above the 15-V boost disable threshold, the V_{VDD} starts to decay back to the rectified auxiliary winding voltage minus the forward voltage drop of the boost diode (D_B). Also, when V_O gets close to the target regulation level, V_{CST} starts to reduce from $V_{CST(MAX)}$.

11. Time interval K: V_O and V_{CST} settle, and the auxiliary winding takes over the VDD supply.
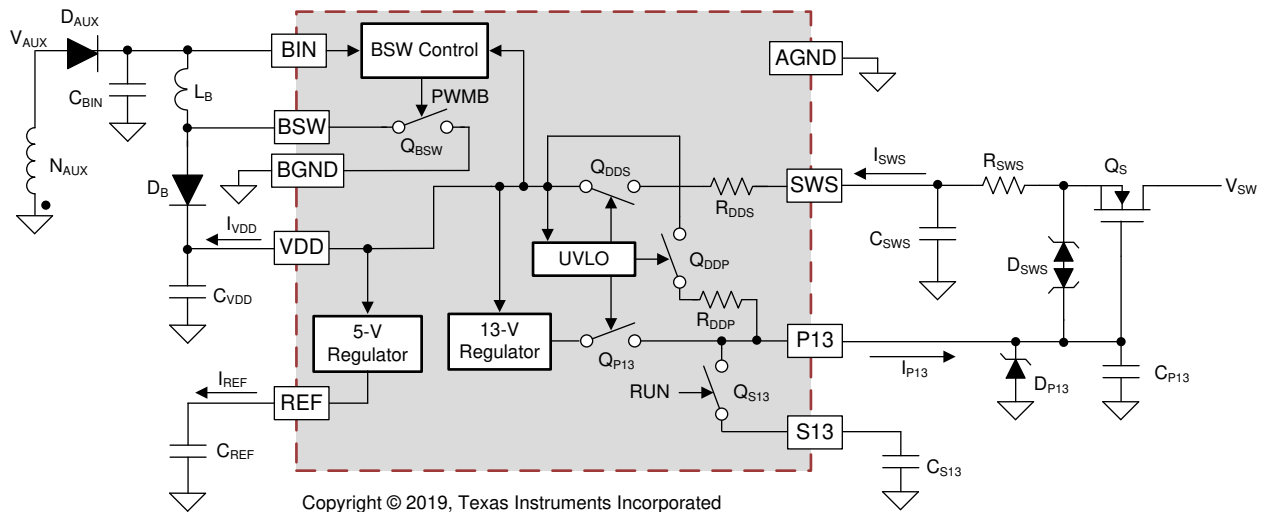
Figure 8-31. Functional Startup Block Diagram
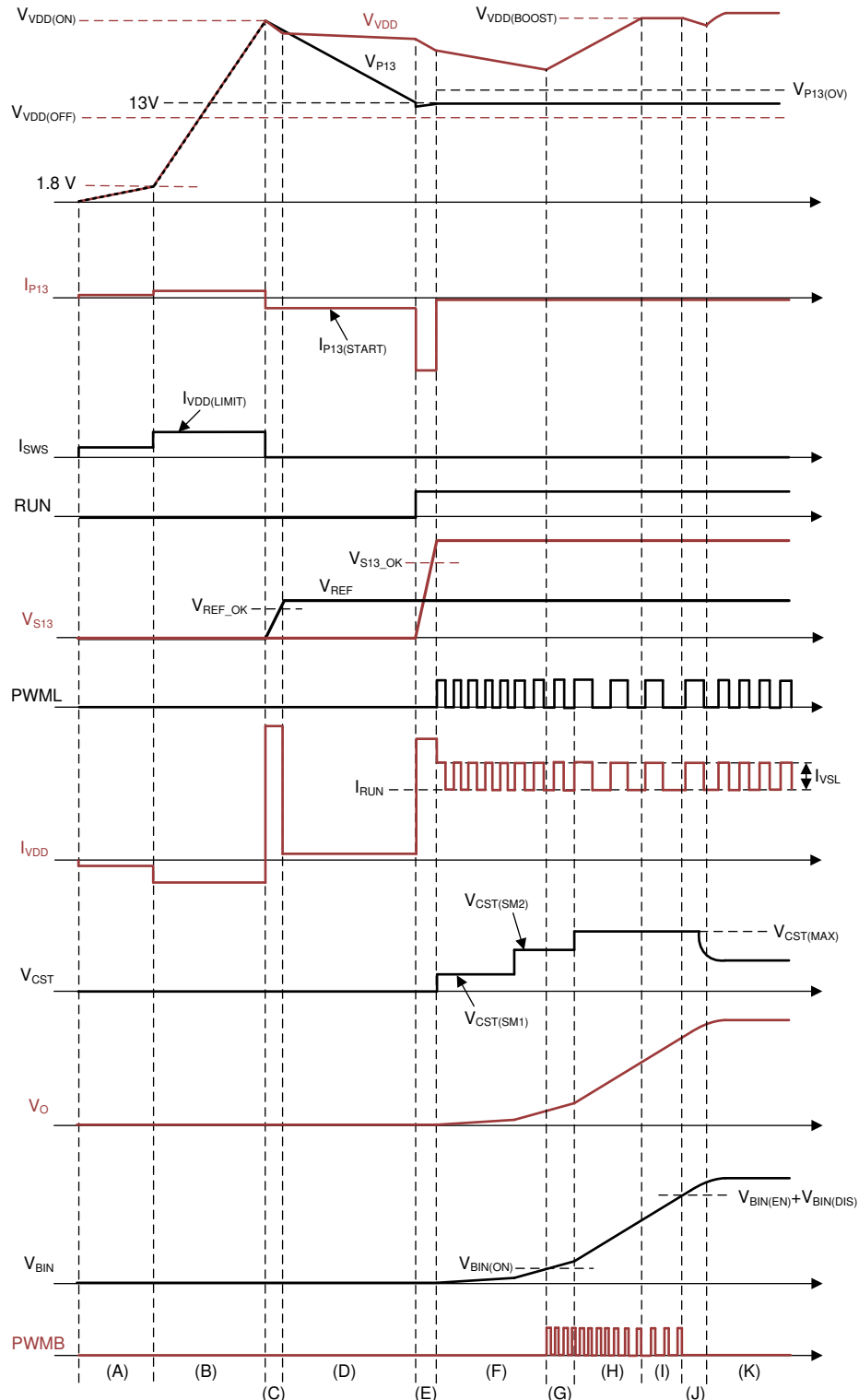
Copyright © 2019, Texas Instruments Incorporated

Figure 8-32. Startup Timing Waveforms

8.4.11 Survival Mode of VDD (INT_STOP)

When an output voltage overshoot occurs during step-down load transients, the V_O feedback loop commands the UCC28782 to stop switching quickly by increasing I_{FB}, in order to prevent additional energy from aggravating

Product Folder Links: *UCC28782*

the overshoot. Since V_{VDD} drops during this time, the typical way to prevent a controller from shutting down is to oversize the VDD capacitor (C_{VDD}) so as to hold V_{VDD} above $V_{VDD(OFF)}$. Instead, UCC28782 is equipped with survival-mode operation to hold V_{VDD} above $V_{VDD(OFF)}$ during a transient event. Therefore, the size of C_{VDD} can be significantly reduced and the PCB footprint for the auxiliary power can be minimized. Specifically, there is a ripple comparator to regulate V_{VDD} above a 13-V threshold, which is $V_{VDD(OFF)}$ plus $V_{VDD(PCT)}$ in the electrical table. The ripple regulator is enabled when the V_O feedback loop requests the UCC28782 to stop switching due to V_O overshoot.

The regulator initiates unlimited PWML pulses when V_{VDD} drops lower than 13 V, and stops switching after V_{VDD} rises above 13 V. Since V_{VDD} or V_{BIN} is lower than the reflected output voltage overshoot, most of the magnetizing energy is delivered to the auxiliary winding and brings V_{BIN} above 2.2 V or V_{VDD} above 13 V quickly. After V_O moves back to the regulation level, V_O feedback loop forces the UCC28782 to begin switching again by reducing I_{FB}, and the PWML and PWMH pulses are then controlled by the normal operating mode.

To prevent the controller from getting stuck in survival mode continuously or toggling between SBP and survival mode at zero load, some guidelines on the auxiliary power delivery path to VDD should be considered:

1. For fixed output voltage applications where the switching bias regulator is not required, the normal V_{VDD} level under regulated V_O must be designed to be above the 13-V threshold by an appropriate turns count for the auxiliary winding.
2. C_{VDD} should not be over-sized, but designed just large enough to hold $V_{VDD} > V_{VDD(OFF)}$ under the longest V_O soft-start time.
3. For variable output voltage applications where the bias regulator is used, C_{VDD} voltage can be ramped up faster if the turns count of the auxiliary winding (N_{AUX}) can be increased, because the switching bias regulator can process more energy from its input, especially under the lowest output voltage condition. The design limitation on N_{AUX} is the maximum voltage rating of BIN and BSW pins under the highest output voltage condition.
4. The BIN-pin capacitor (C_{BIN}) provides energy storage for the bias regulator. Higher C_{BIN} value, such as >33 uF, can help avoid excess survival-mode operation and reduce the potential increase of V_O under no-load conditions.
5. When the bias regulator is not required, an auxiliary resistor in series with the auxiliary rectifier diode (D_{AUX}) should not be too large of value, because the lower series impedance can help the VDD capacitor to charge faster.
6. When the bias regulator is used, a series auxiliary resistor should not be used since it limits the energy transfer to C_{BIN}. When the resistor is removed, one effective way to prevent C_{BIN} from being overcharged by high leakage inductance or other potential energy source is to parallel a small 24-V TVS diode between the BIN pin and the AGND pin. If there is a layout limitation which forces the TVS diode connected to BGND pin instead, the impedance between BGND and AGND needs to be as small as possible, such that the TVS diode can clamp the voltage below the two pin ratings more effectively.
7. If the output voltage dynamic range is very wide, such as from 3.3 V to 20 V, low auxiliary winding resistance less than 0.1 Ω and a Schottky-type auxiliary diode are recommended, such that the majority of the survival mode energy can be transferred to C_{BIN} instead of diverting to the output capacitor under the lowest output voltage condition.
8. Ensure good coupling between the auxiliary winding (N_{AUX}) and the secondary winding (N_S) of the transformer.

When the control loop is inevitably stuck in the survival mode at no load, it is important to ensure that the high-side switch can be responsive to the PWMH signal of the survival mode switching pattern entirely, such that the survival mode energy can be diverted to the boost converter and the risk of output voltage drifting higher than the regulation level can be mitigated. It is essential to choose the high-side driver with short power-on delay less than 10 µs.

8.4.12 Capacitor Voltage Balancing Function

ACF contains two energy storage devices on primary and secondary sides. One is the clamping capacitor (C_{CLAMP}) and the other is the output capacitor. When the PWMH signal is enabled, the clamping capacitor voltage (V_{CLAMP}) is close to the reflected output voltage (N_{PS} x V_O). When the PWMH is disabled in LPM mode, V_{CLAMP} becomes higher, because some of the leakage energy will be stored on C_{CLAMP}, instead of recycling

to the output, as it does in AAM and ABM. During the control mode transition from LPM to ABM, the capacitor voltage balancing current in the first PWMH on time is normally bigger than the following PWMH pulses. If the PWMH on time is too short to discharge C_{CLAMP}, a high di/dt change of the switching current will flow through the transformer winding at the turn-off instant of the high side switch, so the leakage inductance will introduce a high voltage stress across the secondary-side rectifier. Instead of using a strong RC snubber to damp the voltage spike or a lossy bleed resistor in parallel with C_{CLAMP}, UCC28782 automatically extends the first PWMH pulse width around 140% longer than the following PWMH pulse. When the high side switch turns off at lower di/dt current instance, the voltage stress can be reduced, and the efficiency compromise can be eliminated with this new voltage balancing function. Moreover, another possibility of triggering the on-time extension function is under the output voltage ramp down condition, which is a very common transient event of a USB-PD adapter. If the USB-PD controller on the secondary side is able to program the step size of the reference output voltage change, the LPM-to-ABM transition will occur during the voltage change. This behavior allows the V_{CLAMP} to follow the reflected output voltage change, and minimize the voltage stress on the rectifier.

However, some USB-PD controllers can not smoothly change the reference output voltage, but only offer a one-step voltage change to a lower reference level. This rapid change prevents the controller from switching in general, so the chance of voltage balancing during voltage transition is gone. Once the output voltage is settled to the lower level and PWMH is enabled back again, a big voltage difference between V_{CLAMP} and the reflected voltage occurs, and the magnitude of the balancing current may be large enough to create a high voltage stress and damage the secondary rectifier. In order to resolve this issue, UCC28782 utilizes a patent pending unique switching pattern in the survival mode to achieve the capacitor voltage balancing, as shown in the following figure.

With a rapid reference voltage ($V_{REF(Vo)}$) change, the feedback current (i_{FB}) increases and the controller enters into SBP1 mode. Since this event is like an output overshoot condition, the output voltage feedback loop prevents the ACF from switching and V_{VDD} drops. When V_{VDD} reaches the 13-V survival mode threshold, the unique burst packet contains a series of PWML pulses followed by a long PWMH pulse. The PWML pulse train helps to charge up the bootstrap capacitor voltage, so that the high-side switch can respond to the PWMH command. When the PWMH is in on state, the unbalanced voltage between V_{CLAMP} and the reflected V_{BIN} forces the additional energy to charge up C_{BIN}. The charge current becomes a useful energy source to keep V_{VDD} away from $V_{VDD(OFF)}$. At the same time, C_{CLAMP} can be discharged gradually. Through the multiple survival mode events, V_{CLAMP} can be discharged to be very close to the reflected output voltage, so the voltage stress can be reduced. The minimum number of PWML pulses of the first survival-mode event is 9. The rest survival-mode burst packets contain at least 3 PWML pulses.
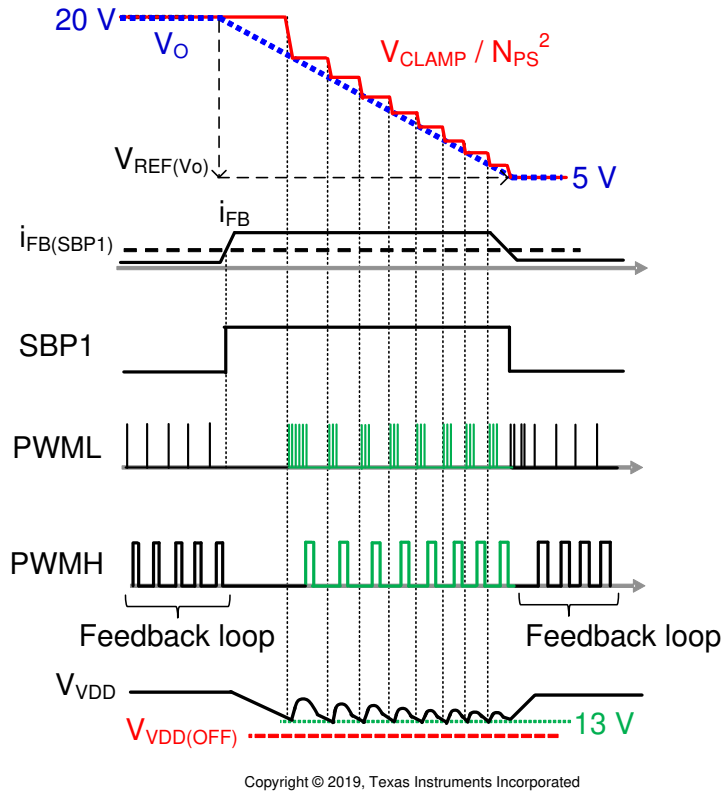
Figure 8-33. Capacitor Balancing During Output Voltage Transition

8.4.13 Device Functional Modes for Bias Regulator Control

When there is no overlapping between PWML on time and BSW on time and the survival mode is not triggered, there are two operating modes for the bias regulator when V_{BIN} is between the UVLO(ON) threshold and the disable threshold. The first is the constant peak current (CPC) control mode for a heavier VDD load condition, and the second is the burst mode (BM) control for a light VDD load condition. The 18.5-V regulation in CPC is maintained by varying the boost switching frequency, and the peak current of the boost inductor is fixed at approx. 0.33 A. The 18.5-V regulation in BM is maintained by changing the burst frequency with a constant peak current for each switching cycle of a burst packet. There are at least 3 switching cycles in a burst packet for BM. E.g. when a 22-µH boost inductor (L_B) is used, the mode transition point is at approx. 3-mA VDD load.

In CPC mode, the V_{VDD} regulation is achieved by changing the boost switching frequency (f_{BSW}) with a fixed 0.33-A peak current. When f_{BSW} is reduced to the minimum controllable frequency, the control loop will automatically transition into BM. Figure 8-34 illustrates the switching pattern in CPC mode operating in the transition mode or discontinuous conduction mode (DCM). The internal ZCD detection on BSW pin only allows the turn on instant of the next boost switching cycle to happen after the BSW-pin voltage falls below the BIN-pin voltage, so that the boost inductor current drops to zero first.

DCM Operation in CPC Mode

CCM Operation in COT Mode
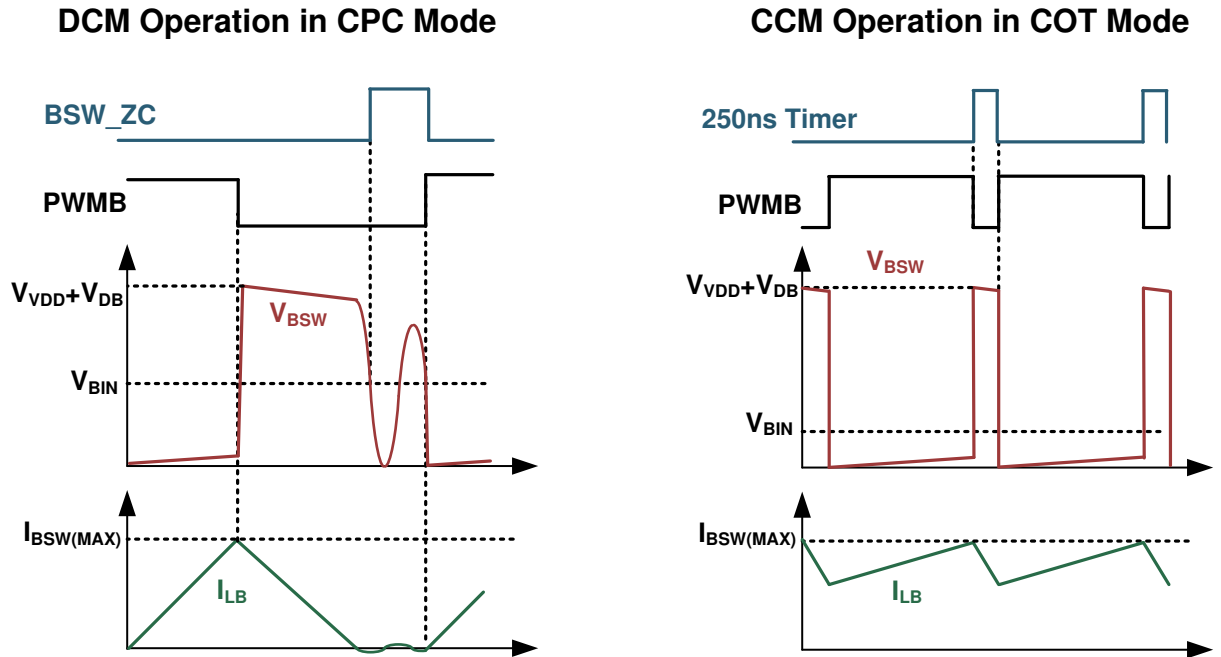
Copyright © 2019, Texas Instruments Incorporated

Figure 8-34. Switching Pattern of Boost Converter in CPC and COT Modes

If survival mode is enabled, the regulator will start switching regardless of V_{BIN} level and enter into constant off time (COT) control mode. The COT control mode disables the ZCD detection on the BSW pin and creates a 250-ns off time in order to force the regulator into the continuous conduction mode (CCM). More energy per cycle can transfer from the BIN-pin capacitor to the VDD capacitor in CCM, so V_{VDD} can be ramped up above the 13-V survival mode threshold faster than DCM, and minimize the survival mode energy transfer to the output capacitor on the ACF secondary side, as a result of the drop in V_{BIN}. When V_{VDD} is higher than 13 V, the regulator will automatically change the operation mode back to CPC or BM.

Besides survival mode, when the voltage difference between V_{VDD} and V_{BIN} is less than 1 V, the regulator will also disable ZCD detection and allows CCM operation. If ZCD is not disabled, the low voltage difference makes the demagnetization time of the boost inductor current very long, so V_{VDD} would not be able to build up to the regulation level. The CCM operation can transfer the energy to VDD capacitor quickly, so V_{VDD} can recover back to the regulation level.

8.4.13.1 Mitigation of Switching Interaction with ACF Converter

When the ACF control law is in AAM and ABM modes, the high side switch and ZVS control loop are enabled. In order to desensitize the boost switching noise interfering with the peak current loop and the ZVS control loop of the ACF converter, a unique switching misalignment function is activated for these two modes. When the ACF control law enters into LPM, SBP1, and SBP2 modes, the high side switch is disabled and the converter operates in valley switching, so switching misalignment function is disabled.

Since the bias regulator switch (Q_{BSW}) turns off at the highest peak current of the boost inductor, the lumped parasitic inductance from the BGND-pin bond wire and the PCB traces may create a voltage disturbance on the current sense signal, and might potentially result in prematurely turn-off of the PWML signal. When the PWML on time is disturbed, the ZVS control loop may introduce a small calculation error in the PWMH on time, so the ZVS switching may not be maintained for all switching cycles. To resolve this effect in UCC28782, the switching misalignment function will automatically avoid the intersection between the Q_{BSW} turn off edge and the PWML turn off edge to mitigate the noise interference. Specifically, if Q_{BSW} still stays in the on-state when the PWML signal reaches 70% on time, Q_{BSW} will be forced to be turned off earlier, so that the turn off instant for both the boost converter and ACF converter will not be aligned. Therefore, it is normal that the peak current of the boost inductor may not be consistent in AAM and ABM because of this misalignment function.
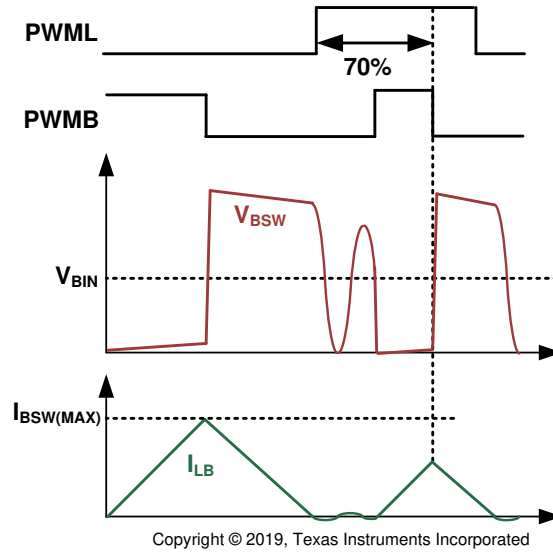
Figure 8-35. Switching Misalignment Function

Besides the above di/dt coupling effect, both the dV/dt coupling through the parasitic capacitance of the boost switching node on the BSW pin and the dB/dt coupling through the inductor flux change need to be considered in the design. It is important that the noise-sensitive traces or components must be kept away from the high dV/dt BSW node and the high dB/dt boost inductor flux loop in order to minimize the coupling. A shielded chip ferrite inductor or a powder core chip inductor is preferred to minimize the flux coupling. If a non-shielding chip ferrite inductor has to be used, the inductor must not be close to the noise-sensitive components and controller pins.

8.4.13.2 Protection Functions for the Bias Regulator

The protection features for the integrated bias regulator are summarized in Table 8-2.

Table 8-2. Fault Protections of the Bias Regulator

PROTECTION	SENSING	THRESHOLD	DELAY TO ACTION	ACTION
UVLO ON in boost mode	BIN voltage	$V_{BIN} \leq V_{BIN(ON)}$	None	Disable BSW switching
UVLO OFF in boost mode	BIN voltage	$V_{BIN} \leq V_{BIN(OFF)}$	1 Min. BSW LEB time (t_{BLEB})	Disable BSW switching
Max. disable threshold of boost mode	BIN voltage	$V_{BIN} \geq V_{BIN(DIS)} + V_{BIN(EN)}$	1 Min. BSW LEB time (t_{BLEB})	Disable BSW switching
Max. enable threshold of boost mode	BIN voltage	$V_{BIN} \geq V_{BIN(EN)}$	None	Disable BSW switching
Over current protection of boost mode	BSW current	$I_{BSW} \geq I_{BSW(MAX)}$	1 Min. BSW LEB time (t_{BLEB})	Minimum off-time of 4 µs before another BSW cycle
Missing ZCD timeout	BSW and BIN voltages	$V_{BSW} \geq V_{BIN}$	1 BSW pulse	Delay 700 µs and retry
VDD over-voltage protection	VDD voltage	$V_{VDD} \geq V_{BOVPTH}$	None	Disable BSW switching, and retry after $V_{VDD} \leq V_{BOVPR}$

8.4.13.3 BIN-Pin Related Protections

The 2.2-V UVLO(ON) threshold, 1-V UVLO(OFF) threshold, and the 30-V Max. voltage rating on the BIN pin allows the switching bias regulator to generate a usable bias power for a wide output voltage range application. The 15-V boost mode disable threshold allows the rectified auxiliary winding voltage to supply the bias power directly without the boost conversion loss. For example, when a 3.3-V to 21-V output voltage range is needed, the turns ratio between the auxiliary winding and the secondary winding should be set to one. The boost mode

operation will regulate V_{VDD} at 18.5 V for the 3.3-V to 14.9-V output range. The boost operation is disabled in the 15-V to 21-V output voltage range, V_{VDD} follows the output voltage change with a boost diode drop.

8.4.13.4 BSW-Pin Related Protections

In constant peak current (CPC) mode, the zero crossing detect (ZCD) on the BSW pin is critical to trigger the switching instant of the next cycle, so the missing ZCD timeout feature can avoid the risk of inability to sense ZCD in a given switching cycle. The normal peak current threshold is approx. 0.33 A for every BSW switching cycle. In DCM operation of the CPC mode, the ZCD detection is enabled to allow the boost inductor current to decay to zero before the next switching cycle. The internal detection network compares the V_{BSW} and V_{BIN} to qualify for a valid ZCD event. If the ZCD event can not be detected for a given cycle, a 700-μs timer is enabled and then the next switching cycle occurs after the 700-μs has expired.

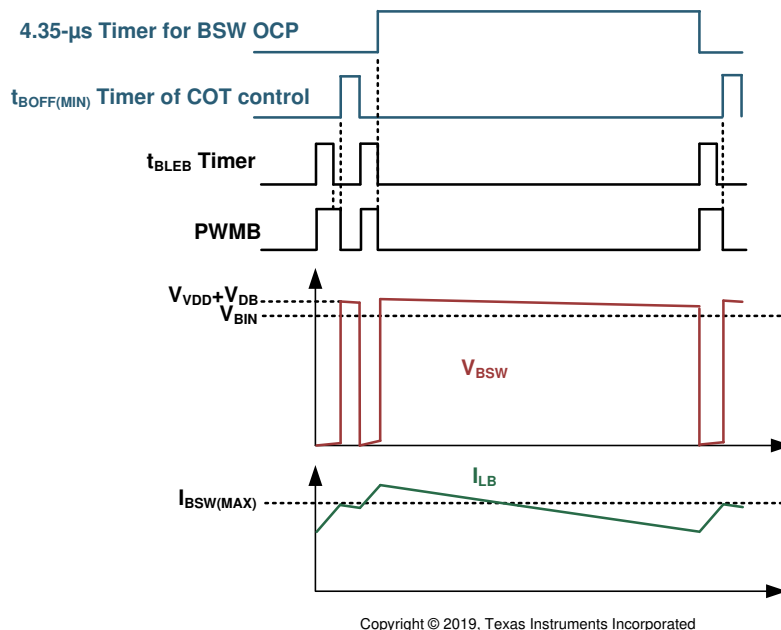

Copyright © 2019, Texas Instruments Incorporated

Figure 8-36. Operation Principle of Over Current Protection in Boost Mode

In constant off time (COT) mode, it is critical to prevent the inductor from reaching the saturation limit. Due to the CCM operation of COT mode, if the peak current is higher than 0.33 A after the 190-ns leading edge blank time, a 4.35-μs timer is enabled and then the next switching cycle cannot be initiated until after the 4.35 μs has elapsed. The operating principle is shown in Figure 8-36. This built-in over current protection prevents the chance of accumulated peak current overshoot in CCM, so the risk of boost inductor saturation can be eliminated.

8.4.14 System Fault Protections

The UCC28782 provides extensive protections on different system fault scenarios. The protection features are summarized in Table 8-3.

- The system fault responses of UCC28782A and UCC28782AD are all auto-recovery.
- The fault responses of UCC28782BDL are latch-off for OVP, OPP, PPL, OCP, SCP, OTP on the FLT pin, and OTP on the CS pin. The remaining faults are auto-recovery.
- The fault responses of UCC28782CD are latch-off for OVP and OTP on the FLT pin. The remaining faults are auto-recovery.

The response for any latch-off fault will disable the switching until a latch-reset event is detected. Resetting a latched fault can be achieved by either discharging $V_{VDD} < V_{VDD(RST)}$ or triggering the LZC detection on the XCD pin. Due to the large input bulk capacitor, V_{VDD} can stay above $V_{VDD(RST)}$ for a long time at no output load after the AC line is removed. If there is a need to reset the fault condition quickly for fast recovery of the output

voltage, the application circuit for the XCD pin can be used. The detection timing of the XCD pin allows the latch to be reset and initiate the switching attempt, after reapplying the AC line in less than 2 seconds.

Table 8-3. System Fault Protection

PROTECTION	SENSING	THRESHOLD	DELAY TO ACTION	ACTION BY UCC28782A, UCC28782AD	ACTION BY UCC28782BDL	ACTION BY UCC28782CD
VDD UVLO	VDD voltage	$V_{VDD(OFF)} \leq V_{VDD} \leq V_{VDD(ON)}$	None	UVLO reset	UVLO reset	UVLO reset
Brown-in detection	VS current	$I_{VSL} \leq I_{VSL(RUN)}$	4 PWML pulses	UVLO reset	UVLO reset	UVLO reset
Brown-out detection	VS current	$I_{VSL} \leq I_{VSL(STOP)}$	t_{BO} (60ms) plus 3 confirming PWML pulses	UVLO reset	UVLO reset	UVLO reset
Over-power protection (OPP)	CS voltage	$V_{CST(OPP)} \leq V_{CST} \leq V_{CST(MAX)}$	t_{OPP} (160 ms)	t_{FDR} restart (1.5s)	Latch off	t_{FDR} restart
Peak-power limit (PPL)	CS voltage	$V_{CST} \leq V_{CST(MAX)}$				
Over-current protection (OCP)	CS voltage	$V_{CS} \geq V_{OCP}$	3 PWML pulses	t_{FDR} restart	Latch off	t_{FDR} restart
Output short-circuit protection (SCP)	CS, VS, and VDD voltages	(1) $V_{VDD} = V_{VDD(OFF)}$ & $V_{CST} \geq V_{CST(OPP)}$; (2) $V_{VDD} = V_{VDD(OFF)}$ & $V_{VS} \leq V_{VS(SM2)}$	$\leq t_{OPP}$	t_{FDR} restart	Latch off	t_{FDR} restart
Output over-voltage protection (OVP)	VS voltage	$V_{VS} \geq V_{OVP}$	3 PWML pulses	t_{FDR} restart	Latch off	Latch off
Over-temperature protection on FLT pin (OTP)	FLT voltage	$R_{NTC} \leq R_{NTCTH}$	$t_{FLT(NTC)}$ (50 µs)	UVLO reset until $R_{NTC} \geq R_{NTCR}$	Latch off	Latch off
Over-temperature protection on CS pin (OTP)	CS voltage	$V_{CS} \geq V_{OCP}$	2 PWMH pulses	t_{FDR} restart	Latch off	t_{FDR} restart
Input over-voltage protection (IOVP)	FLT voltage	$V_{FLT} \geq V_{IOVPTH}$	$t_{FLT(IOVP)}$ (750 µs)	UVLO reset until $V_{FLT} < V_{IOVPTH} - V_{IOVPR}$	UVLO reset until $V_{FLT} < V_{IOVPTH} - V_{IOVPR}$	UVLO reset until $V_{FLT} < V_{IOVPTH} - V_{IOVPR}$
Thermal shutdown	Junction temperature	$T_J \geq T_{J(STOP)}$	3 PWML pulses	UVLO reset	UVLO reset	UVLO reset

8.4.14.1 Brown-In and Brown-Out

The VS pin senses the negative voltage level of the auxiliary winding during the on-time of the low-side switch (Q_L) to detect an under-voltage condition of the input AC line. When the bulk voltage (V_{BULK}) is too low, UCC28782 stops switching and no V_O restart attempt is made until the AC input line voltage is back into normal range. As Q_L turns on with PWML, the negative voltage level of the auxiliary winding voltage (V_{AUX}) is equal to V_{BULK} divided by primary-to-auxiliary turns ratio (N_{PA}) of the transformer, which is N_P / N_A. During this time, the voltage on VS pin is clamped to about 250 mV below GND. As a result, V_{AUX} can create a line-sensing current (I_{VSL}) out of the VS pin flowing through the upper resistor of the voltage divider on VS pin (R_{VS1}). With I_{VSL} proportional to V_{BULK}, it can be used to compare against two under-voltage thresholds, $I_{VSL(RUN)}$ and $I_{VSL(STOP)}$.

The target brown-in AC voltage ($V_{AC(BI)}$) can be programmed by the proper selection of R_{VS1}. For every UVLO cycle of VDD, there are at least four initial test pulses from PWML to check I_{VSL} condition. I_{VSL} of the first test pulse is ignored. If $I_{VSL} \leq I_{VSL(RUN)}$ is valid for the next three consecutive test pulses, the controller stops switching, the RUN pin goes low, and a new UVLO start cycle is initiated after V_{VDD} reaches $V_{VDD(OFF)}$. On the other hand, if $I_{VSL} > I_{VSL(RUN)}$ occurs, V_O soft start sequence is initiated.

$$R_{VS1} = \frac{V_{AC(BI)}\sqrt{2}}{N_{PA} \times I_{VSL(RUN)}} = \frac{N_A}{N_P} \frac{V_{AC(BI)}\sqrt{2}}{365\mu A}$$

(16)

The brown-out AC voltage ($V_{AC(BO)}$) is set internally by approximately 83% of $V_{AC(BI)}$, which provides enough hysteresis to compensate for possible sensing errors through the auxiliary winding.

$$V_{AC(BO)} = \frac{I_{VSL(STOP)}}{I_{VSL(RUN)}} V_{AC(BI)} = 0.83 \times V_{AC(BI)}$$

(17)

A 60-ms timer (t_{BO}) is used to bypass the effect of line ripple content on the I_{VSL} sensing. Only when the $I_{VSL} \leq I_{VSL(STOP)}$ condition lasts longer than 60 ms (i.e. typically three line cycles of 50 Hz) and 3 additional switching cycles verify the condition, the brown-out fault is triggered. If switching is interrupted, the brown-out fault will remain pending without shut-down until the 3 verification cycles complete. The fault is reset after V_{VDD} reaches $V_{VDD(OFF)}$. Figure 8-37 shows an example of the timing sequence of brown-out and brown-in protections for the case of an actual input brown-out condition.
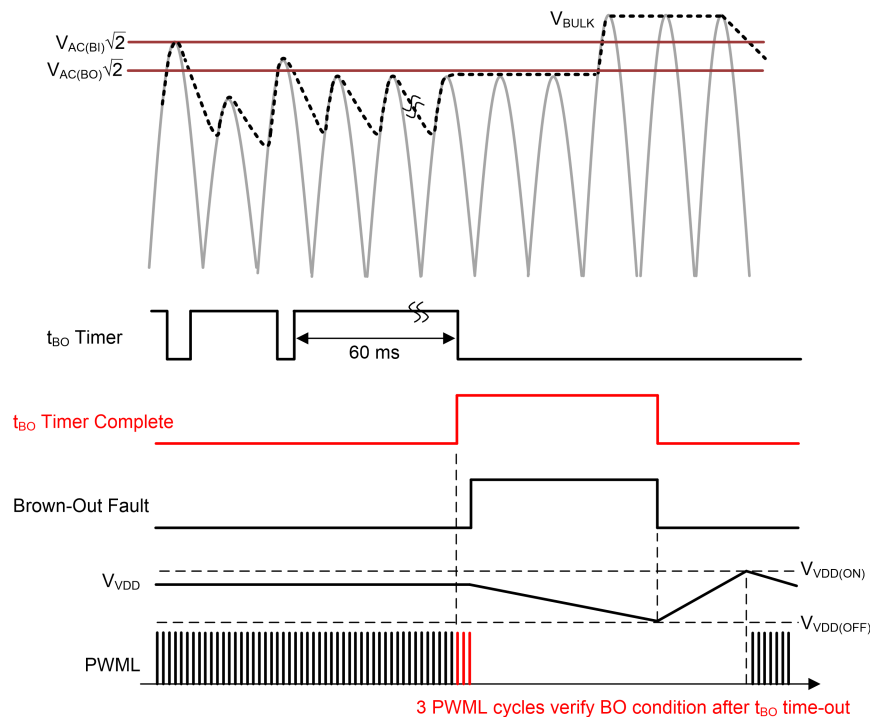

Figure 8-37. Timing Diagram of Brown-Out/Brown-In Response on AC Line Events

The t_{BO} timer is started at the moment $I_{VSL} \leq I_{VSL(STOP)}$ is detected during the PWML on-time. The timer is cleared when $I_{VSL} > I_{VSL(STOP)}$ is detected. In the case of an overshoot voltage on the output, switching will stop until the output voltage recovers to the regulation level. If the t_{BO} timer is triggered by $I_{VSL} \leq I_{VSL(STOP)}$ while in the valley of the bulk ripple voltage, and then switching is stopped the status of I_{VSL} cannot be detected and updated. The timer cannot be cleared without switching to sample I_{VSL}, and the 60-ms timer may elapse even though no brown-out condition exists. To prevent an unwarranted shut-down, the 3 additional switching cycles sample the condition once switching does resume, to verify or dismiss the pending apparent brown-out fault. An

extended output overshoot condition longer than t_{BO} can result from a sudden load drop combined with a drop in the regulation reference due to reduction of cable compensation. Figure 8-38 shows an example of the timing sequence for the case of an apparent brown-out cancelled by 3 verifying pulses.
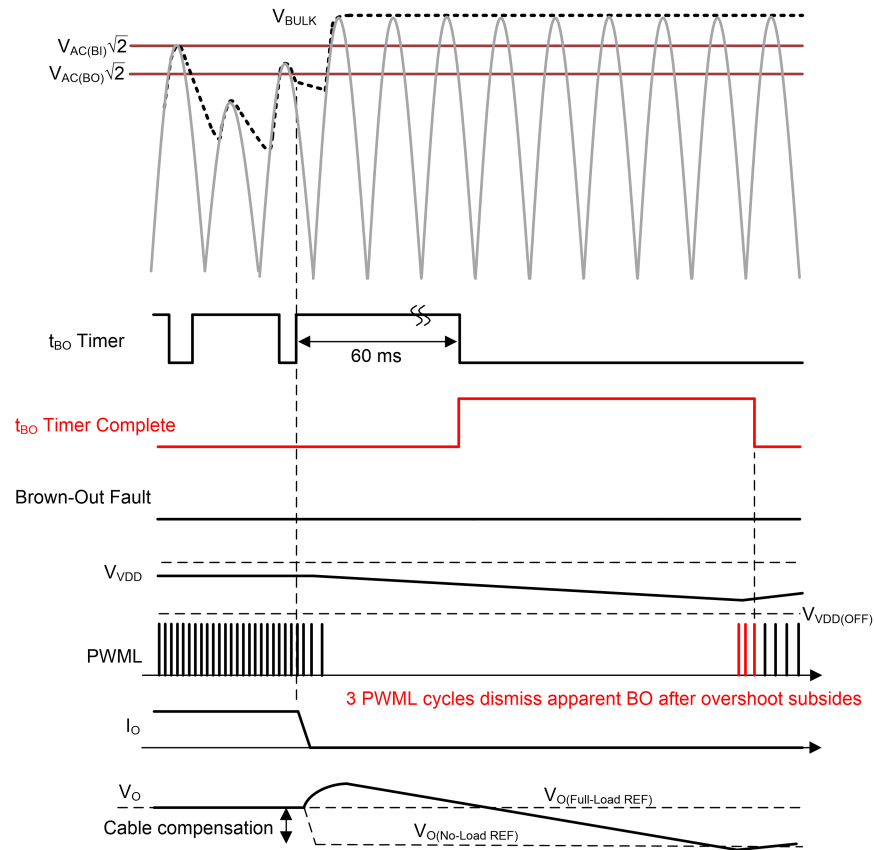

Figure 8-38. Timing Diagram of Brown-Out Response on Extended Output Overshoot

8.4.14.2 Output Over-Voltage Protection (OVP)

The VS pin is used to sense the positive voltage level of the auxiliary winding voltage (V_{AUX}) to detect an over-voltage condition of V_O. When an OVP event is triggered, the auto-recovery version of OVP stops switching and there is a 1.5-s fault recovery time (t_{FDR}) before any V_O restart attempt is made. As Q_L turns off, the settled V_{AUX} is equal to (V_O+V_F) x N_{AS}, where N_{AS} is the auxiliary-to-secondary turns ratio of the transformer, N_A / N_S, and V_F is the forward voltage drop of the secondary-side rectifier. The VS pin senses V_{AUX} through a voltage divider formed by R_{VS1} and R_{VS2}. The pin voltage (V_{VS}) is compared with an internal OVP threshold (V_{OVP}). If $V_{VS} \geq V_{OVP}$ condition is qualified for three consecutive PWML pulses, the controller stops switching, brings RUN pin low, and initiates the 1.5-s time delay. During this long delay time, only the UVLO-cycle of V_{VDD} is active, and there are no test pulses of PWML. After the 1.5-s timeout is completed and V_{VDD} reaches the next $V_{VDD(OFF)}$, a normal start sequence begins. The calculation of R_{VS2} is

$$R_{VS2} = \frac{R_{VS1} \times V_{OVP}}{N_{AS} \times (V_{O(OVP)} + V_F) - V_{OVP}} = \frac{R_{VS1} \times 4.5V}{(N_A / N_S)(V_{O(OVP)} + V_F) - 4.5V}$$

(18)

The long t_{FDR} timer helps to protect the power stage components from the large current stress during every restart. After OVP is triggered, V_O may be brought down quickly by the output load current. If OVP were reset directly after one UVLO cycle of VDD without the 1.5-s delay, the first PWMH pulse turns on Q_H under the condition of a large voltage difference between the high clamp capacitor voltage (V_{CLAMP}) and the low reflected voltage. A large current can flow through the clamp switch (Q_H) and secondary rectifier. Therefore, the 1.5-s timer of UCC28782 allows V_{CLAMP} to drop to a lower voltage level through a bleeding resistor (R_{BLEED}) in parallel

with C_{CLAMP} before the next V_O restart attempt, such that the current stress can be minimized. A large R_{BLEED} can be used with the long time-out to minimize the impact on standby power. For example, to discharge V_{CLAMP} to 10% of its normal level in 1.5 s, only 3 mW of additional standby power is added with R_{BLEED} = 2.8 MΩ and C_{CLAMP} = 220 nF. The Timing Diagram of C_{CLAMP} Discharging During 1.5-s Recovery Time illustrates the timing sequence as V_{CLAMP} is discharged to a residual voltage ($V_{RESIDUAL}$) in 1.5 s. R_{BLEED} also helps to reduce the voltage overcharge on the clamp capacitor in LPM, SBP1, and SBP2 modes in which PWMH is disabled, so the voltage stress in the passive-clamp operation can be controlled.
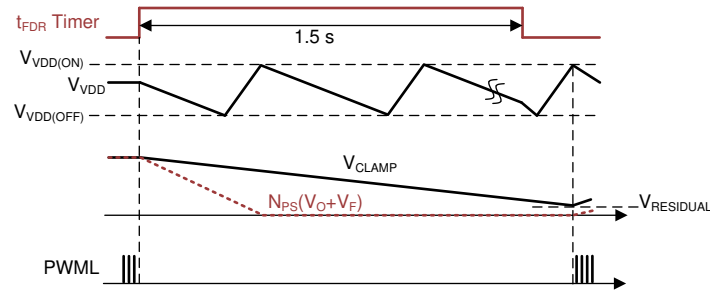

Figure 8-39. Timing Diagram of C$_{CLAMP}$ Discharging During 1.5-s Recovery Time

8.4.14.3 Input Over Voltage Protection (IOVP)

The UCC28782 provides an input OVP function on the FLT pin. Figure 8-40 shows the application circuit for the input OVP sensing. A resistor divider senses the bulk capacitor voltage, and the IOVP fault is triggered when V_{FLT} > 4.5 V for longer than 750 μs. The 750 μs delay helps to desensitize the abrupt bulk voltage spike during the line surge condition, such that the output voltage will not drop accidentally. After the IOVP fault is asserted, the switching will be terminated immediately and V_{VDD} will restart. When V_{VDD} reaches $V_{VDD(ON)}$ of the following VDD cycle, the controller will check V_{FLT} first before switching, to avoid the switching device from being exposed to a high-voltage stress condition. The fault will be cleared when V_{FLT} < 4.43 V.

If longer than 750 μs delay is required, a filter capacitor between the FLT pin and AGND pin can create additional programmable delay. If the filter capacitor is too large, it may trigger the OTP fault on the FLT pin, if the ramp up time for V_{FLT} to rise above V_{NTCTH} is longer than $t_{FLT(NTC)}$ after the RUN pin is pulled high. The resistor divider design does not need to consider the offset voltage effect from the 50 μA current source out of the FLT pin, because the controller will disable the current source once V_{FLT} > 2.5 V.

The goal of the internal 5.5-V clamp device on the FLT pin is to protect the pin from exceeding the voltage limit when one of the IOVP upper sensing resistor fails short. The maximum clamp current is 150 μA, so the resistor divider design needs to consider this limitation.
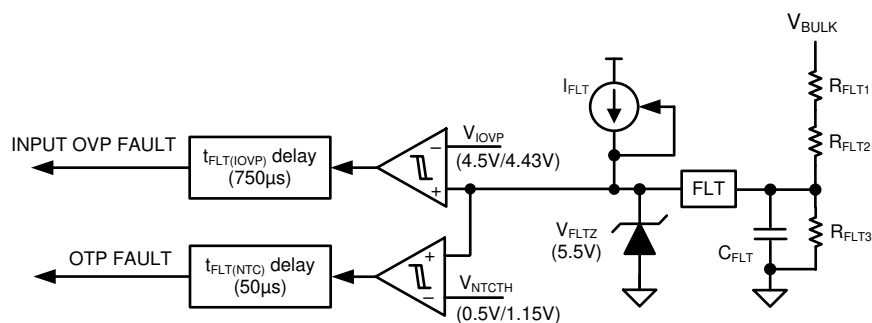
Copyright © 2019, Texas Instruments Incorporated

**Figure 8-40. Bulk Capacitor Voltage Sensing for Input OVP**

8.4.14.4 Over-Temperature Protection (OTP) on FLT Pin

The UCC28782 uses an external NTC resistor (R_{NTC}) tied to the FLT pin to program a thermal shutdown temperature near the hotspot of the converter. The NTC shutdown threshold (V_{NTCTH}) of 0.5 V with an internal 50-µA current source flowing through R_{NTC} results in a 10-kΩ thermistor shutdown threshold. If the NTC resistance stays lower than 10 kΩ for more than 50 µs, an OTP fault event is triggered. The 50-µs delay ($t_{FLT(NTC)}$) allows a filter capacitor (C_{FLT}) to be placed between the FLT pin and the AGND pin, when the NTC resistor is located far away from the controller but close to the hot spot. To avoid the OTP fault from false trigger as RUN goes high, C_{FLT} should be designed to allow V_{FLT} increased above V_{NTCTH} within $t_{FLT(NTC)}$. On the other hand, if the NTC resistor is close to the controller and there is no potential noise coupling path to the sensing traces, C_{FLT} is not needed.

For auto-recovery mode, the 0.5-V threshold is increased to 1.15 V after the OTP fault, so the NTC resistance has to increase above 23 kΩ to reset the OTP fault. This threshold change provides a safe temperature hysteresis to help the hot-spot temperature cool down before the next V_O restart attempt, reducing the thermal stress to the components. If the FLT pin is not used, the pin can be left floating but can not be connected to REF pin, since the line OVP will be falsely triggered.

The thermal issue in the heavy output load condition is the main design consideration for OTP, and the heavy load operating mode, AAM, allows the controller to stay in the run state continuously, so the 50-µs delay allows V_{FLT} to trigger OTP. Based on the practical BUR-pin setting, 50% to 60% load is operated in AAM. The 50-µA current source is disabled in the burst off time of the light load modes such as ABM, LPM, SBP1, and SBP2, in order to save standby power. However, when the run state becomes shorter than the 50-µs in these modes but the current source is disabled in the wait state, the OTP will not be able to trigger because there is not enough time to detect the fault. Therefore, if certain design considerations still require the OTP to be armed in light load modes, a second OTP configuration can be considered by reusing the 4.5-V threshold of input OVP. As shown in Figure 8-41, the upper NTC resistor and the lower resistor form a resistor divider from the REF pin to the FLT pin. The 750-µs delay is independent to the wait state condition of controller, so the OTP fault can still be triggered in the light load mode. This configuration provides auto-recovery mode only.
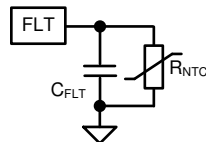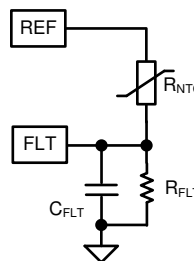
Copyright © 2019, Texas Instruments Incorporated

Figure 8-41. Two Connections to Implement OTP on the FLT Pin

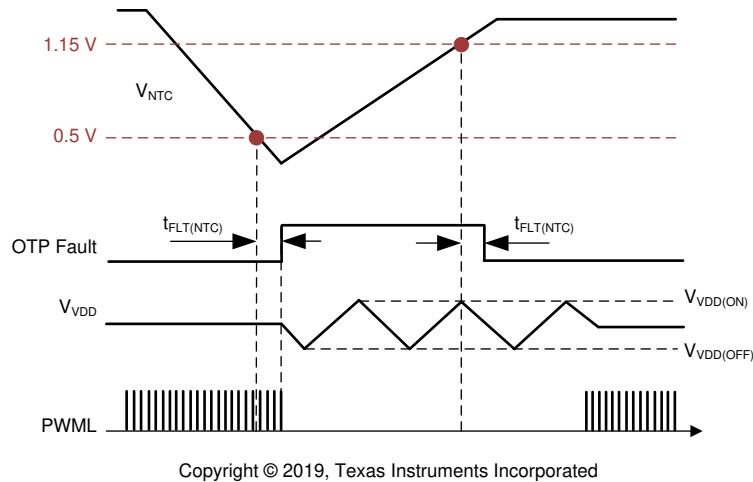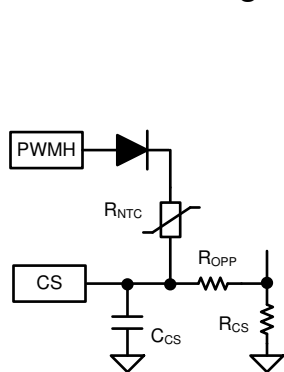Copyright © 2019, Texas Instruments Incorporated

Figure 8-42. OTP Timing Diagram for a NTC between the FLT Pin and AGND Pin

### 8.4.14.5 Over-Temperature Protection (OTP) on CS Pin

In case the FLT pin is already used for the input OVP sensing, UCC28782 provides the third and fourth OTP functions on the CS pin. The two configurations do not affect the current sense signal on the CS pin and the OPP level, because the two sensing circuits are only biased after PWML is off. Figure 8-43 shows the two application circuits. For the third OTP configuration, when the PWMH pin is pulled high, R_{NTC} and R_{OPP} form a resistor divider to create a temperature-dependent voltage signal on the CS pin. When the voltage exceeds the 1.2-V threshold sampled before the end of the demagnetization time (T_{DM}) for two successive cycles, the OTP fault will be triggered. The OTP sensing circuit will not affect the operation of the peak current loop, since the PWMH is pulled low in the PWML on time duration. For auto-recovery mode, the long 1.5-s timer starts and the controller stays in fault state without switching. This long recovery time provides a temperature hysteresis to help the hot-spot temperature cool down before the next V_O restart attempt. Compared with the first OTP configuration on the FLT pin, this configuration allows the OTP armed in both AAM and ABM, so the OTP can still be triggered at around 25% output load. Compared with the second OTP configuration from FLT pin, this configuration supports both auto-recovery and latch-off modes.

The fourth configuration with a small-signal PMOS is the most comprehensive way to cover a wide output load range and support both auto-recovery and latch-off modes at the same time. The RUN pin is used to bias the sensing circuit, and the PMOS gate is controlled by the PWML pin to only allow the detection to occur when PWML is low.

3rd OTP Sensing   **4th OTP Sensing**
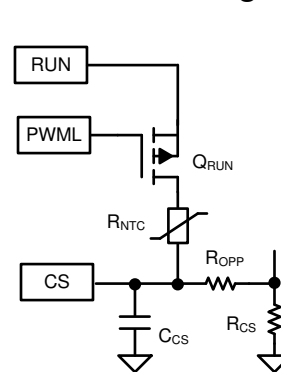
Copyright © 2019, Texas Instruments Incorporated

Figure 8-43. Two Connections to Implement OTP on the CS Pin

Product Folder Links: *UCC28782*

8.4.14.6 Programmable Over-Power Protection (OPP)

The over-power protection (OPP) enables the ACF to operate in an over-power condition for a limited amount of time, so the UCC28782 can support a power stage design with peak power requirements. As shown in Figure 8-44, when V_{CST} is higher than the threshold voltage of the OPP curve ($V_{CST(OPP)}$), a 160-ms timer starts. For the auto-recovery mode, if V_{CST} remains higher than $V_{CST(OPP)}$ continuously for 160 ms, the 1.5-s timer starts and the controller stays in fault state without switching. This long recovery time reduces the average current during a sustained over-power event. The system benefits includes the reduction of thermal stress in high density adapters and the protection of its output cable.

The OPP function uses I_{VSL} as a line feed-forward signal to vary $V_{CST(OPP)}$ depending on V_{BULK}, in order to make the OPP trigger point constant over a wide line voltage range. The UCC28782 allows programmability of the OPP curve by adding a line-compensation offset voltage on the CS pin through a resistor (R_{OPP}) connected between the CS pin and current-sense resistor (R_{CS}). An internal current source flowing out of CS pin creates the offset voltage on R_{OPP}. This current level is equal to I_{VSL} divided by a constant gain of K_{LC}. As R_{OPP} increases, the OPP trigger point becomes lower at high line, so lower peak magnetizing current is allowed to run continuously.

The OPP function uses V_{VS} as an output voltage feed-forward signal to modify the line-dependent $V_{CST(OPP)}$ curve into the two different sets, such that the OPP trigger point can be more consistent across a wide output voltage range. The higher OPP threshold under $V_{VS} > 2.5$ V contains two piece-wise linear regions, and the lower OPP threshold under $V_{VS} < 2.4$ V contains one piece-wise linear region.

The highest threshold of OPP curve ($V_{CST(OPP1)}$) of 0.6 V helps to determine R_{CS} value at $V_{BULK(MIN)}$.

$$R_{CS} = \frac{V_{CST(OPP1)}}{\dfrac{P_{O(OPP)}}{V_{BULK(MIN)}\eta}\dfrac{2}{D_{MAX}} - \dfrac{V_{BULK(MIN)}t_{D(CST)}}{L_M}}$$

(19)

where $P_{O(OPP)}$ is the output power that triggers OPP, and $t_{D(CST)}$ is the sum of all delays in the peak current loop which contributes additional peak current overshoot. $t_{D(CST)}$ consists of propagation delay of the low-side driver, current sense filter delay (R_{OPP} x C_{CS}), internal CS comparator delay ($t_{D(CS)}$), and nonlinear capacitance delay of Q_L. After R_{CS} is determined, R_{OPP} can be adjusted to keep a similar OPP point at highest line. Note that setting the OPP trigger point too far away from the full power may introduce more challenge on the thermal design, since the converter runs continuously with more power as long as the corresponding peak current is slightly less than OPP threshold.
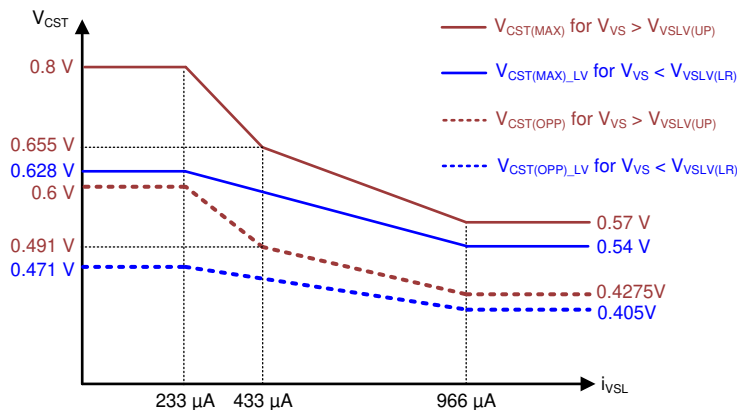
Copyright © 2019, Texas Instruments Incorporated
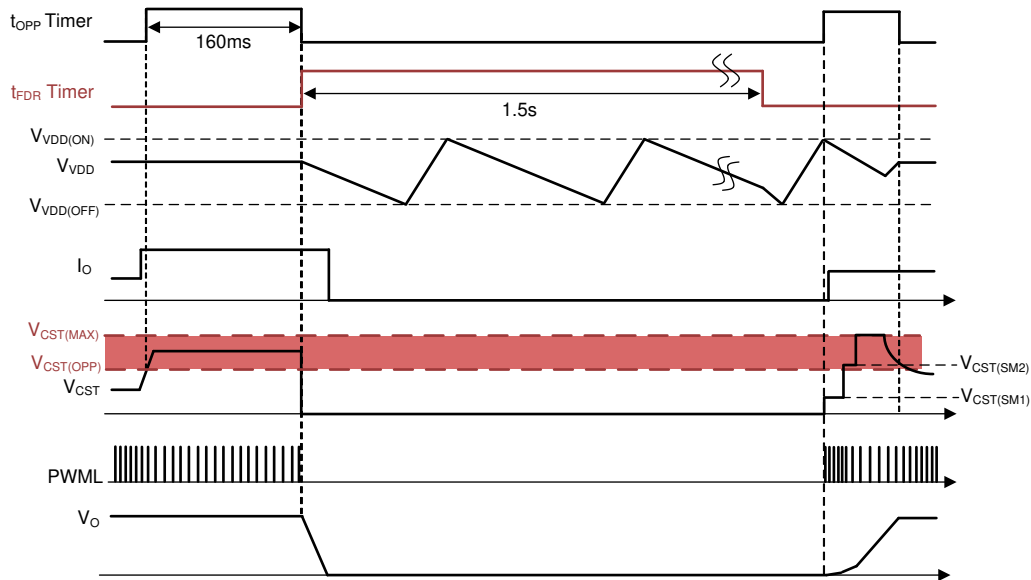
Figure 8-44. V_{CST} OPP curve across I_{VSL}

Product Folder Links: *UCC28782*

Figure 8-45. Timing Diagram of OPP

8.4.14.7 Peak Power Limit (PPL)

The peak current threshold of the OPP curve is used to initiate the 160-ms timer, while the peak power limit (PPL) determines the highest controllable peak current of the peak current loop, $V_{CST(MAX)}$. Regardless of V_{VS}, the ratio between $V_{CST(MAX)}$ and $V_{CST(OPP)}$ is fixed at approx. 4/3. In other words, this feature provides the highest "short duration" peak power ($P_{O(MAX)}$) that the converter can reach. The line-dependent PPL curve is able to achieve a consistent peak power level over a wide input voltage range. For example, to supply a highest peak power of 150%, R_{CS} should be chosen to ensure that the peak current at 150% load and $V_{BULK(MIN)}$ must not be above $V_{CST(MAX)}$. Then, the threshold of the OPP power ($P_{O(OPP)}$) can be programmed to around 112% to support 150% peak power design, based on the following equation. Additionally, before V_O reaches steady state during V_O soft-start, the highest V_{CST} can also reach to $V_{CST(MAX)}$. The transformer must have enough design margin separating its maximum flux density from the saturation limit of the core material under the peak current level in PPL.

$$P_{O(OPP)} = \frac{V_{CST(OPP1)}}{V_{CST(MAX)}} P_{O(MAX)} = \frac{0.6V}{0.8V} P_{O(MAX)}$$

(20)

8.4.14.8 Output Short-Circuit Protection (SCP)

When an output short-circuit is applied, the peak current reaches the PPL limit and triggers the 160-ms OPP fault timer. During this event, the VDD power supply is lost due to the auxiliary winding voltage being close to 0 V. Without additional short-circuit detection, if V_{VDD} reaches $V_{VDD(OFF)}$ before the 160-ms timeout, the 1.5-s recovery time for the OPP fault cannot be triggered but only a UVLO recycle is performed. To remedy this scenario, as V_{VDD} reaches $V_{VDD(OFF)}$, the auto-recovery version of UCC28782 checks two additional parameters to identify the short-circuit event at the output, and triggers the fault response without waiting for 160 ms to expire. Specifically, when V_{VDD} reaches $V_{VDD(OFF)}$, if either V_{CST} is greater than the OPP threshold ($V_{CST(OPP)}$) or the VS-pin voltage is less than 0.5 V, the 1.5-s recovery delay is initiated for auto-recovery mode. With this additional layer of intelligence, the average load current during continued short-circuit event can be greatly reduced, and thus also the thermal stress on the power supply.

8.4.14.9 Over-Current Protection (OCP)

The UCC28782 operates with cycle-by-cycle primary-peak current control. The normal operating range of the CS pin is between $V_{CST(MIN)}$ and $V_{CST(MAX)}$. If the CS-pin voltage exceeds the 1.2-V over-current level, any time after the internal leading edge blanking time (t_{CSLEB}) and before the end of the transformer demagnetization, for three consecutive PWML cycles, the device stops switching, RUN pin goes low, and the fault response is triggered.

Similar to OVP, OPP, and SCP, only the UVLO-cycle of VDD is active, there are no test PWML pulses at all. For auto-recovery mode, after the 1.5-s time-out is completed and V_{VDD} reaches the next $V_{DD(OFF)}$, a normal start sequence begins.

8.4.14.10 External Shutdown

The REF pin can be used as an external shutdown function by shorting this pin to AGND with a small-signal control switch. This provides an additional design flexibility for the control function extension with external circuitry. When the REF-pin voltage drops lower than its power good threshold, the switching action will be terminated and V_{VDD} will drop to $V_{VDD(OFF)}$, so the controller will need to restart V_{VDD}. When the external switch keeps shorting the REF pin continuously, switching action is inhibited until the external pull-down on REF is released. During the switch-short condition, the falling slope of V_{VDD} will drop faster than normal case because the 17-mA over-current limit of the REF regulator discharges VDD capacitor faster than the normal I_{VDD} current in run state and wait state.

8.4.14.11 Internal Thermal Shutdown

The internal over-temperature shutdown threshold is higher than 125°C. If the junction temperature of the device reaches this threshold, the device initiates a UVLO reset and restart fault cycle. If the temperature is still high at the end of the UVLO cycle, the protection cycle repeats. This internal protection is not suitable as a substitute for the NTC for hot-spot temperature protection. The NTC thermistor can provide more accurate and remote temperature sensing with less compromise on PCB layout.

8.4.15 Pin Open/Short Protections

As summarized in Table 8-4, UCC28782 strengthens the protections of several critical pins under "open" and "short" conditions, such as CS, P13, RDM, and RTZ pins. The pin protections are all in auto-recovery modes. UCC28782A does not have the XCD-pin over voltage protection. All "short" conditions are defined as short-circuits to AGND.

Table 8-4. Protections for Open and Short of Critical Pins

PROTECTION	SENSING	CONDITION	DELAY TO ACTION	ACTION
CS pin short	PWML on-time at first PWML pulse only	> 2 μs (V_{SET} = 5 V)	none	t_{FDR} restart (1.5 s)
		> 2 μs (V_{SET} = 0 V, $R_{RDM} \geq R_{RDM(TH)}$)		
		> 1 μs (V_{SET} = 0V, $R_{RDM} < R_{RDM(TH)}$)		
CS pin open	CS voltage	$V_{CS} \geq V_{OCP}$	3 PWML pulses	t_{FDR} restart (1.5 s)
P13 pin open	P13 voltage at $UVLO_{ON}$	V_{P13} drops to 14 V within 10 μs	none	UVLO reset
P13 pin over voltage	P13 voltage	$V_{P13} \geq V_{P13(OV)} + V_{P13(REG)}$	3 PWML pulses	UVLO reset
RDM pin short	RDM current at $UVLO_{ON}$	V_{RDM} = 0 V, self-limited I_{RDM}	none	UVLO reset
RDM pin open	RDM current at $UVLO_{ON}$	RDM = Open	none	UVLO reset
RTZ pin short	RTZ current at $UVLO_{ON}$	V_{RTZ} = 0 V, self-limited I_{RTZ}	none	UVLO reset
RTZ pin open	RTZ current at $UVLO_{ON}$	RTZ = Open	none	UVLO reset
XCD pin over voltage	XCD voltage	$V_{XCD} > V_{XCD(OVP)}$	750 μs	UVLO reset

8.4.15.1 Protections on CS pin Fault

UCC28782 identifies a fail-short event on the CS pin by monitoring the on-time pulse width of the first PWML pulse after V_{VDD} startup is completed. As shown in Figure 8-32, the normal first on-time pulse width should be limited by the clamped $V_{CST(SM1)}$ level of 0.2 V and the rising slope of the current-loop feedback signal from the current-sense resistor (R_{CS}) to the CS pin. When the current feedback path is gone due to a CS pin short to GND, the peak magnetizing current increases and potentially can damage the power stage. Therefore, a maximum on-time of the first PWML pulse for V_{SET} = 5 V, t_{CSF1} of 2 μs in the electrical table, is used to limit the first peak-current stress of the silicon-based converter and then will trigger a CS pin short protection which initiates the t_{FDR} recovery of 1.5 s in auto-recovery mode.

Additionally, t_{CSF0} in the electrical table confines the maximum on-time of the first PWML pulse on the GaN-based converter with V_{SET} = 0 V. There are two corresponding values based on two predetermined ranges of the RDM pin setting in order to provide the protection over a wider switching frequency range. Specifically, t_{CSF0} is set at 2 μs with R_{RDM} higher than the $R_{RDM(TH)}$ threshold of 55 kΩ, while t_{CSF0} is reduced to 1 μs under $R_{RDM} < R_{RDM(TH)}$. Since a GaN-based converter is capable of operating at higher switching frequency with lower magnetizing inductance (L_M), it is possible that the peak current can be increased higher than a lower switching-frequency design under the same $V_{CST(SM1)}$ level and same on-time of PWML. The RDM pin can provide a good indication of the switching frequency range of a GaN power stage, since the lower L_M requires smaller R_{RDM} setting. With a different t_{CSF0} setting, the CS pin fault adapts to a wide switching frequency range.

Unlike a CS pin short protection which senses only the first on-time pulse width of PWML only, CS pin open protection monitors the fail-open condition cycle-by-cycle. An internal 4-μA current source out of the CS pin is used to pull the CS pin voltage up to 3.3 V as the CS pin exhibits high impedance during a fail-open condition. If the CS voltage is higher than the 1.2-V threshold of the OCP limit and lasts for three consecutive PWML pulses, the CS pin open protection is triggered which initiates the 1.5-s recovery.

8.4.15.2 Protections on P13 pin Fault

As shown in Figure 8-32, after V_{VDD} reaches $V_{VDD(ON)}$, an internal 13-V regulator on the P13 pin should force V_{P13} back to the regulation level before PWML starts switching. If the recommended P13-pin capacitor (C_{P13}) of

1 µF and the connection to the depletion-mode MOSFET (Q_S) are in place, the settling time of V_{P13} to 14 V is much longer than 10 µs with a limited 1.9-mA sink current of the regulator ($I_{P13(START)}$) to discharge C_{P13}.

The first fault scenario is that if C_{P13} is too small, or the P13 pin is open, the pin is not able to control Q_S correctly for the high-voltage sensing function of ZVS control, so no switching action will be performed. When either two situations happen, V_{P13} settles to 13 V very quickly instead. Therefore, after a 10-µs delay from the instant of V_{VDD} reaching $V_{VDD(ON)}$, UCC28782 checks if V_{P13} is below 14 V for the pin-fault detection, and then performs one UVLO cycle of VDD directly without switching as the protection response.

The above protection is to prevent the controller from generating PWM signals. However, when the P13 pin is open and disconnected from the Q_S gate, the source voltage of Q_S keeps increasing. To protect the P13-pin open event, a small Zener diode (D_{P13}) between Q_S gate to AGND should be used to limit the Q_S source voltage. D_{P13} should be higher than $V_{VDD(ON)}$, so as to prevent interference with normal VDD startup. A 20-V Zener diode is recommended.

The second fault scenario is the over-voltage condition of P13 pin after the converter starts switching. When the switch-node voltage (V_{SW}) rises with a high dV/dt condition, there is a charge current flowing through the junction capacitance of Q_S, and part of the current can charge up C_{P13}. If the overshoot is too large, the voltage on the SWS pin also increases due to the nature of depletion-mode MOSFET operation. UCC28782 detects the overshoot event on P13 pin with a 15-V over-voltage threshold cycle-by-cycle. When V_{P13} is higher than 15 V for three consecutive PWML pulses, the P13 over-voltage protection is triggered which performs one UVLO cycle of VDD.

The third fault scenario is an P13 pin short event at the beginning of VDD startup, and Q_S is unable to charge up the VDD capacitor to $V_{DD(ON)}$, so there is no chance to enable the controller.

8.4.15.3 Protections on RDM and RTZ pin Faults

Since RDM and RTZ pins are the critical programming pins for ZVS control, UCC28782 offers both open-circuit and short-to-GND protections for those pins. At initial start-up when V_{VDD} reaches $V_{VDD(ON)}$ and before switching begins, a fixed voltage level is applied to each pin and the corresponding current level flowing out of the pin is sensed to detect a pin-fault condition. As a result, too small of a current represents the pin-open state, and too large of a current represents the pin-short state where the short-circuit current level is self-limited.

In general, maintain 2 kΩ < R_{RDM} < 500 kΩ and 20 kΩ < R_{RTZ} < 1.1 MΩ with ample margins to avoid triggering one of these faults. When a pin-fault condition is identified, no switching is allowed and one UVLO cycle of VDD is triggered as the protection response. The normal start-up sequence will proceed on the next VDD cycle after the fault condition is removed.

9 Application and Implementation

Note

Information in the following applications sections is not part of the TI component specification, and TI does not warrant its accuracy or completeness. TI's customers are responsible for determining suitability of components for their purposes. Customers should validate and test their design implementation to confirm system functionality.

9.1 Application Information

A typical application of a high-frequency active-clamp flyback (ACF) converter, using the UCC28782 ACF controller, is to enable high-density AC-to-DC power supply design which complies with stringent global efficiency standards and high-density power packaging. Both Silicon (Si) and Gallium Nitride (GaN) power MOSFETs may be used, with appropriate gate drivers for each.

9.2 Typical Application Circuit

The following 65-W USB-PD application circuit applies to a GaN-based power stage with the SET pin connected to the AGND pin.
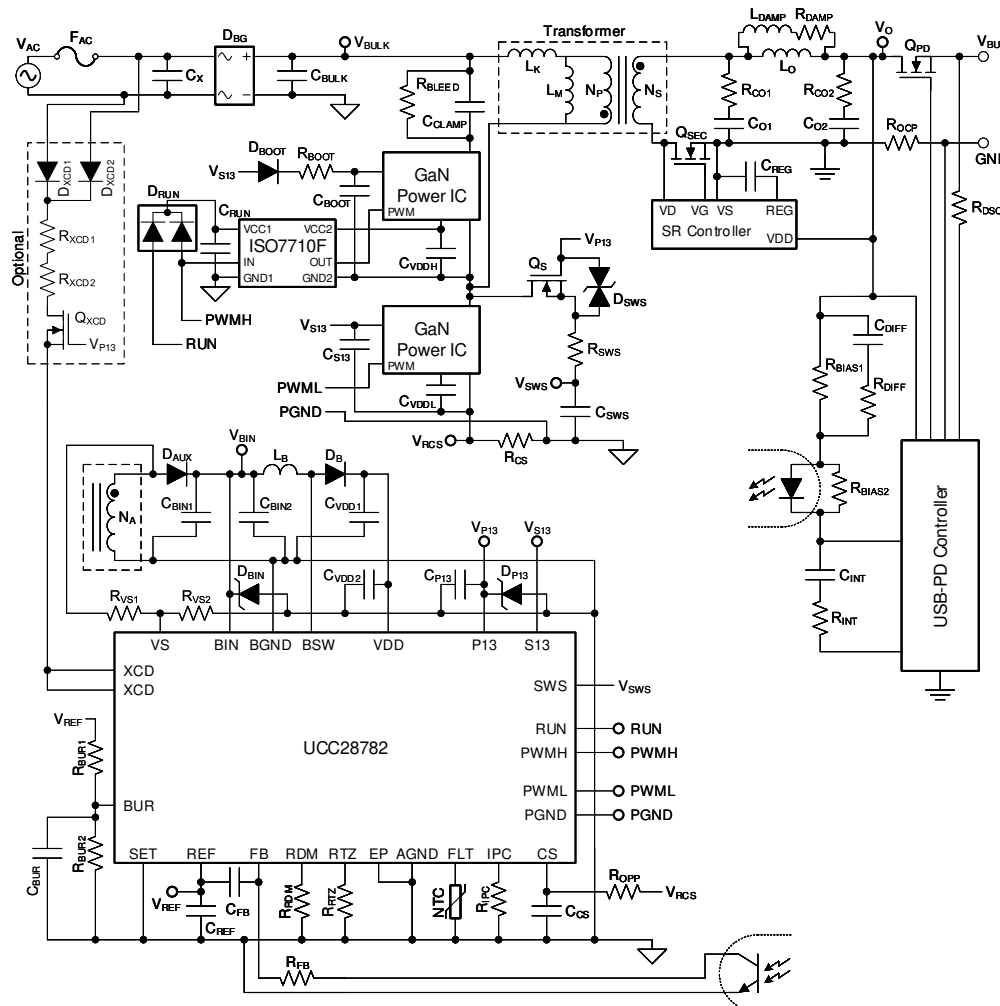

Figure 9-1. Typical Application Circuit

9.2.1 Design Requirements for a 65-W USB-PD Adapter Application

Table 9-1. UCC28782 Electrical Performance Specifications for GaN FET[1]

PARAMETER		TEST CONDITIONS	MIN	TYP	MAX	UNIT
INPUT CHARACTERISTICS						
V_{IN}	Input line voltage (RMS)		90	115 / 230	264	V
f_{LINE}	Input line frequency		47	50 / 60	63	Hz
P_{STBY}	Input power at no-load, V_O = 5 V	V_{IN} = 230 V_{RMS}, I_O = 0 A		55	70	mW
		V_{IN} = 115 V_{RMS}, I_O = 0 A		45	70	mW
$P_{0.25W}$	Input power at 0.25-W load, V_O = 20 V	V_{IN} = 230 V_{RMS}, P_O = 250 mW		399	470	mW
		V_{IN} = 115 V_{RMS}, P_O = 250 mW		359	470	mW
OUTPUT CHARACTERISTICS						
V_O	Output voltage, 20-V setting	V_{IN} = 90 to 264 V_{RMS}, I_O = 0 A to 3.25 A		19.95		V
	Output voltage, 15-V setting	V_{IN} = 90 to 264 V_{RMS}, I_O = 0 A to 3 A		15.06		
	Output voltage, 9-V setting	V_{IN} = 90 to 264 V_{RMS}, I_O = 0 A to 3 A		9.05		
	Output voltage, 5-V setting	V_{IN} = 90 to 264 V_{RMS}, I_O = 0 A to 3 A		5.05		
$I_{O(FL)}$	Full-load rated output current, 20-V setting	V_{IN} = 90 to 264 V_{RMS}, V_O = 20 V		3.25		A
$I_{O(FL2)}$	Full-load rated output current, 15-V, 9-V, 5-V settings	V_{IN} = 90 to 264 V_{RMS}, V_O = 15 V, 9 V, 5V		3.00		A
V_{O_pp}	Output ripple voltage, peak to peak 20-V setting	V_{IN} = 90 to 264 V_{RMS}, I_O = 0 A to 3.25 A		150	600	mVpp
	Output ripple voltage, peak to peak 15-V setting	V_{IN} = 90 to 264 V_{RMS}, I_O = 0 A to 3 A		150	450	
	Output ripple voltage, peak to peak 9-V setting	V_{IN} = 90 to 264 V_{RMS}, I_O = 0 A to 3 A		150	300	
	Output ripple voltage, peak to peak 5-V setting	V_{IN} = 90 to 264 V_{RMS}, I_O = 0 A to 3 A		150	200	
$P_{O(OPP)}$	Over-power protection threshold	V_{IN} = 90 to 264 V_{RMS}		70		W
t_{OPP}	Over-power protection duration	V_{IN} = 90 to 264 V_{RMS}, P_O > $P_{O(OPP)}$		160		ms
ΔV_O	Output voltage deviation during step-load transient	V_O = 20 V, I_O step between 0 A to $I_{O(FL)}$ at 100 Hz		-604 / +340	±1000	mVpp
SYSTEM CHARACTERISTICS						
η_{FL_20}	Full-load efficiency[3], V_O = 20 V	V_{IN} = 230 V_{RMS}, I_O = 3.25 A	94%	94.2%		
		V_{IN} = 115 V_{RMS}, I_O = 3.25 A	94%	94.2%		
		V_{IN} = 90 V_{RMS}, I_O = 3.25 A	93%	93.3%		
η_{avg_20}	4-point average efficiency[2], V_O = 20 V	V_{IN} = 230 V_{RMS}	89%	93.4%		
		V_{IN} = 115 V_{RMS}	89%	92.4%		
$\eta_{10\%\_20}$	Efficiency at 10% load, V_O = 20 V	V_{IN} = 230 V_{RMS}, I_O = 10% of $I_{O(FL)}$	79%	83.8%		
		V_{IN} = 115 V_{RMS}, I_O = 10% of $I_{O(FL)}$	79%	89.0%		
T_{AMB}	Ambient operating temperature range	V_{IN} = 90 to 264 V_{RMS}, V_O = 20 V, I_O = 0 to 3.25 A		25°C		

(1)   The performance listed in this table is achieved using secondary-resonance and based on the test results from a single board.
(2)   Average efficiency of four load points, I_O = 100%, 75%, 50%, and 25% of $I_{O(FL)}$.
(3)   Power loss from external cable is not included in efficiency results.

9.2.2 Detailed Design Procedure

9.2.2.1 Input Bulk Capacitance and Minimum Bulk Voltage

In an off-line rectified-AC application, the total input bulk capacitor (C_{BULK}) should be sized to provide energy from the peak of the minimum input AC line voltage ($V_{IN(MIN)}$) to the minimum allowable voltage ($V_{BULK(MIN)}$) to the power conversion stage. Due to the transition-mode operation, too low of $V_{BULK(MIN)}$ selection results in higher RMS current at $V_{IN(MIN)}$ and affects the full load efficiency, while too high of $V_{BULK(MIN)}$ enlarges the volume of the bulk capacitor. This equation does not account for the hold-up time requirement over AC-line dips and drop-outs.

$$C_{BULK(MIN)} = \frac{\frac{P_O}{\eta} \times [0.5 + \frac{1}{\pi} \times \arcsin(\frac{V_{BULK(MIN)}}{\sqrt{2} \times V_{IN(MIN)}})]}{(2 \times V_{IN(MIN)}{}^2 - V_{BULK(MIN)}{}^2) \times f_{LINE}}$$

(21)

C_{BULK} may be made up of more than one capacitor. Select standard values with sufficient margin to the calculated $C_{BULK(MIN)}$ to allow for tolerance and aging.

9.2.2.2 Transformer Calculations

9.2.2.2.1 Primary-to-Secondary Turns Ratio (N_{PS})

N_{PS} is a ratio of primary winding turns to secondary winding turns and although each winding must have a whole number of turns, the ratio of the two is not required to be a whole number. The choice of N_{PS} influences the design tradeoffs on the voltage ratings between primary and secondary switches, and the balance between the magnetic core and winding loss of the transformer, which are explained in detail as follows:

1. Maximum N_{PS} ($N_{PS(MAX)}$) is limited by the maximum derated drain-to-source voltage of Q_L ($V_{DS\_QL(MAX)}$). In the expression below, ΔV_{CLAMP} is a voltage deviation above the reflected output voltage. It can be either the ripple voltage of C_{CLAMP} in AAM mode, or the voltage over-charge of C_{CLAMP} by the leakage inductance energy when Q_H is disabled in LPM. V_O is the output voltage, and V_F is the forward voltage drop of the secondary rectifier.

$$N_{PS(MAX)} = \frac{V_{DS\_QL(MAX)} - V_{BULK(MAX)} - \Delta V_{CLAMP}}{V_O + V_F}$$

(22)

2. Minimum N_{PS} ($N_{PS(MIN)}$) is limited by the maximum derated drain-to-source voltage of the secondary rectifier ($V_{DS\_SR(MAX)}$). In the expression for $N_{PS(MIN)}$, ΔV_{SPIKE} should account for any additional voltage spike higher than $V_{BULK(MAX)}/N_{PS}$ that occurs when Q_H is active and turns-off at non-zero current in AAM mode.

$$N_{PS(MIN)} = \frac{V_{BULK(MAX)}}{V_{DS\_SR(MAX)} - V_O - \Delta V_{SPIKE}}$$

(23)

3. Since the high-frequency transformer is usually a core-loss limited design instead of a saturation-limited design, the minimum duty cycle (D_{MIN}) at $V_{BULK(MAX)}$ is more important. Lower D_{MIN} increases core loss at $V_{BULK(MAX)}$, so this constraint creates another limitation on $N_{PS(MIN)}$.

$$N_{PS(MIN)} = \frac{D_{MIN}V_{BULK(MAX)}}{(1 - D_{MIN})(V_O + V_F)}$$

(24)

4. The winding loss distribution between the primary and secondary side of the transformer is the final consideration. As N_{PS} increases, primary RMS current reduces, while secondary RMS current increases. Conversely, as N_{PS} decreases, primary RMS current increases, while secondary RMS current reduces.

9.2.2.2.2 Primary Magnetizing Inductance (L_M)

After N_{PS} is chosen, L_M can be estimated based on minimum switching frequency ($f_{SW(MIN)}$) at $V_{BULK(MIN)}$, maximum duty cycle (D_{MAX}), and output power at highest nominal output voltage, nominal full-load current ($P_{O(FL)}$). The choice of $f_{SW(MIN)}$ should consider the expected range of switching frequency as bulk voltage

increases from minimum to maximum and as load falls from maximum to the burst mode threshold. K_{RES} represents the duty cycle loss to wait for the switch-node voltage transition from the reflected output voltage to zero. Typically, f_{SW} may extend to 200% to 300% $f_{SW(MIN)}$ or higher. A K_{RES} value of 5% to 6% is used as an initial estimate for GaN-based power stages, while ~10% is more appropriate for Si-based designs. The selection of minimum switching frequency ($f_{SW(MIN)}$) should consider the impact on full-load efficiency and EMI filter design.

$$D_{MAX} = \frac{N_{PS}(V_O + V_F)}{V_{BULK(MIN)} + N_{PS}(V_O + V_F)} \tag{25}$$

$$L_M = \frac{D_{MAX}^2 V_{BULK(MIN)}^2 \eta}{2P_{O(FL)}} \times \frac{(1 - K_{RES})}{f_{SW(MIN)}} \tag{26}$$

9.2.2.2.3 Primary Winding Turns (N_P)

The turn number on the primary side of the transformer (N_P) is determined by two design considerations:

1. The maximum flux density (B_{MAX}) must be kept below the saturation limit (B_{SAT}) of the magnetic core under the highest peak magnetizing current ($I_{M+(MAX)}$) condition, a given cross-section area (A_E) of the core geometry, and highest core temperature. When $I_{FB} = 0$ A, such as V_O soft-start or step-up load transient, the peak magnetizing current reaches $I_{M+(MAX)}$, since $V_{CST} = V_{CST(MAX)}$ in those conditions. $I_{M+(MAX)}$ can be calculated based on the output power triggering an OPP fault ($P_{O(OPP)}$) with $V_{CST} = V_{CST(OPP1)}$ at $V_{BULK(MIN)}$.

$$I_{M+(MAX)} = \frac{2P_{O(OPP)}}{D_{MAX}V_{BULK(MIN)}\eta} \frac{V_{CST(MAX)}}{V_{CST(OPP1)}} \tag{27}$$

$$B_{MAX} = \frac{L_M I_{M+(MAX)}}{N_P A_E} < B_{SAT} \tag{28}$$

2. The AC flux density (ΔB) affects the core loss of a transformer. For a transition-mode active clamp flyback, the core loss is usually highest at high line, since the switching frequency is highest and duty cycle is smallest for a given load condition. The following equation is the ΔB calculation including the contribution of negative magnetizing current (I_{M-}), used to put into the Steinmetz equation for more accurate core loss estimation. For $V_{BULK} \geq N_{PS}(V_O + V_F)$, I_{M-} is calculated with V_{BULK} divided by the characteristic impedance of L_M and the lumped time-related switch-node capacitance (C_{SW}). The expression of f_{SW} is derived based on the triangular approximation of the magnetizing current, which also considers I_{M-} effect over wide AC line condition.

$$I_{M-} = -\sqrt{\frac{C_{SW}}{L_M}}V_{BULK} \tag{29}$$

$$I_{IN} = \frac{P_{O(FL)}}{\eta} \frac{1}{V_{BULK}} \tag{30}$$

$$D = \frac{N_{PS}(V_O + V_F)}{V_{BULK} + N_{PS}(V_O + V_F)} \tag{31}$$

$$f_{SW} = \frac{D^2 V_{BULK}}{2L_M I_{IN} - DL_M I_{M-} + DV_{BULK} \times 0.5\pi\sqrt{L_M C_{SW}}} \tag{32}$$

Product Folder Links: *UCC28782*

$$I_{M+} = \sqrt{\frac{2P_{O(FL)}}{\eta L_M f_{SW}} + I_{M-}^{\ 2}}$$

(33)

$$\Delta B = \frac{L_M(I_{M+} - I_{M-})}{N_P A_E}$$

(34)

9.2.2.2.4 Secondary Winding Turns (N$_S$)

After N$_P$ is chosen, N$_S$ can be calculated through N$_{PS}$. N$_S$ and N$_P$ are adjusted to the nearest suitable integers. With the new N$_{PS}$, Section 9.2.2.2.2 and follow-on parameters are recalculated to update the parameter change.

$$N_S = \frac{N_P}{N_{PS}}$$

(35)

9.2.2.2.5 Auxiliary Winding Turns (N$_A$)

Turns of the auxiliary winding (N$_A$) is an integer value usually chosen to provide a nominal V$_{VDD}$ that satisfies all devices powered from V$_{VDD}$, such as a gate driver, UCC28782, etc. N$_A$ is determined by the following design considerations:

1. V$_{VDD}$ must be lower than the maximum rating voltage of VDD pin (V$_{VDD(MAX)}$) at maximum output voltage and rectifier forward drop (V$_{O(MAX)}$ + V$_F$). V$_{VDD(MAX)}$ is also limited by the lowest voltage rating of any other devices connected to the VDD pin. Use the lower result of the two following options, where applicable.
    a. For designs with a fixed output voltage or a narrow output range, the maximum Auxiliary winding turns (N$_{A(MAX)}$) is given by the following equation.

$$N_{A(MAX)} = \frac{V_{VDD(MAX)}}{V_{O(MAX)} + V_F} N_S$$

(36)

    b. For designs with wide-output voltage range (such as with USB-PD or PPS or similar) where the boost circuit is likely to be used, leakage inductance may peak-charge the BIN capacitance. The internal boost switch has a maximum rating of 30 V, so a 24-V Zener diode is often used as a clamping device to avoid overstress on BSW. This clamping voltage sets a lower limit on N$_{A(MAX)}$ and is given by the following equation.

$$N_{A(MAX)} < \frac{24V}{V_{O(MAX)} + V_F} N_S$$

(37)

2. The nominal V$_{VDD}$ should consider the impact on the stand-by power. Higher V$_{VDD}$ results in a static-loss increase with the total bias current of the devices connected to the VDD pin.
3. V$_{VDD}$ should be higher than the 13-V threshold voltage of survival mode (which is the sum of V$_{VDD(OFF)}$ and V$_{VDD(PCT)}$) at the minimum sustained output voltage (V$_{O(MIN)}$). ΔV here represents the voltage difference between the nominal V$_{VDD}$ and the survival-mode threshold. A minimum of 3 V is a recommended design margin for ΔV.

$$N_{A(MIN)} = \frac{V_{VDD(OFF)} + V_{VDD(PCT)} + \Delta V}{V_{O(MIN)} + V_F} N_S$$

(38)

N$_{A(MIN)}$ must also accommodate the highest V$_{VDD(OFF)}$ threshold of other devices powered by VDD, if any. Select an integer value for N$_A$ between the lowest N$_{A(MAX)}$ and the highest N$_{A(MIN)}$ with consideration of #2. For best performance, design the DC resistance of the auxiliary winding to be < 0.1 Ω.

9.2.2.2.6 Winding and Magnetic Core Materials

Besides the choice of AC flux density (ΔB) with L_M and N_P , the core loss of the transformer can also be significantly reduced by a proper selection of the magnetic core material. For converters operating at full-load switching frequencies up to 250 kHz, ferrite materials such as 3C97 and 3C98 (by Ferroxcube) exhibit low core loss density. For converters operating at full-load switching frequencies over 400 kHz, materials such as 3F36 from Ferroxcube and N49 from TDK/Epcos exhibit low core loss density. Other ferrite materials with equivalent or similar loss characteristics may also be used. Litz wires are recommended for both primary and secondary windings, in order to reduce the R_{AC} winding loss caused by the proximity effect and the skin effect of the transformer windings.

9.2.2.3 Clamp Capacitor Calculation

There are two resonant approaches for an active clamp flyback (ACF) converter, primary resonance and secondary resonance, which affect the design guidance on the clamp capacitor (C_{CLAMP}). Referring to Figure 9-1, if C_{O1} serves as the main energy-storage capacitor at the output with large capacitance and C_{O2} is a smaller high-frequency decoupling capacitor, leakage inductance of transformer (L_K) mainly resonates with C_{CLAMP} during the demagnetization time of L_M. This configuration is called the primary-resonance ACF converter. On the other hand, if C_{O2} serves as the main energy-storage capacitor at the output with larger capacitance and C_{O1} is much smaller than the equivalent capacitance of C_{CLAMP} reflected to the secondary side ($C_{CLAMP}*N_{PS}{}^2$), L_K mainly resonates with C_{O1}. This configuration is called the secondary-resonance ACF converter.

9.2.2.3.1 Primary-Resonance ACF

For primary-resonance ACF, the design tradeoff between conduction loss and turn-off switching loss of Q_H needs to be considered. Higher C_{CLAMP} results in less RMS current flowing through the transformer windings and switching devices, so the conduction loss can be reduced. However, a higher C_{CLAMP} design results in Q_H turning-off before the clamp current returns to zero. The condition of not having zero current switching (ZCS) increases the turn-off switching loss of Q_H. This is aggravated if the turn-off speed of Q_H is not fast enough. Therefore, C_{CLAMP} needs to be fine-tuned based on the loss attribution. If the resonance between L_K and C_{CLAMP} is designed to be completed by the time Q_H is turned-off, the clamp current should reach close to zero at approximately three quarters of the resonant period. The following equation can be used to design C_{CLAMP} for obtaining ZCS at $V_{BULK(MIN)}$ and full load. This design results in a non-ZCS condition at $V_{BULK(MAX)}$, since the switching frequency at $V_{BULK(MAX)}$ is higher in transition-mode operation. A low-ESR clamp capacitor is recommended to minimize the conduction loss. If a ceramic capacitor is used as the low-ESR capacitor, the DC-bias effect on capacitance reduction also needs to be considered.

$$C_{CLAMP} = \frac{1}{L_K}[\frac{L_M I_{M+(FL)}}{1.5\pi N_{PS}(V_O + V_F)}]^2$$

(39)

9.2.2.3.2 Secondary-Resonance ACF

For secondary-resonance ACF, C_{O1} is used to adjust the resonant time with L_K to fulfill the ZCS condition, so a large C_{CLAMP} will not compromise ZCS. Besides, during the on-time of low-side switch (Q_L), the small C_{O1} is partially discharged by the load current at the same time. After Q_L turns off and the resonance begins, the discharged C_{O1} makes the initial resonance voltage lower than the reflected clamp capacitor voltage across C_{CLAMP}, which forces more magnetizing current to be delivered to the output, so the conduction loss is reduced with less RMS current flowing through Q_H and the primary winding.

9.2.2.4 Bleed-Resistor Calculation

R_{BLEED} is used to discharge the clamp capacitor voltage to a residual voltage ($V_{RESIDUAL}$) during the 1.5-s fault delay recovery time (t_{FDR}). After the converter recovers from the fault mode, lower $V_{RESIDUAL}$ reduces the maximum current stress ($I_{SHORT(MAX)}$) flowing through the switching devices within their respective safe operating areas, even if the output voltage is shorted. $V_{RESIDUAL}$ can be determined by the target $I_{SHORT(MAX)}$ multiplied with the characteristic impedance between the leakage inductance (L_K) and the clamp capacitor (C_{CLAMP}). $I_{SHORT(MAX)}$ is based on the de-rated maximum pulse current of Q_H or the output-rectifier current reflected to the primary side, whichever is lower. This design guide can be applied to both primary and

secondary resonance ACF converters. An excessively low value of R_{BLEED} results in over-discharging of C_{CLAMP}, and introduces excess continuous power loss which affects standby power.

$$V_{RESIDUAL} \approx I_{SHORT(MAX)} \sqrt{\frac{L_K}{C_{CLAMP}}}$$

(40)

$$R_{BLEED} = \frac{t_{FDR}}{C_{CLAMP} \ln[\frac{N_{PS}(V_O + V_F) + \Delta V_{CLAMP}}{V_{RESIDUAL}}]}$$

(41)

9.2.2.5 Output Filter Calculation

The bulk output capacitor of active clamp flyback (ACF) converters, C_{O1} of the primary-resonance ACF or C_{O2} of the secondary-resonance ACF, is often determined by the load-step transient-response requirement from no-load to full-load transition. For a target output voltage undershoot (ΔV_O) with the load step-up transient of ΔI_O, the minimum bulk output capacitance ($C_{O(MIN)}$) can be expressed as

$$C_{O(MIN)} = \frac{\Delta I_0 t_{RESP}}{\Delta V_0 - \Delta I_0 R_{Co}}$$

(42)

where t_{RESP} is the response time delay from the moment ΔI_O is applied to the moment when I_{FB} falls below 10 µA. At ~10 µA, full power is available to prevent further drop of V_O and to recharge C_O. The response delay time consists of the time for the secondary regulator to stop driving the opto-coupler input plus the time for the opto-coupler output transistor to turn off. R_{Co} is the equivalent series resistance (ESR) of the output capacitor C_O.

The output filter inductor (L_O) is an essential component for the secondary-resonance ACF, not only to filter the large switching voltage ripple across C_{O1} but also to decouple the effect of C_{O2} on the resonant period. The sum of L_O impedance, ESR of C_{O2} (R_{Co2}), and C_{O2} impedance at minimum switching frequency ($f_{SW(MIN)}$) must be much higher than C_{O1} impedance at the same frequency to force most of switching resonant current to flow through C_{O1} only. L_O is chosen with minimal ESR to achieve minimal conduction loss.

$$L_O >> \frac{1}{(2\pi f_{SW(MIN)})^2 C_{O1}} - \frac{1}{(2\pi f_{SW(MIN)})^2 C_{O2}} - \frac{R_{Co2}}{2\pi f_{SW(MIN)}}$$

(43)

One benefit of lowering the ESR on C_{O1} (R_{Co1}) is to help to reduce the switching ripple on the output voltage. Another benefit is reducing the conduction loss of C_{O1} for the secondary-resonance ACF converter. However, the issue is that the damping between L_O and C_{O1} is weakened. Without proper damping, the magnitude of low-frequency resonant ripple between L_O and C_{O1} enlarges output ripple, affects the loop stability, and affects the operation of synchronous rectifier (Q_{SEC}). The secondary-resonance ACF converter is the most vulnerable since C_{O1} with low capacitance significantly weakens the damping. To resolve this issue, it is found that a serial damping network formed by L_{DAMP} and R_{DAMP} is a very effective way to minimize the impact. However, too much damping results in noticeable conduction loss increase and full-load efficiency drop. Therefore, it is recommended that L_{DAMP} and R_{DAMP} should be higher than the theoretical strong damping value as the following equations suggest. Even though the damping network is an additional component, the physical size or the footprint is much smaller than L_O, not only because of the small value but also the wide availability of small-size chip inductors with high winding resistance can provide "free" R_{DAMP}. For the 65-W secondary-resonance ACF design with primary GaN FETs and a polymer-type C_{O2}, when a 0.68-µH chip inductor is in parallel with a 1-µH output filter inductor, there is only 0.15% full-load efficiency drop at 90-V AC input, and there is a negligible efficiency difference at 230-V AC input.

$$L_{DAMP} > 0.13 \times L_O$$

(44)

$$R_{DAMP} > \sqrt{\frac{L_O}{C_{O1}}}$$

(45)

The equation for R_{DAMP} assumes that $C_{O2} >> C_{O1}$. Select a standard component available with parameter values that satisfy both of these two equations. It is usually not necessary to use two separate components.

9.2.2.6 Calculation of ZVS Sensing Network

There are three components in the application circuit to help the depletion MOSFET (Q_S) perform ZVS sensing safely: C_{SWS}, R_{SWS}, and D_{SWS}. Design considerations and selection guidelines for the values of these components are given here.

At the rising edge of the switch node voltage, the fast dV/dt coupling through the drain-to-source capacitance of Q_S ($C_{OSS(Qs)}$) generates a charge current flowing into the circuit loading on the Q_S source pin. The result is a possible voltage overshoot on both the SWS pin and across the gate-to-source of Q_S ($V_{GS(Qs)}$) since the gate is tied to P13. The SWS pin, with an absolute maximum voltage rating of 38 V, can handle higher voltage stress than $V_{GS(Qs)}$. Therefore, a capacitor (C_{SWS}) between the SWS pin and GND should be selected properly to prevent the voltage overshoot from damaging the Q_S gate. Since $C_{OSS(Qs)}$ and C_{SWS} form a voltage divider, the minimum C_{SWS} ($C_{SWS(MIN)}$) can be derived as

$$C_{SWS(MIN)} = \frac{C_{OSS(Qs)} \times \left[V_{BULK(MAX)} + N_{PS}(V_O + V_F) \right]}{V_{P13} + V_{GS\_MAX(Qs)}}$$

(46)

where $V_{GS\_MAX(Qs)}$ is the de-rated maximum gate-to-source voltage of Q_S and V_{P13} is the steady-state voltage level of 13 V.

Without resistive damping, both the charge current on the rising edge of V_{SW} and the discharge current on the falling edge of V_{SW} are oscillatory with the parasitic series inductance within the ZVS sensing network resonating with C_{SWS}. Therefore, a series resistor (R_{SWS}) between SWS pin and source-pin of Q_S is used to dampen any high-frequency ringing, helping to obtain a cleaner sensing signal on the SWS pin and preventing any high-frequency current from interfering with other noise-sensitive signals. R_{SWS} can be expressed as:

$$R_{SWS} > \sqrt{\frac{L_{SWS}}{C_{SWS} + C_{Dz}}}$$

(47)

where L_{SWS} is the lumped parasitic inductance including the packaging of Q_S and PCB traces of Q_S and C_{SWS} return path.

A bidirectional TVS across BSS126 gate and source should be added to protect the gate-to-source voltage from potential abnormal voltage stress. The clamping voltage of TVS should be less than BSS126 voltage rating but greater than 15 V. The resistor should be slightly higher than 500 Ω. The resistor and a 22-pF ceramic capacitor between the SWS pin and the bulk input capacitor ground form a small sensing delay to help the internal detection circuit to identify the ZVS characteristic correctly.

Based on the above design guide, even though R_{SWS} and C_{SWS} may be sufficient to manage the voltage overshoot in normal operation, a low-capacitance bi-directional TVS diode (D_{SWS}) across BSS126 gate and source is highly recommended to serve as a safety backup of the ZVS sensing network. Regular Zener diodes are not suitable due to high capacitance and slow clamping response. The clamping voltage of TVS should be less than BSS126 voltage rating but greater than 15 V.

A general recommendation is to use a 50-V 22-pF C0G-type ceramic capacitor for C_{SWS}, a 510-Ω chip resistor for R_{SWS}, and a bi-directional TVS diode with clamp voltage of 18 V for D_{SWS}. Too large of R_{SWS} or C_{SWS} introduces a sensing delay between the actual V_{SW} and the SWS pin, causing the ZVS control to unnecessarily extend t_{DM} in order to pull down V_{SW} earlier than expected before the end of t_Z . As shown in Figure 8-5, the larger R_{SWS} is, the smaller supply current to charge the VDD capacitor. If the reduced charge current (I_{SWS}) is

lower than the total consumed current from the controller (I_{START}) and from the external circuitry on the VDD pin and P13 pin, V_{VDD} may not be able to reach $V_{VDD(ON)}$ and the controller can not initiate any switching event.

9.2.2.7 Calculation of BUR Pin Resistances

Referring back to Section 8.3.1, it is recommended that ABM is entered at no higher than 50% to 60% of full load. Equation 1 and Equation 2, or Equation 1 and Equation 4, provide two equations for calculating two unknowns for the BUR-pin resistor values. However, first the target values of $V_{CST(BUR)}$, $\Delta V_{BUR(AAM)}$, and $\Delta V_{BUR(LPM)}$ must be chosen. Since the ratio of $I_{BUR(AAM)}$ to $I_{BUR(LPM)}$ is fixed at 1.852 (5 µA / 2.7 µA), it is necessary to target $\Delta V_{BUR(AAM)}$ = 185 mV to ensure that $\Delta V_{BUR(LPM)}$ = 100 mV, per guidance in Section 8.3.1.

The procedure to determine the value of $V_{CST(BUR)}$ is quite complex and is not provided in this datasheet. Instead, the UCC28782 Excel Calculator Tool automatically calculates this value based on user input and determines the V_{BUR} target voltage V_{BUR_tgt}. Using this target value, it further determines the appropriate values for R_{BUR2} and R_{BUR1} to meet the BUR pin targets based on user selections for the following set of equations. Note that expected values are used to determine recommended resistances, then actual resistances are selected from standard value series and the resulting actual voltages are calculated from the selected resistor values. Actual voltage results should be close to the targeted values.

Calculate expected $\Delta V_{BUR(LPM)}$ value based on $\Delta V_{BUR(AAM)}$ target value.

$$\Delta V_{BUR(LPM)} = \Delta V_{BUR(AAM)} \times \frac{I_{BUR(LPM)}}{I_{BUR(AAM)}} = \Delta V_{BUR(AAM)} \times 0.54$$

(48)

Calculate the expected value for the parallel combination of R_{BUR1} with R_{BUR2}.

$$R_{BUR1} || R_{BUR2} = \Delta V_{BUR(AAM)} / I_{BUR(AAM)}$$

(49)

Calculate the recommended value for R_{BUR1} and choose a standard 1% tolerance value for R_{BUR1_act} that is close to the recommended value.

$$R_{BUR1\_rec} = \frac{\Delta V_{BUR(AAM)}}{I_{BUR(AAM)}} \times \left(\frac{V_{REF}}{V_{BUR\_tgt} + \Delta V_{BUR(AAM)}} \right)$$

(50)

Calculate the recommended value for R_{BUR2} using R_{BUR1_act} and choose a standard 1% tolerance value for R_{BUR2_act} that is close to the recommended value.

$$R_{BUR2\_rec} = R_{BUR1} \times \left[\frac{\left(V_{BUR\_tgt} + \Delta V_{BUR(AAM)} \right)}{V_{REF} - \left(V_{BUR\_tgt} + \Delta V_{BUR(AAM)} \right)} \right]$$

(51)

Calculate the actual values for V_{BUR}, $\Delta V_{BUR(AAM)}$, and $\Delta V_{BUR(LPM)}$ using R_{BUR1_act} and R_{BUR2_act}.

$$V_{BUR\_act} = V_{REF} \times \left(\frac{R_{BUR2}}{R_{BUR1} + R_{BUR2}} \right) - I_{BUR(AAM)} \times \left(\frac{R_{BUR1} \times R_{BUR2}}{R_{BUR1} + R_{BUR2}} \right)$$

(52)

$$\Delta V_{BUR(AAM)} = I_{BUR(AAM)} \times \left(\frac{R_{BUR1} \times R_{BUR2}}{R_{BUR1} + R_{BUR2}} \right)$$

(53)

$$\Delta V_{BUR(LPM)} = I_{BUR(LPM)} \times \left(\frac{R_{BUR1} \times R_{BUR2}}{R_{BUR1} + R_{BUR2}} \right)$$

(54)

Finally, verify that the total summation of the BUR voltage with hysteresis does not exceed the BUR-pin upper clamp voltage of 2.4 V.

$$V_{BUR\_act} + \Delta V_{BUR(AAM)} + \Delta V_{BUR(LPM)} \leq 2.4V$$

(55)

9.2.2.8 Calculation of Compensation Network

UCC28782 integrates two control concepts to benefit high-efficiency operation: peak current-mode control and burst-ripple control. The peak current loop in AAM can be analyzed based on the linear control theory, so the compensation target is to obtain enough phase margin and gain margin for the given small-signal characteristic of an active clamp flyback converter. For Transition-Mode operation, the power stage can be modeled as a voltage-controlled current source charging an output capacitor (C_O) with an equivalent-series resistance (R_{Co}) and the output load (R_O) as shown in Figure 9-2. The first-order plant characteristic and high switching frequency operation in AAM make the peak current loop easier to stabilize than ABM.
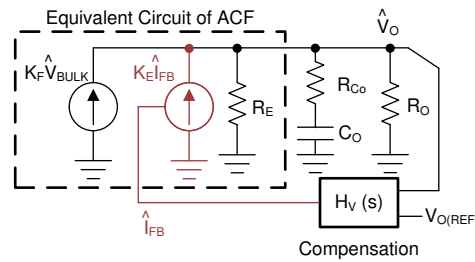
Copyright © 2018, Texas Instruments Incorporated

Figure 9-2. Small-Signal Model of ACF in AAM Loop

The adaptive burst mode (ABM) uses ripple-based control, so the linear control theory for AAM cannot be applied. As illustrated in Figure 8-4, the internal ramp compensation feature of UCC28782 stabilizes the ABM control loop, so the external compensation network can be simplified.
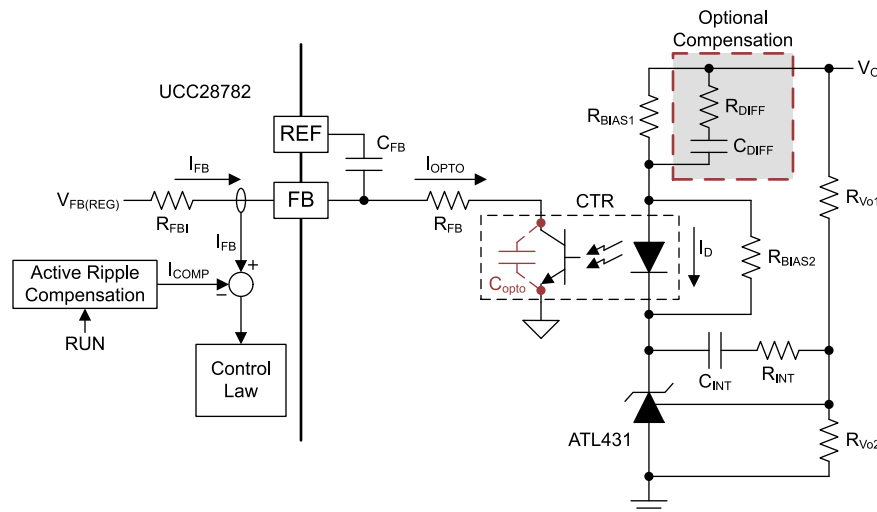

Figure 9-3. Compensation Network, H_v(s)

The transfer function from I_{FB} to V_O guides the pole/zero placement of the general secondary-side compensation network in Figure 9-3. In the primary-side control circuitry, two poles at ω_{FB} and ω_{OPTO} introduce phase-delay on I_{FB}. ω_{FB} pole is formed by the external filter capacitor C_{FB} and the parallel resistance of the internal R_{FBI} and the external current-limiting resistor (R_{FB}). ω_{OPTO} pole is formed by the parasitic capacitance of the optocoupler output (C_{OPTO}) and the series resistance of R_{FBI} and R_{FB}. For C_{FB} = 220 pF, R_{FBI} = 8 KΩ, and R_{FB} = 20 KΩ, the delay effect of ω_{FB} pole located at 139 kHz is negligible. C_{OPTO} is in the range of a few nF contributed by the Miller effect of the collector-to-base capacitance of the BJT in the optocoupler output, so ω_{OPTO} pole is located at less than 10 kHz. If the control loop bandwidth needs to be designed at higher frequency for a faster transient response, the phase delay effect of ω_{OPTO} on the stability margin must be taken into account. Therefore, an RC network (R_{DIFF} and C_{DIFF}) in parallel with R_{BIAS1} is used to compensate the phase-delay of the optocoupler, which introduces an extra pole/zero pair located at ω_{P1} and ω_{Z1} respectively. The basic design guide is to place the ω_{Z1} zero close to the ω_{OPTO} pole, and to place ω_{P1} pole away from highest f_{BUR}. On the other hand, if the

Product Folder Links: UCC28782

stability margin and transient response are sufficient to meet the requirements without R_{DIFF} and C_{DIFF}, then these two components are optional for UCC28782.

$$\frac{I_{FB}(s)}{V_O(s)} = \frac{CTR}{R_{BIAS1}} \frac{1+(s/\omega_{Z0})}{(s/\omega_{Z0})} \frac{1}{1+(s/\omega_{P1})} \frac{1+(s/\omega_{Z1})}{1+(s/\omega_{OPTO})} \frac{1}{1+(s/\omega_{FB})}$$
(56)

$$\omega_{Z0} = \frac{1}{(R_{Vo1}+R_{INT})C_{INT}}$$
(57)

$$\omega_{Z1} = \frac{1}{(R_{DIFF}+R_{BIAS1})C_{DIFF}}$$
(58)

$$\omega_{P1} = \frac{1}{R_{DIFF}C_{DIFF}}$$
(59)

$$\omega_{OPTO} = \frac{1}{(R_{FB}+R_{FBI})C_{OPTO}}$$
(60)

$$\omega_{FB} = \frac{1}{(R_{FBI}//R_{FB})C_{FB}}$$
(61)

The step-by-step design procedure of the compensator without R_{DIFF} and C_{DIFF} is:

1. R_{FB} selection needs to consider both the output voltage regulation and compensation challenge on the low-frequency pole at ω_{OPTO}. R_{FB} should be less than the maximum value of 28 kΩ to provide a sufficient feedback current of 95 µA for the output voltage regulation in SBP2 mode, under the worst-case $V_{FB(REG)}$ and R_{FBI}. However, R_{FB} = 28 kΩ and C_{OPTO} = 2 nF result in an ω_{OPTO} pole located at 2.8 kHz. This low-frequency pole may reduce phase margin at the cross-over frequency. If the control bandwidth is around this frequency range, R_{FB} value should be designed even lower to move the pole to a higher frequency.

$$R_{FB(MAX)} = \frac{V_{FB(REG)}-V_{CE(OPTO)}}{I_{FB(SBP)}} - R_{FBI}$$
(62)

2. R_{BIAS1} is determined based on a given current transfer ratio (CTR) of the optocoupler, $\Delta V_{O(ABM)}$, and target 4~5 µA of ΔI_{FB} as example. At collector currents less than 100 µA, the CTR of most optocouplers can be as low as 10%, or 0.1 (used in this example), although some high performance devices can have higher CTR.

$$R_{BIAS1} = \frac{CTR}{\Delta I_{FB}}\Delta V_{O(ABM)} = \frac{0.1}{5\mu A}\Delta V_{O(ABM)}$$
(63)

3. R_{INT} selection is not designed for the small-signal compensation, but to resolve the slow large-signal response of the shunt regulator. Specifically, after a step-down load change from heavy load to no load occurs, the output voltage overshoot and the long settling time forces ATL431 to reduce the cathode voltage continuously by the integrator configuration until the output voltage gets back to normal regulation level. If the load step-up transient happens before the output voltage is settled from the previous load step-down event, the low voltage across ATL431 becomes the initial voltage level for the integrator to move to a new steady-state. Since the time for ATL431 to move from lower voltage to a high voltage delays i_{FB} reduction, the controller response from SBP mode to AAM mode is delayed as well, which slows down the energy delivery to the output and results in a large voltage undershoot.
To resolve this problem, R_{INT} behaves like a current-limiting resistor for C_{INT}, which slows down the reduction of the cathode voltage of ATL431. R_{INT} needs to be adjusted based on the voltage undershoot requirement under the highest repetitive rate of load change.

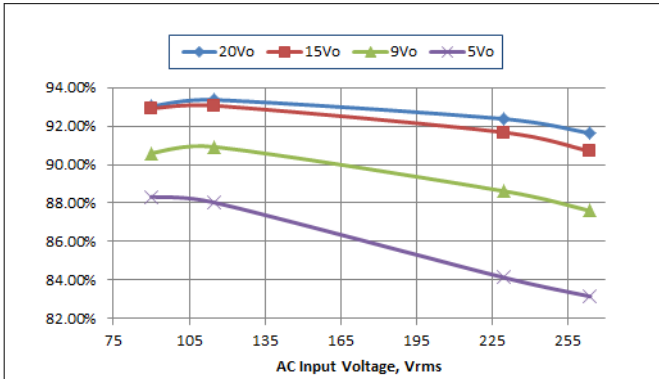### 9.2.3 Application Curves

Figure 9-4. 4pt-Average Efficiency vs. Input Voltage
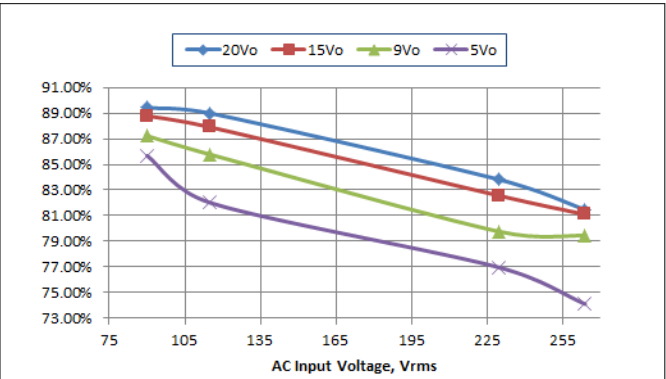

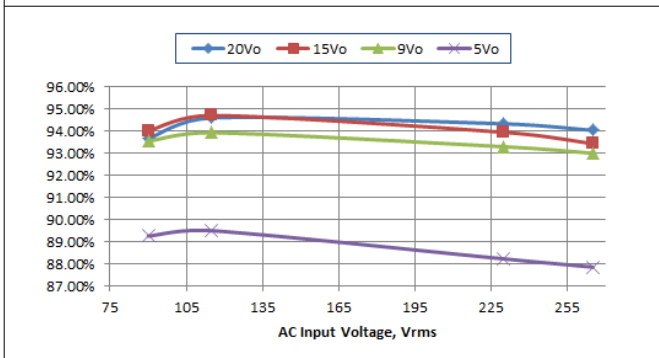Figure 9-5. 10%-Load Efficiency vs. Input Voltage

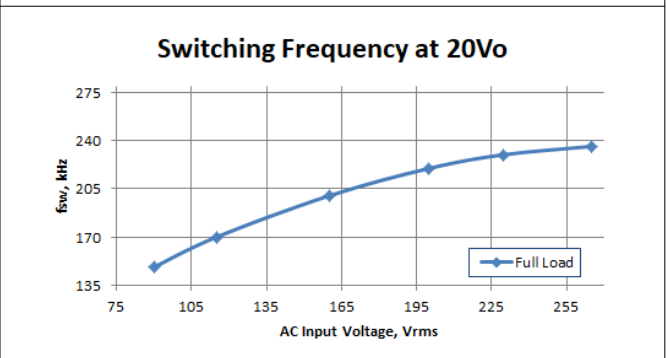Figure 9-6. Full-Load Efficiency vs. Input Voltage

Figure 9-7. Average Switching Frequency vs. Input Voltage for 20-V Output, Full-load

Product Folder Links: *UCC28782*

10 Power Supply Recommendations

The UCC28782 is intended to control active-clamp flyback (ACF) converters in high-efficiency off-line applications, and is optimized to be used with universal AC input, from 85 V_{AC} to 265 V_{AC}, at 47 Hz to 63 Hz. An external depletion-mode MOSFET connected between the switch node of the converter and the SWS / P13 pins of this controller is required to charge the VDD capacitor during start-up, and to perform ZVS sensing during normal operation.

Once the V_{VDD} reaches the UVLO turn-on threshold at 17 V (typical), the VDD rail should be kept within the bias supply operating voltage range listed in the Recommended Operating Conditions table in Section 7.3 . To avoid the possibility that the device might stop switching, V_{VDD} should not be allowed to fall below the maximum UVLO turn-off threshold at 11.17 V.

Under the condition of LPM operation, the clamp capacitor C_{CLAMP} is charged higher than the reflected voltage by the primary leakage inductance energy. On transition from LPM to ABM, this over-charge of C_{CLAMP} is delivered to the output during the first event where PWMH is high. The peak current is determined by the impedance formed by the resonance of the leakage inductance with the clamp capacitance, and it may be quite high. On the secondary side, the primary current is multiplied by the transformer turns-ratio. Verify that the pulse-current ratings of the high-side MOSFET and the output rectifier are adequate for these peak currents.

During power-stage switching, high dv/dt may appear to induce positive or negative noise on various pins of the UCC28782 that apparently exceeds their respective Absolute Maximum ratings. This kind of noise is often less than 10~20 ns in duration. If such measurements are made, ensure that "tip & barrel" probing techniques are used to eliminate ground-bounce and noise pickup on oscilloscope probe grounding wires. Make sure that the probe's GND reference is an AGND node as close to the IC as possible. If excess voltage is still measured, verify that the maximum source or sink current of the pin is not exceeded.

Under certain special circumstances, such as a brief short-circuit or an extended overshoot on the converter output, switching slows or stops until the condition clears and the clamp capacitor C_{CLAMP} may be overdischarged by a low R_{BLEED} value. A low V_{CLAMP} reflects to the Auxiliary winding and may cause VS to go low before PWMH goes low. If this happens the UCC28782 will stop switching and VDD will fall to the UVLO threshold and cycle through a restart. If this situation occurs, it may be mitigated by one or more of the following steps:

- Use an edge-triggered (not level-triggered) isolator/driver with short power-up delay for the high-side switch on the primary side.
- Ensure the value of R_{BLEED} is not too low.
- Reduce the value of the RDM resistor judiciously.
- In cases where there is no DCM ringing after PWMH goes low, try adding a positive offset voltage to VS to raise the apparent ZCD threshold.

Mitigation of Voltage Stresses on the Output Rectifier

The rectifier on the output winding may be a P-N diode, a Schottky diode, or a synchronous-rectifier (SR) MOSFET for higher efficiency. The current rating of this rectifier should be appropriate for the resonant flyback current and its peak current rating should accomodate the C_{CLAMP} charge balancing peak current. Besides the output voltage plus reflected bulk voltage impressed across the rectifier during PWML on-time, consideration for additional voltage spikes from various transient conditions should be made. Sources of voltage spikes on the rectifier include: hard switching of the low-side MOSFET on the primary, non-ZCS turn-off of the high-side MOSFET on the primary, and non-ZCS turn-off of an SR-MOSFET.

Regardless of cause of each of these spike sources, it is important to ensure that the peak voltage across the rectifier does not exceed its maximum rating. This may be accomplished in several ways, by implementing one or more of the alternative methods listed here:
- Choose a rectifier with a higher voltage rating.
- Add a TVS-type voltage-clamping device across the rectifier.
- Add or improve an R-C snubber across the rectifier.
- Slow down falling dv/dt of the low-side switch on the primary side.

- Minimize leakage inductance of the transformer secondary winding.
- Use an edge-triggered (not level-triggered) isolator/driver with short power-up delay for the high-side switch on the primary side.
- Minimize the stray inductance in the V_{DS}-sense path of the SR controller.
- In case of reverse current conduction, choose an SR controller with shorter minimum on-time.
- Add or increase the value of a resistor in series with the gate of the SR-MOSFET, to slow down its di/dt during non-ZCS turn-off.
- Reduce the value of the RDM resistor judiciously, to reduce the maximum negative peak primary current by reducing maximum PWMH on-time.

11 Layout

11.1 Layout Guidelines

The active clamp flyback converter (ACF) designed with the UCC28782 not only recovers clamp energy but also eliminates switching loss with minimum circulating energy, so higher switching frequencies, efficiencies, and greater power densities can be achieved. However, when designing for higher switching frequencies, good layout practices as discussed below should be followed to ensure a reliable and robust design.

11.1.1 General Considerations

Designing for high power density requires consideration of noise coupling and thermal management. A four-layer PCB structure is highly recommended to use inner layers to help reduce current-loop areas and provide heat-spreading for surface-mount semiconductors.

- Provide internal-layer copper areas to improve heat dissipation of high-power SMDs, particularly for switching MOSFETs and power diodes. Use multiple thermal-vias to conduct heat from outer pads to inner-layers and supporting copper areas.
- To avoid capacitive noise coupling, do not cross outer-layer signals over copper areas that carry high-frequency switching voltage.
- To avoid inductive noise coupling, keep switching current loops as small as possible, and do not run signal tracks in parallel with such loops.
- Arrange the conducted-EMI filter components such that they do not allow switching noise to bypass them and affect the input. Avoid running switching signals through the EMI filter area.
- Use multiple vias to connect high-current tracks and planes between layers.

Figure 11-1 summarizes the critical layout guidelines, and more detail is further elaborated in the descriptions below.

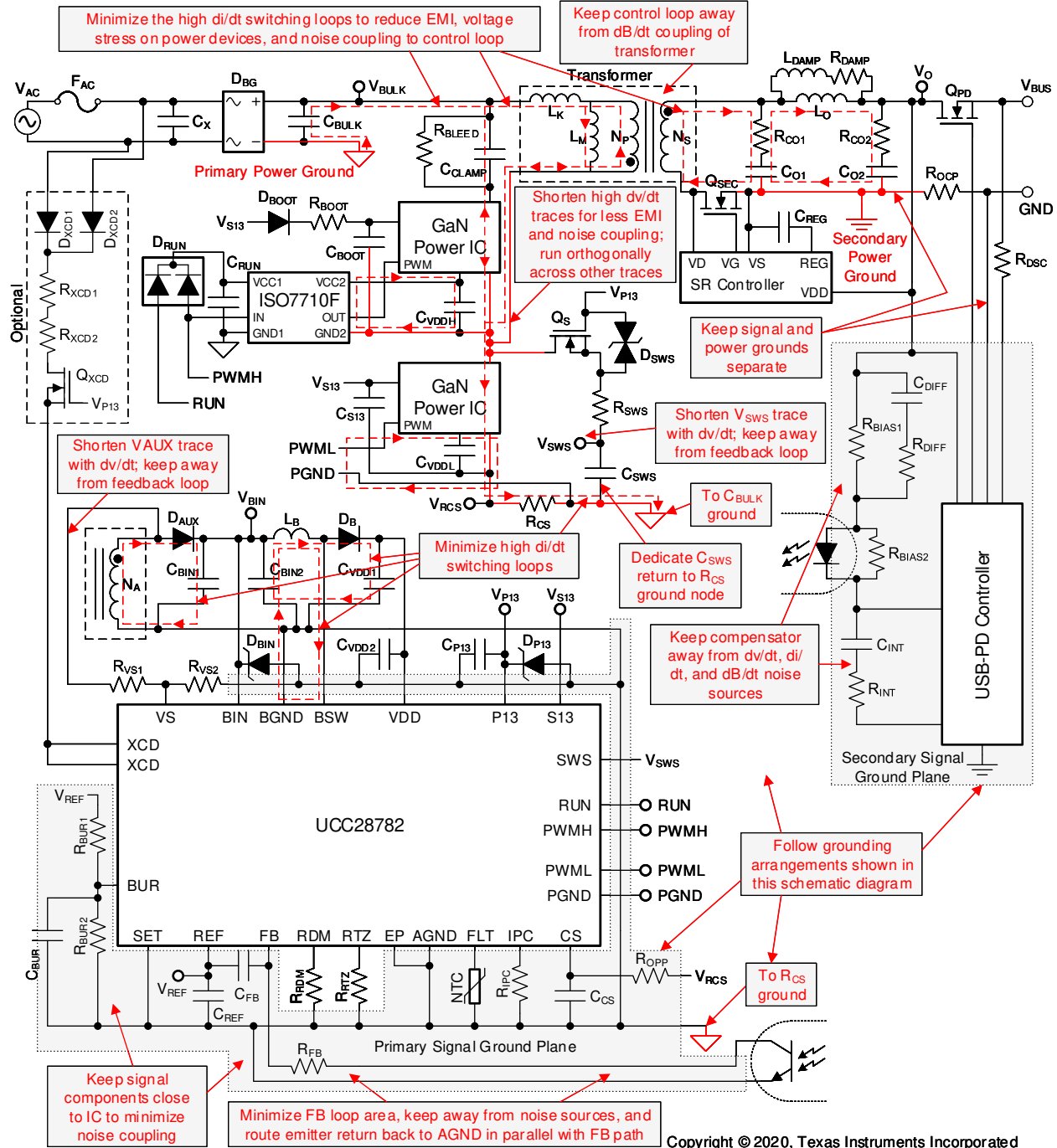Product Folder Links: *UCC28782*

Figure 11-1. Typical Schematic with Layout Considerations

11.1.2 RDM and RTZ Pins

Minimize stray capacitance to RDM and RTZ pins.

- Place R_{RDM} and R_{RTZ} as close as possible between the controller pins and AGND pin.
- Avoid putting ground plane or any other tracks under RDM and RTZ pins to minimize parasitic capacitance. This can be accomplished by putting cutouts in the layers below these pins.

11.1.3 SWS Pin

Minimize potential stray noise coupling from SWS pin to noise-sensitive signals.

- Keep some distance between SWS network and other connections.
- The RC damping network (R_{SWS}, C_{SWS}) and the TVS diode (D_{SWS}) should be as close to the source pin of Q_S as possible instead of SWS pin, so the gate-to-source pin of Q_S can be effectively protected.
- Keep the return path for di/dt current through C_{SWS} and D_{SWS} separate from the IC local GND and FB signal return paths. Return C_{SWS} back to the ground node at R_{CS}, not at the IC.

11.1.4 VS Pin

Minimize stray capacitance at the VS pin to reduce the time-delay effect on ZVS control.

- Avoid putting GND plane under VS pin to reduce parasitic capacitance. This can be accomplished by putting a cutout in the ground plane below this pin pad and the tracks an pads of components connected to VS. minimize the track length of the VS net.
- Do not run other tracks or planes over or under the VS net.
- Do not run other tracks or planes under R_{VS1} and R_{VS2}.

11.1.5 BUR Pin

The resistor divider (R_{BUR1} and R_{BUR2}) and the filter capacitor (C_{BUR}) on the BUR pin should to be as close to the BUR pin and IC AGND as possible.

- It is recommended to provide shielding on the BUR-pin trace with ground planes to minimize the noise-coupling effect on peak current variation during burst-mode operation. This can be accomplished by adding a ground plane under the BUR traces and pins.

11.1.6 FB Pin

This pin can be noise-sensitive to capacitive coupling from the high dV/dt switch nodes, or the flux coupling from magnetic components and high di/dt switching loops.

- Minimize the loop area for the PCB traces from the opto-coupler to the FB pin in order to avoid the possible flux coupling effect. Run the opto-coupler emitter return track from AGND at the IC in parallel with the FB to collector path, to minimize loop-area.
- Keep PCB traces away from the high dv/dt signals, such as the switch node of the converter (V_{SW}), the auxiliary winding voltage (V_{AUX}), and the SWS-pin voltage (V_{SWS}). If possible, it is recommended to provide shielding for the FB trace with ground planes.
- The filter capacitor between FB pin and REF pin (C_{FB}) needs to be as close to the two IC pins as possible.
- The current-limiting resistor of FB pin (R_{FB}) should be as close to the FB pin as possible to enhance the noise rejection of nearby capacitively-coupled noise sources.

11.1.7 CS Pin

The OPP-programming resistor (R_{OPP}) and the filter capacitor (C_{CS}) should be as close to the CS pin as possible to improve the noise rejection of nearby capacitively-coupled noise sources, and to filter any ringing that may be present during non-ZVS conditions.

11.1.8 BIN Pin

This pin monitors the boost input voltage to determine if the level is correct to allow the boost circuit to switch. When the boost circuit is used, the BIN signal usually originates from the rectified and filtered Auxiliary voltage.

- Place the AUX voltage rectifier and main filter capacitor (C_{BIN1}) near the transformer pins to minimize the AUX switching current loop. Return that capacitor's negative lead directly back to the transformer pin. Then run the negative track to the BGND pin and the positive net to the boost inductor input.
- Place another filtering capacitor (C_{BIN2}) at the input to the boost inductor and return that negative lead directly to the BGND pin to minimize boost switching current loop area.
- Connect the BIN pin to (C_{BIN2}) at the input of the boost inductor.

If the boost circuit is not used, connect BIN directly to BGND.

11.1.9 BSW Pin

The BSW pin is the drain of the internal boost switch and carries high-frequency switching current internally to BGND. To avoid self-generated noise and interference with control signals, minimize the boost switching current loop area.

- Place the boost inductor (L_B) close to the controller to minimize the track length from the inductor output to the BSW pin. To avoid inducing switching noise into control signals, do not run such signal tracks over, under, or through the boost switching loop.
- Place the boost output diode (D_B) at the output of the boost inductor is such a way that minimized the loop area with the boost output filter capacitor (C_{VDD1}) and return that capacitor's negative lead directly to the BGND pin to minimize boost switching current loop area.

If the boost circuit is not used, connect BSW directly to BGND.

11.1.10 AGND Pin

The AGND pin is the bias-power and signal-ground connection for the controller. The effectiveness of the filter capacitors on the signal pins depends upon the integrity of this ground return.

- Place the decoupling capacitors for VDD, REF, CS, BUR, and P13 pins as close as possible to the device pins and AGND pin with short traces.
- The device ground and power ground should meet at the return of the current-sense resistor (R_{CS}). Try to ensure that high frequency/high current from the power stage does not go through the signal ground.
- The thermal pad of the QFN package should be tied to the AGND pin with a short trace, and be connected to the signal ground plane with multiple vias which becomes a low-impedance ground return of external components to the AGND pin.

11.1.11 BGND Pin

The BGND pin is the boost ground connection for the controller. The effectiveness of the filter capacitors on the boost input and output depends upon the integrity of this ground return.

- Place the filter capacitors on BIN and VDD as close as possible to the device pins and BGND pin with short traces.
- Minimize the loop areas of the boost circuit and BGND to avoid coupling boost switching noise to other circuits.
- BGND should be tied to AGND at a location such that switching currents in the BGND return do not pass into the AGND network. Only low-ripple DC current should pass from BGND to AGND.

11.1.12 PGND Pin

The PGND pin is the gate-drive return for the PWML signal. It is NOT a ground return; do not confuse it as a power ground pin. It is not connected to AGND or BGND within the IC.

- The PGND signal is normally connected to the source pin of the low-side switching device, and run in parallel with PWML to minimize loop area.
- In certain cases, PGND may be connected to AGND at a location where PWML return currents do not create ground noise to disturb control signals referenced to AGND.
- For the individual low-side GaN power IC with logic PWM input, it is recommended to connect PGND to the bottom of the current sense resistor (R_{CS}) directly.

11.1.13 EP Thermal Pad

The EP pad is internally connected to the device substrate by an indeterminate impedance. Connect this pad externally to AGND at the AGND pin and at other pins that may be tied to AGND for the application. This pad also functions as a thermal dissipater for the device. Use multiple vias to connect this pad to other copper planes and areas to help dissipate heat and maintain the lowest GND impedance for signal integrity.

11.2 Layout Example

The layout techniques described in above sections were applied to the layout of the 65-W USB-PD high-density GaN active clamp flyback converter.
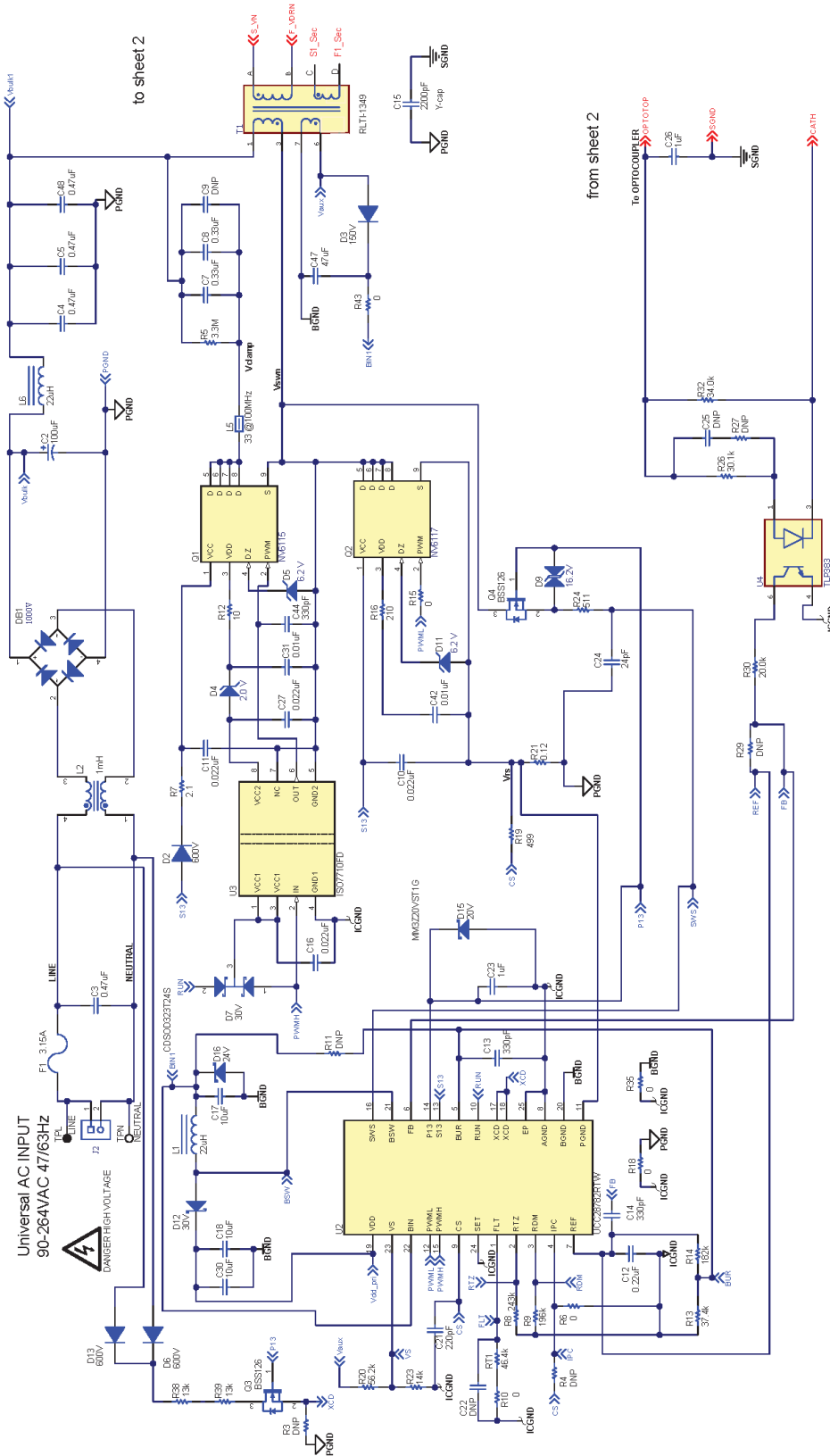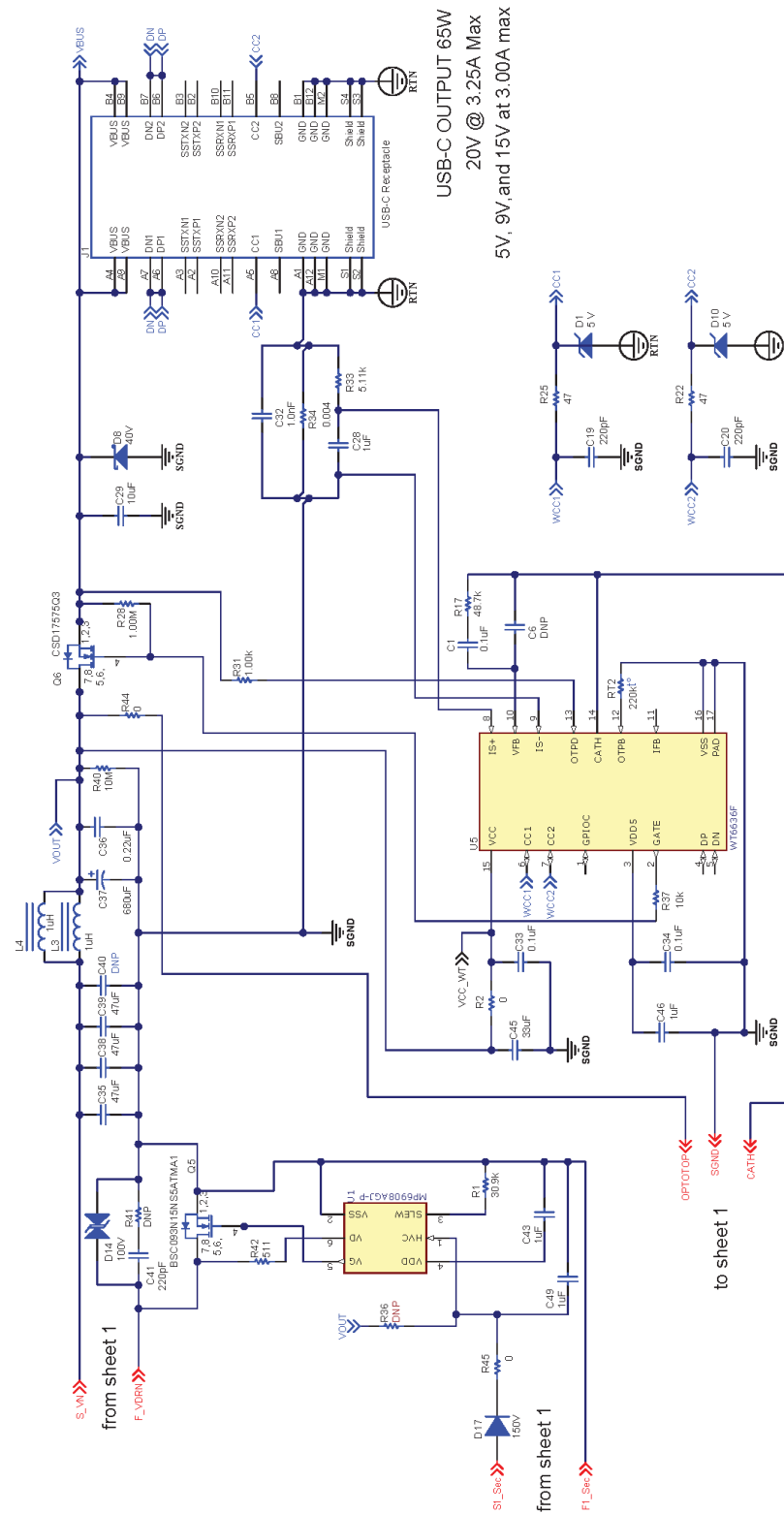
Figure 11-2. Schematic Page 1 of the 65-W EVM

Product Folder Links: *UCC28782*

Figure 11-3. Schematic Page 2 of the 65-W EVM
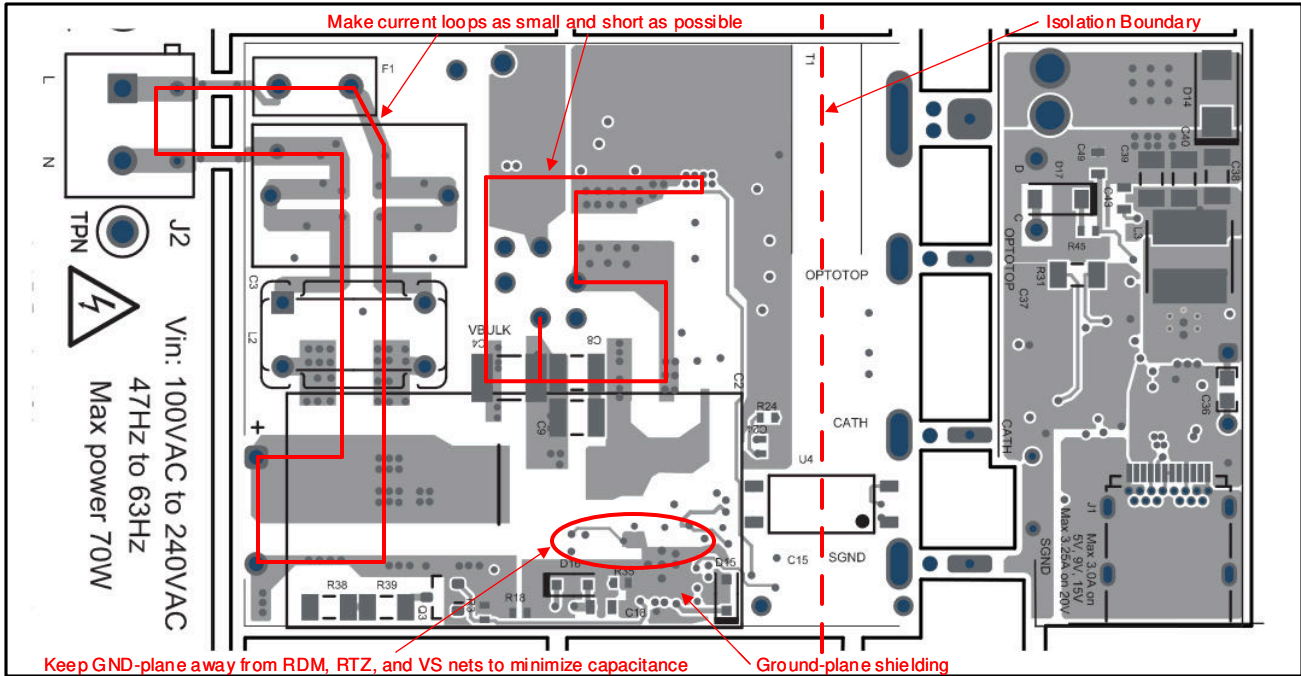
Figure 11-4. Top Assembly and Top (First Layer) of PCB
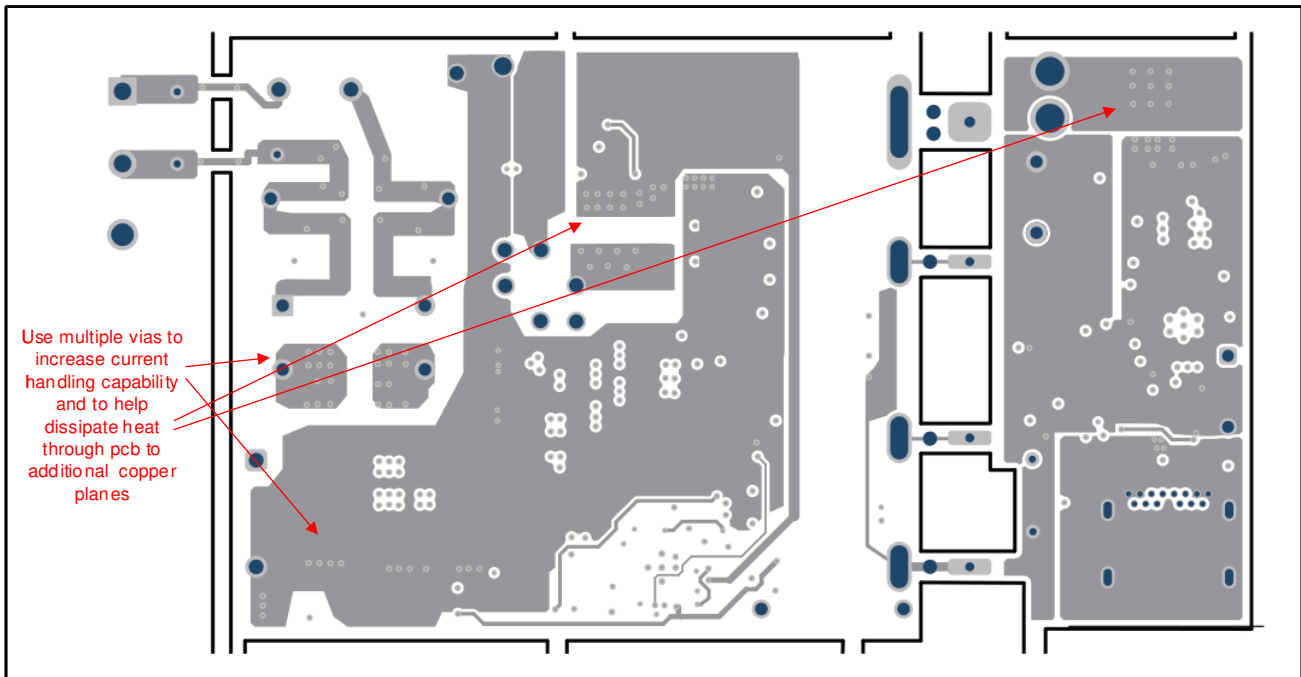
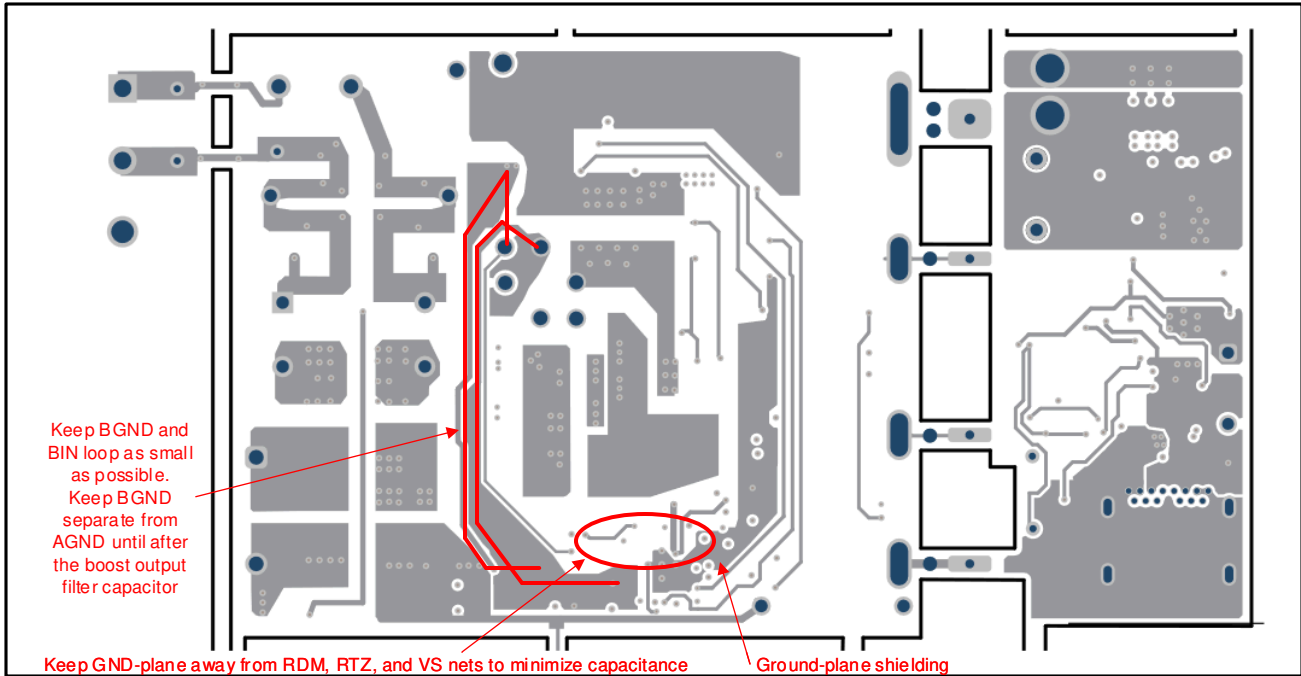
Figure 11-5. Inner Layer 1 (Second Layer) of PCB

Product Folder Links: *UCC28782*

Figure 11-6. Inner Layer 2 (Third Layer) of PCB
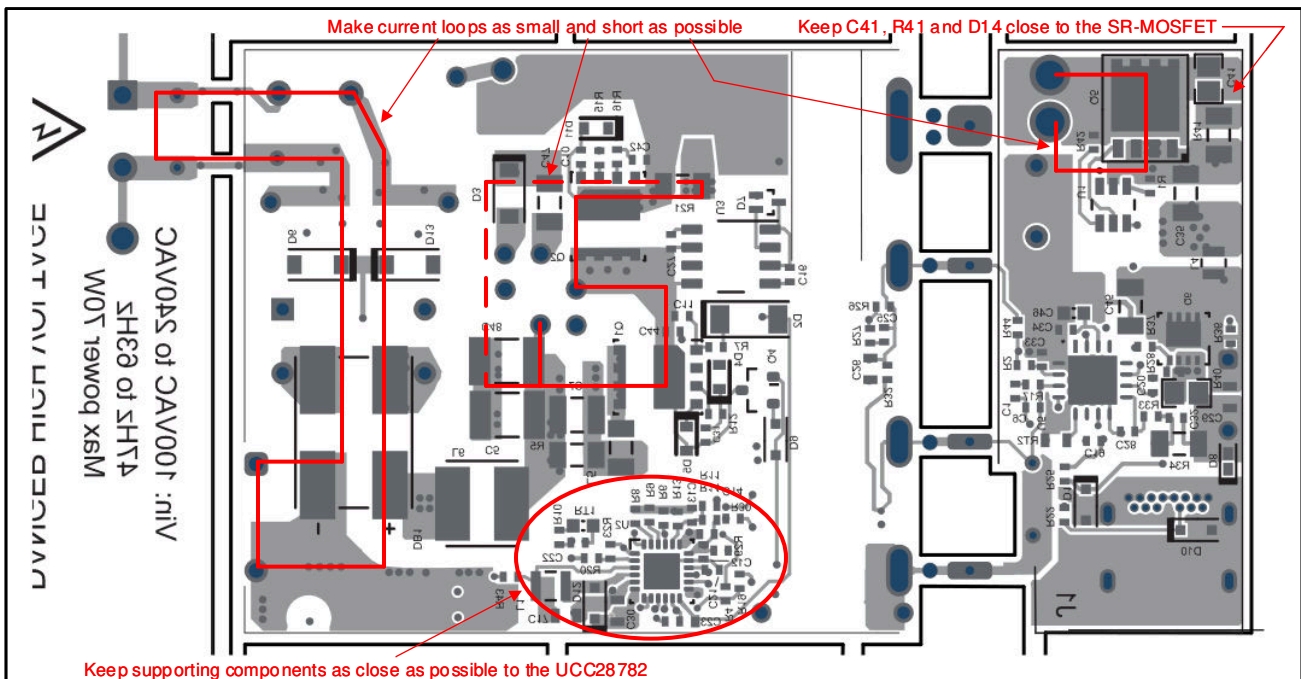
Figure 11-7. Bottom Assembly and Bottom (Fourth Layer) of PCB

12 Device and Documentation Support

12.1 Documentation Support

12.1.1 Related Documentation

For related documentation see the following:
- UCC28782 Design Calculator Tool is an Excel-based calculation tool for UCC28782 design
- Using the UCC28782EVM-030 65-W USB-C PD High-Density Active-Clamp Flyback Converter is a User Guide for the EVM

12.2 Receiving Notification of Documentation Updates

To receive notification of documentation updates, navigate to the device product folder on ti.com. In the upper right corner, click on *Alert me* to register and receive a weekly digest of any product information that has changed. For change details, review the revision history included in any revised document.

12.3 Support Resources

TI E2E™ support forums are an engineer's go-to source for fast, verified answers and design help — straight from the experts. Search existing answers or ask your own question to get the quick design help you need.

Linked content is provided "AS IS" by the respective contributors. They do not constitute TI specifications and do not necessarily reflect TI's views; see TI's Terms of Use.

12.4 Trademarks

TI E2E™ is a trademark of Texas Instruments.
All trademarks are the property of their respective owners.

12.5 Electrostatic Discharge Caution

This integrated circuit can be damaged by ESD. Texas Instruments recommends that all integrated circuits be handled with appropriate precautions. Failure to observe proper handling and installation procedures can cause damage.

ESD damage can range from subtle performance degradation to complete device failure. Precision integrated circuits may be more susceptible to damage because very small parametric changes could cause the device not to meet its published specifications.

12.6 Glossary

TI Glossary   This glossary lists and explains terms, acronyms, and definitions.

13 Mechanical, Packaging, and Orderable Information

The following pages include mechanical, packaging, and orderable information. This information is the most current data available for the designated devices. This data is subject to change without notice and revision of this document. For browser-based versions of this data sheet, refer to the left-hand navigation.

PACKAGING INFORMATION

Orderable Device	Status (1)	Package Type	Package Drawing	Pins	Package Qty	Eco Plan (2)	Lead finish/ Ball material (6)	MSL Peak Temp (3)	Op Temp (°C)	Device Marking (4/5)	Samples
UCC28782ADRTWR	ACTIVE	WQFN	RTW	24	3000	RoHS & Green	NIPDAU	Level-2-260C-1 YEAR	-40 to 125	28782AD	Samples
UCC28782ARTWR	ACTIVE	WQFN	RTW	24	3000	RoHS & Green	NIPDAU	Level-2-260C-1 YEAR	-40 to 125	28782A	Samples
UCC28782ARTWT	ACTIVE	WQFN	RTW	24	250	RoHS & Green	NIPDAU	Level-2-260C-1 YEAR	-40 to 125	28782A	Samples
UCC28782BDLRTWR	ACTIVE	WQFN	RTW	24	3000	RoHS & Green	NIPDAU	Level-2-260C-1 YEAR	-40 to 125	8782BDL	Samples
UCC28782CDRTWR	ACTIVE	WQFN	RTW	24	3000	RoHS & Green	NIPDAU	Level-2-260C-1 YEAR	-40 to 125	28782CD	Samples

(1) The marketing status values are defined as follows:
ACTIVE: Product device recommended for new designs.
LIFEBUY: TI has announced that the device will be discontinued, and a lifetime-buy period is in effect.
NRND: Not recommended for new designs. Device is in production to support existing customers, but TI does not recommend using this part in a new design.
PREVIEW: Device has been announced but is not in production. Samples may or may not be available.
OBSOLETE: TI has discontinued the production of the device.

(2) **RoHS:** TI defines "RoHS" to mean semiconductor products that are compliant with the current EU RoHS requirements for all 10 RoHS substances, including the requirement that RoHS substance do not exceed 0.1% by weight in homogeneous materials. Where designed to be soldered at high temperatures, "RoHS" products are suitable for use in specified lead-free processes. TI may reference these types of products as "Pb-Free".
RoHS Exempt: TI defines "RoHS Exempt" to mean products that contain lead but are compliant with EU RoHS pursuant to a specific EU RoHS exemption.
Green: TI defines "Green" to mean the content of Chlorine (Cl) and Bromine (Br) based flame retardants meet JS709B low halogen requirements of <=1000ppm threshold. Antimony trioxide based flame retardants must also meet the <=1000ppm threshold requirement.

(3) MSL, Peak Temp. - The Moisture Sensitivity Level rating according to the JEDEC industry standard classifications, and peak solder temperature.

(4) There may be additional marking, which relates to the logo, the lot trace code information, or the environmental category on the device.

(5) Multiple Device Markings will be inside parentheses. Only one Device Marking contained in parentheses and separated by a "~" will appear on a device. If a line is indented then it is a continuation of the previous line and the two combined represent the entire Device Marking for that device.
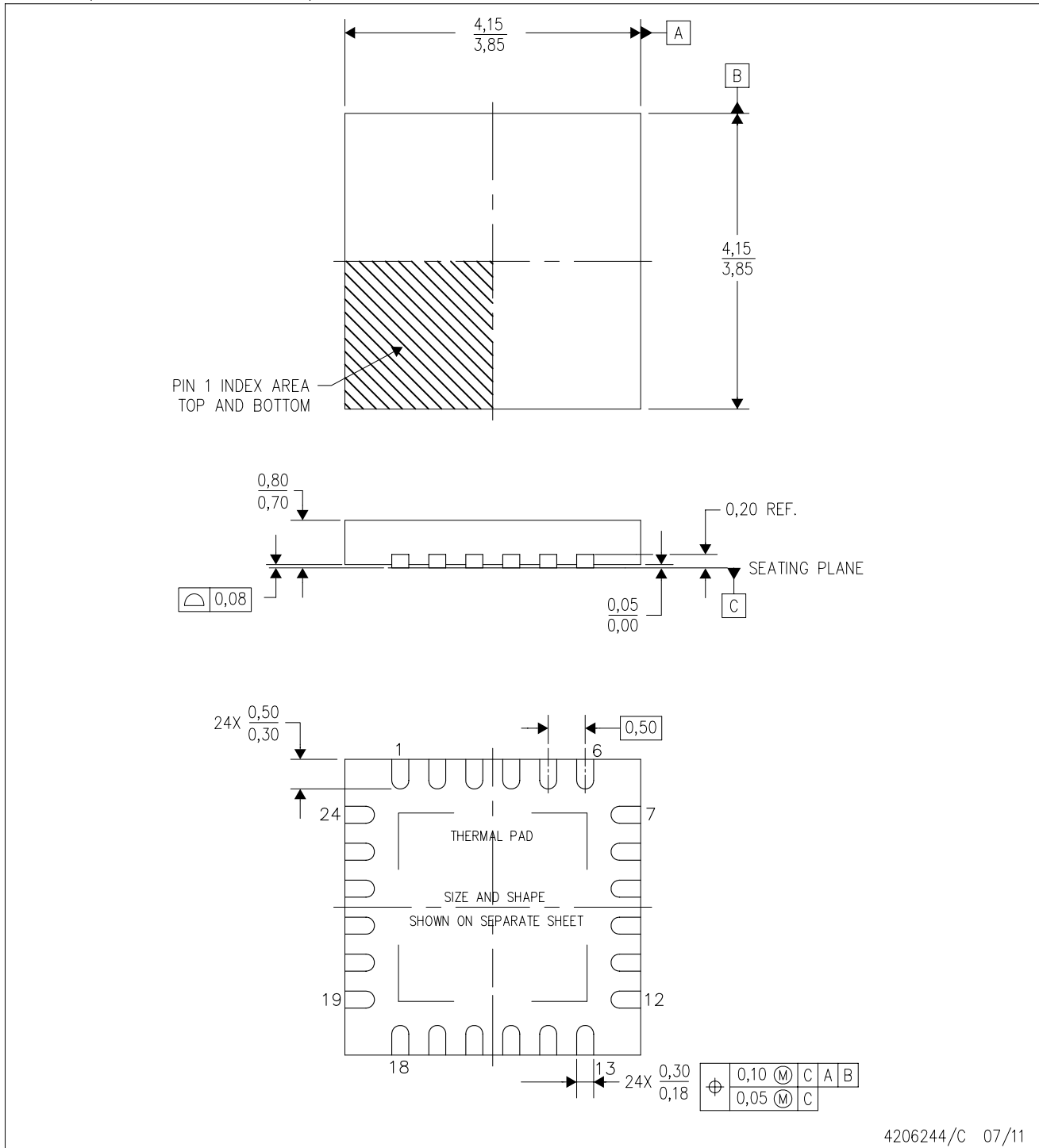
(6) Lead finish/Ball material - Orderable Devices may have multiple material finish options. Finish options are separated by a vertical ruled line. Lead finish/Ball material values may wrap to two lines if the finish value exceeds the maximum column width.

Important Information and Disclaimer: The information provided on this page represents TI's knowledge and belief as of the date that it is provided. TI bases its knowledge and belief on information provided by third parties, and makes no representation or warranty as to the accuracy of such information. Efforts are underway to better integrate information from third parties. TI has taken and continues to take reasonable steps to provide representative and accurate information but may not have conducted destructive testing or chemical analysis on incoming materials and chemicals. TI and TI suppliers consider certain information to be proprietary, and thus CAS numbers and other limited information may not be available for release.

In no event shall TI's liability arising out of such information exceed the total purchase price of the TI part(s) at issue in this document sold by TI to Customer on an annual basis.
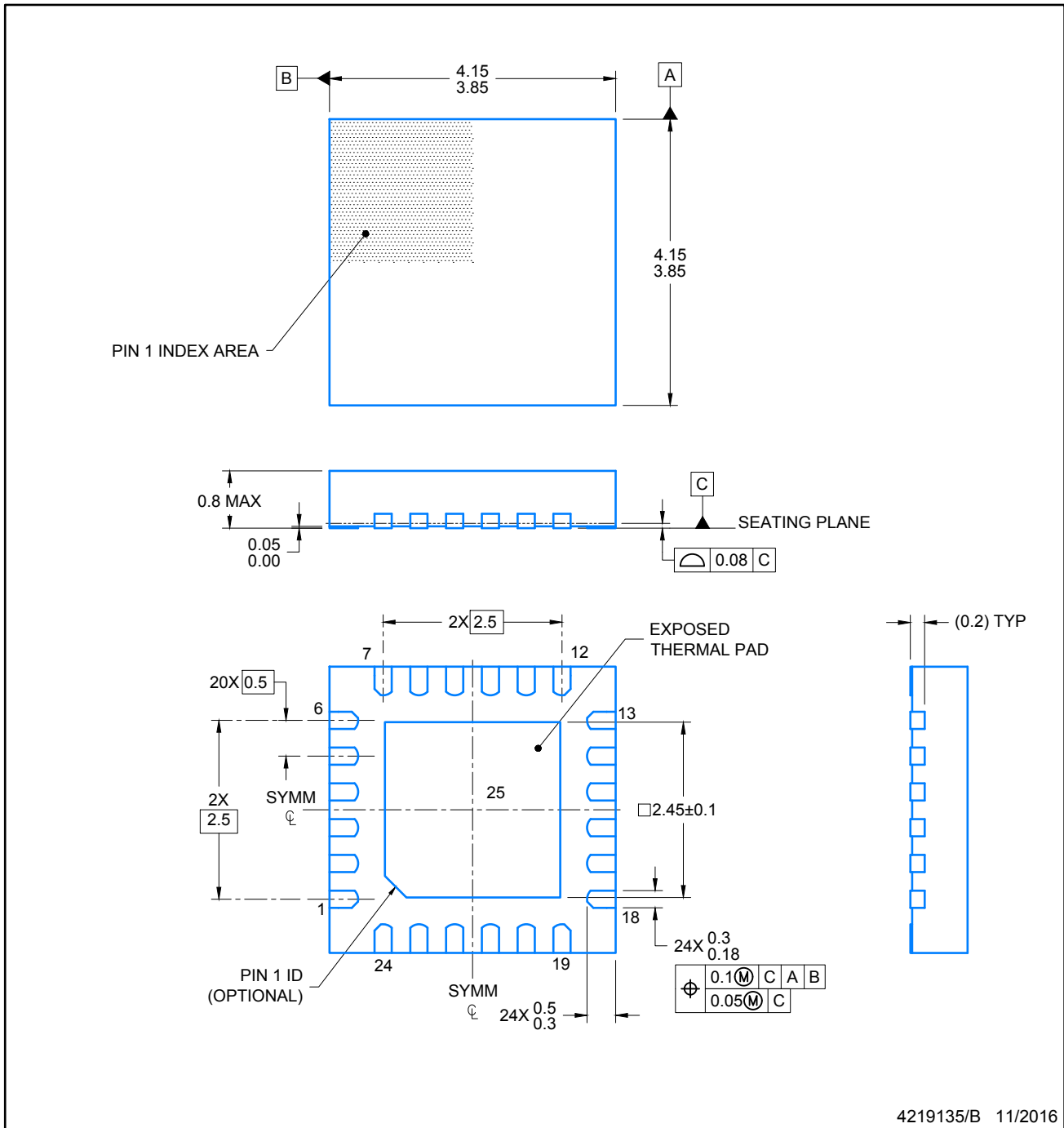
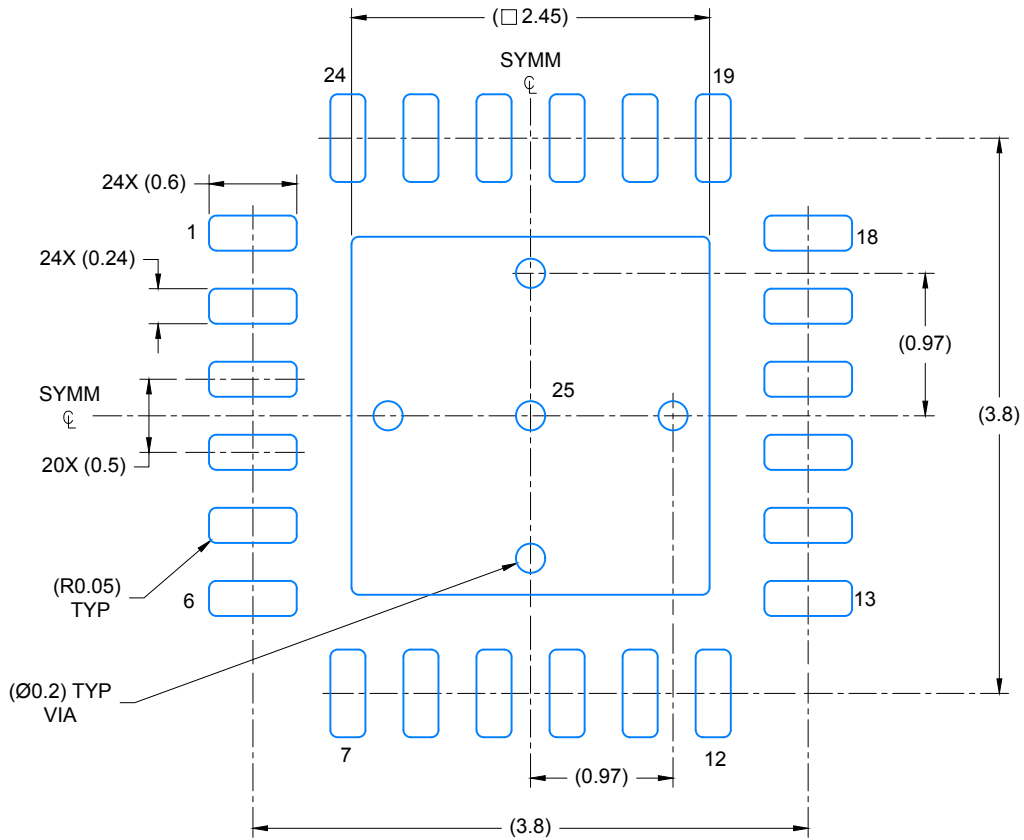RTW (S−PWQFN−N24)   PLASTIC QUAD FLATPACK NO−LEAD

PIN 1 INDEX AREA
TOP AND BOTTOM

$\frac{4,15}{3,85}$

$\frac{4,15}{3,85}$

$\frac{0,80}{0,70}$

0,20 REF.

SEATING PLANE

$\frac{0,05}{0,00}$

0,08

24X $\frac{0,50}{0,30}$

0,50

THERMAL PAD

SIZE AND SHAPE
SHOWN ON SEPARATE SHEET

1   6

24   7

19   12

18   13   24X $\frac{0,30}{0,18}$

⊕	0,10 Ⓜ	C	A	B
	0,05 Ⓜ	C		

4206244/C 07/11

NOTES: A.   All linear dimensions are in millimeters. Dimensioning and tolerancing per ASME Y14.5M−1994.
         B.   This drawing is subject to change without notice.
         C.   Quad Flatpack, No−Leads (QFN) package configuration.
         D.   The package thermal pad must be soldered to the board for thermal and mechanical performance.
         E.   See the additional figure in the Product Data Sheet for details regarding the exposed thermal pad features and dimensions.
         F.   Falls within JEDEC MO−220.

B

4.15
3.85

A

PIN 1 INDEX AREA

4.15
3.85

0.8 MAX

0.05
0.00

C

SEATING PLANE

0.08 C

2X 2.5

7   12

EXPOSED
THERMAL PAD

20X 0.5

6   13

SYMM
℄

2X
2.5

25

□2.45±0.1

1   18

PIN 1 ID
(OPTIONAL)

24   19

SYMM
℄

24X 0.3
0.18

24X 0.5
0.3

0.1 Ⓜ C A B
0.05 Ⓜ C

(0.2) TYP

4219135/B   11/2016

NOTES:

1.   All linear dimensions are in millimeters. Any dimensions in parenthesis are for reference only. Dimensioning and tolerancing
     per ASME Y14.5M.
2.   This drawing is subject to change without notice.

EXAMPLE BOARD LAYOUT

WQFN - 0.8 mm max height

PLASTIC QUAD FLATPACK-NO LEAD

(□ 2.45)

SYMM
℄

24

19

24X (0.6)

1

24X (0.24)

18

SYMM
℄

(0.97)

25

(3.8)

20X (0.5)

(R0.05)
TYP

6

13

(Ø0.2) TYP
VIA

7

(0.97)

12

(3.8)

LAND PATTERN EXAMPLE
SCALE: 20X

0.07 MAX
ALL AROUND

METAL

SOLDER MASK
OPENING

NON SOLDER MASK
DEFINED
(PREFERRED)

0.07 MIN
ALL AROUND

SOLDER MASK
OPENING

METAL UNDER
SOLDER MASK

SOLDER MASK
DEFINED
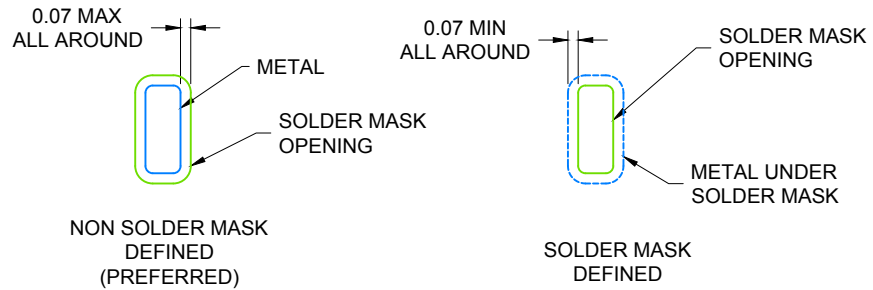
SOLDER MASK DETAILS

4219135/B   11/2016

NOTES: (continued)

3.   For more information, see Texas Instruments literature number SLUA271 (www.ti.com/lit/slua271).

4X(□ 1.08)

(0.64) TYP

(R0.05) TYP

24

19

24X (0.6)

1

25

18

24X (0.24)

(0.64) TYP

20X (0.5)

SYMM ₡

(3.8)

6

13

METAL TYP

7

12

SYMM ₡

(3.8)

SOLDER PASTE EXAMPLE
BASED ON 0.125 mm THICK STENCIL

EXPOSED PAD 25:
78% PRINTED COVERAGE BY AREA UNDER PACKAGE
SCALE: 20X

4219135/B   11/2016
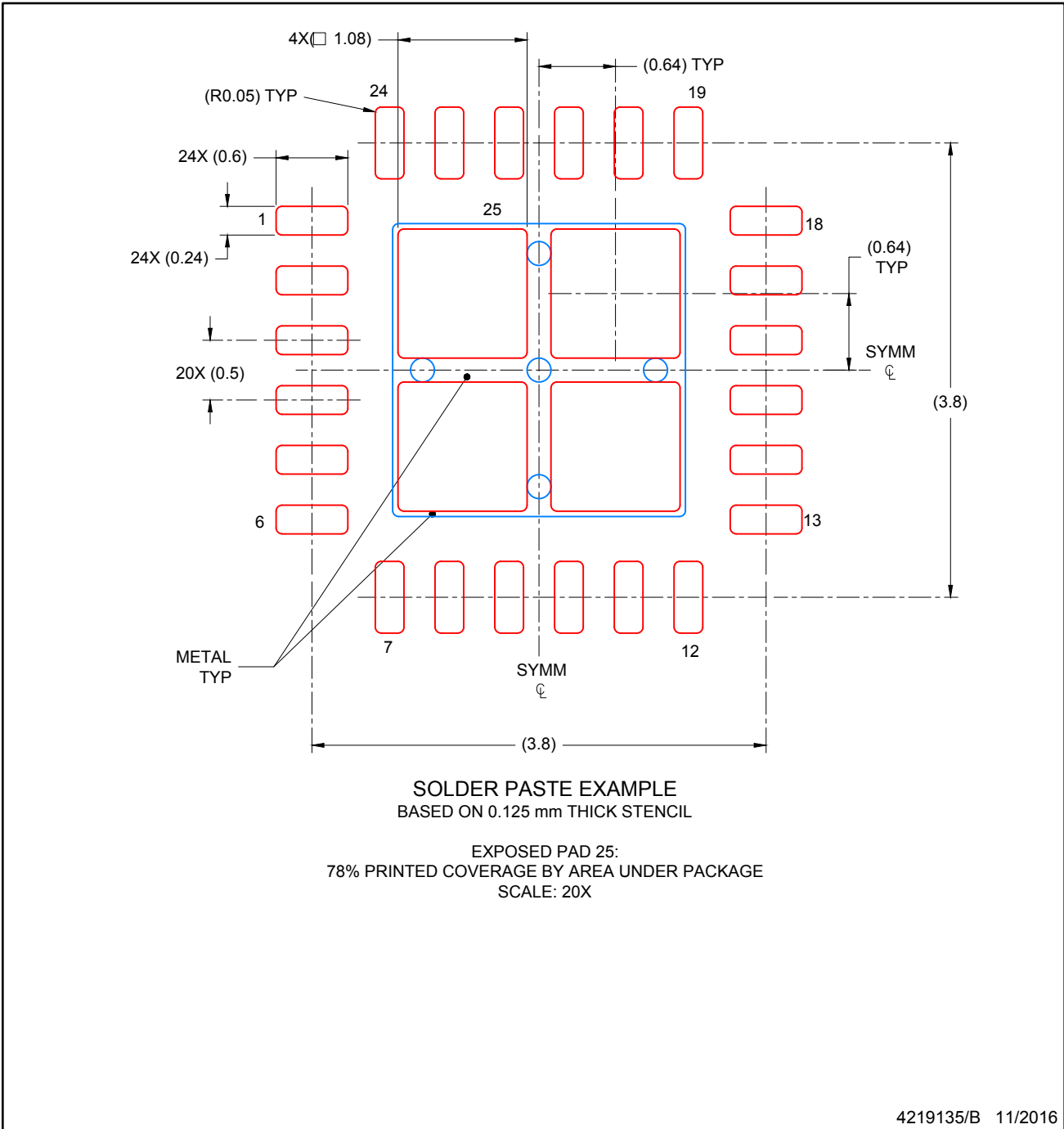
NOTES: (continued)

4. Laser cutting apertures with trapezoidal walls and rounded corners may offer better paste release. IPC-7525 may have alternate design recommendations.

IMPORTANT NOTICE AND DISCLAIMER